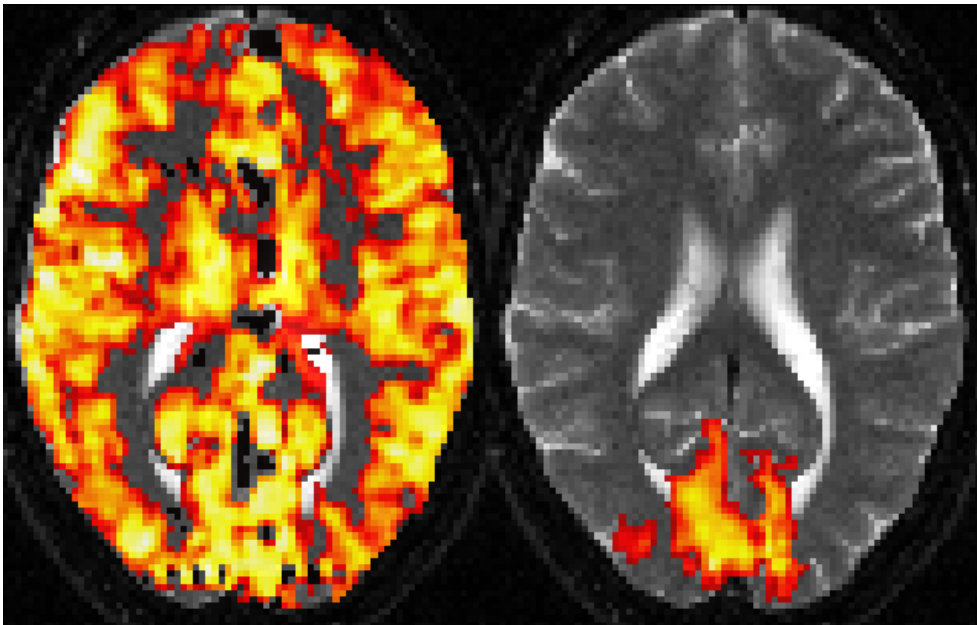


Basic physiology of BOLD imaging



Egill Rostrup

Danish Research Center for Magnetic Resonance,
Copenhagen University Hospital, Hvidovre

6th December 2006

Til Haavard og Vibeke

The illustration on the title page shows the distribution of the BOLD response to either inhalation of 6% CO₂ (left image) or visual stimulation by a flickering checkerboard (right image). The colored regions indicate significant signal increase during the stimulation period (thresholded at $p < 0.001$), data from ref. (85).

Contents

1	Preface	4
2	Introduction	7
3	Theory	10
3.1	Mathematical model	11
3.2	Assumptions	16
3.3	Implementation of model	16
3.4	Determination of constants	17
4	Baseline BOLD signal	19
4.1	Effect of baseline parameters	19
4.2	Capillary heterogeneity	25
4.3	Arterial CO ₂ tension	27
4.4	Arterial O ₂ tension	33
4.5	Breath-holding	38
4.6	Hematocrit	39
4.7	Clinical use	40
4.7.1	Vascular reserve capacity	40
4.7.2	Tumor vascularity	40
5	The BOLD_A response	42
5.1	Basic determinants of the BOLD _A response	42
5.2	Effect of hypo- and hypercapnia	46
5.3	Effect of hypo- and hyperoxia	49
5.4	Hematocrit	53
5.5	Pharmacological perturbation	54
5.6	Other conditions	56
5.6.1	Effects of aging	56
5.6.2	Investigations during sleep	57
6	Using BOLD for quantification	57
6.1	Cerebral blood volume	57
6.2	Regional O ₂ saturation	58
6.3	Oxygen metabolism	59
7	Conclusion	61
	References	63
	Summary in English	77

Dansk Resumé

79

Abbreviations

(see also list of symbols, table 1)

$\Delta\chi$	Relative magnetic susceptibility
ν	Magnetic resonance shift
ω_0	Magnetic resonance frequency
BOLD	Blood Oxygenation Level Dependent signal
BOLD _A	BOLD response, due to neural activation
BOLD _B	BOLD response, due to non-neural CBF change
CBF	Cerebral blood flow
CBV	Cerebral blood volume
CMRO ₂	Cerebral Metabolic Rate for Oxygen, see also M _{O₂}
COX	Cyclooxygenase
DPG	2,3-diphosphoglycerate
EPI	Echo planar imaging
fMRI	Functional magnetic resonance imaging
Hct	Hematocrit
MCHC	Mean red blood Cell Hemoglobin Concentration
M _{O₂}	Effective cerebral metabolic rate for oxygen
M _{O₂} [*]	Maximal cerebral metabolic rate for oxygen (when not limited by O ₂)
MRI	Magnetic resonance imaging
OEF	Oxygen extraction fraction
ODC	Oxygen dissociation curve (binding to hemoglobin)
P _a CO ₂	Arterial CO ₂ tension
P _{ET} CO ₂	End-tidal partial pressure of CO ₂
PET	Positron emission tomography
PS _c O ₂	Permeability-Surface product for O ₂ transport over capillary membrane
R ₂ [*]	Apparent transversal relaxation rate (1/T ₂ [*])
R ₂	Transversal relaxation rate (1/T ₂)
ROI	Region of interest
T ₁	longitudinal relaxation time
T ₂ [*]	Apparent transversal relaxation time
T ₂	Transversal relaxation time

1 Preface

The studies contributing to this thesis were all carried out at the Danish Research Centre for Magnetic Resonance at Hvidovre, and - for the PET studies - at the PET and cyclotron unit in the Dep. of Nuclear Medicine, Rigshospitalet. For many reasons the studies were carried out during over an extended period of time, and though there is a number of disadvantages with this, some advantages also do come to mind. One is that it has been possible to follow the entire evolution of the field of brain imaging using the BOLD technique. Another is that during this period, a large number of skilful people have passed by and contributed to this or other related work in the MR department.

I would like to thank all of them in this preface, and also send my apologies to those that I may forget. Let me begin though, by thanking Jorgen and Margaret Christoffersen who did not contribute directly to the thesis, but who introduced me to scientific method, and image analysis in particular, in my pregraduate years. Although I didn't always follow the advice of repeating experiments until the results fit within the width of a pencil stroke, I'm grateful for this schooling.

The original idea of investigating the newly discovered BOLD response with hypercapnia and hypoxia came from Prof. Ole Henriksen, who was then in charge of the MR-department. The loss of his enthusiasm and knowledge when he unfortunately had to retire much too soon from his position, was a severe setback for this project, as well as for the MR-department in general.

To the first crew of BOLD enthusiasts belongs Henrik Larsson, whom I would like to thank for being a very good friend and knowledgeable colleague ever since our journey to one of the first fMRI conferences in Washington DC, more than 12 years ago.

Among the many people involved in the initial experiments Kim Garde played an important role by setting up the respiratory test equipment, and keeping the volunteers alive! Poul Ring is due to thanks for making the first software to analyse the image results by Mann-Whitney test, for not insisting for too long on its use, and for always being a valuable reference with an extended knowledge of mathematical algorithms.

Ian Law and Morten Blinkenberg entered the scene when PET scanning became part of the project. Thanks for introducing me to that world, and Ian for always, and continuously, maintaining a healthy skepticism towards this new MR business, with all its uncertainties, signal instability etc.

Olaf Paulson became the manager of the department, and a supervisor of great patience! Furthermore, he brought a large number of scientific contacts to the department, notably through the Human Brain Project. Among one of the important contacts was Prof. Seong-Gi Kim, who taught many of us lessons of scientific efficiency and endurance. Also by bravely enduring more than one Christmas party in the MR-group!

Lars Hanson brought back new life to spectroscopy, previously known as the eternal technique of the future, and contributed a lot - although indirectly, and probably without informed consent - to this work, by many an enlightening discussion regarding the world of spins and their secret properties.

In particular I would like to thank a long list of former PhD-students, Sverre Rosenbaum, Peter Born, Ellen Garde, Annika Langkilde, Katja Krabbe, Jacob Marstrand, Elisabeth Kalowska,

Irene Andersen and Karam Sidaros for a fascinating and inspiring collaboration during their PhD-work, and also of course for helping me never needing to be bored, when incidentally not working on my thesis.

Gitte Moos Knudsen's true interest in the work, and valuable comments was instrumental for keeping me on track and finishing some of the key papers. I congratulate those that you supervise! Also I would like to thank Gunhild Waldemar for support and expertise, and - along with Terry Jernigan - for helpful comments and advice during turbulent times.

A lot of the experiments were carried out with the help of technicians, notably Nina Hansen and Helle Simonsen, whose help is gratefully acknowledge.

Also thanks to many volunteers (not the least those of the Chacaltaya expedition) for their participation and brave inhalation of various gas mixtures.

Brave was also the support by my family, Christina and Kjartan, who put up with long working hours and a lot more absent-mindedness than usual, for a long period, while the thesis was being written. Probably, they too had to hold their breaths at times, when nothing else than compartment modelling seemed to matter.

It was a pleasure to work with my brother Claus and Jens Dahl on the layout of the printed version.

Financially, parts of the study were supported by the Medical Research Council.

This thesis was accepted on August 14. 2006 for public defense at the University of Copenhagen. The defense will take place on December 7. 2006, at 2pm in the Auditorium of the Medical Museion, Bredgade 62, Kbh K.

The Thesis is based on the following papers:

- I Rostrup, E., Larsson, H. B., Toft, P. B., Garde, K., Thomsen, C., Ring, P., Sondergaard, L., and Henriksen, O.: Functional MRI of CO₂ induced increase in cerebral perfusion. *NMR Biomed.* 7:29-34, 1994. (quoted as ref. (128)).
- II E. Rostrup, H. B. W. Larsson, P. B. Toft, K. Garde, and O. Henriksen. Signal changes in gradient echo images of human brain induced by hypo- and hyperoxia. *NMR Biomed*, 8:41–47, 1995. (quoted as ref. (126)).
- III E. Rostrup, H. B. W. Larsson, P. B. Toft, K. Garde, P. Ring, and O. Henriksen. Susceptibility contrast imaging of CO₂-induced changes in blood volume of human brain. *Acta Radiologica*, 37:813–822, 1996. (quoted as ref. (127)).
- IV S. G. Kim, E. Rostrup, H. B. W. Larsson, S. Ogawa, and O.B. Paulson. Determination of relative CMRO₂ from CBF and BOLD changes: Significant increase of oxygen consumption rate during visual stimulation. *Magn Reson Med*, 41:1152–61, 1999. (quoted as ref. (85)).
- V E. Rostrup, I. Law, M. Blinkenberg, H. B. W. Larsson, P. Born, S. Holm, and O. B. Paulson. Regional differences in the CBF response to hypercapnia. - a combined PET and MRI study. *Neuroimage*, 11:87 89, 2000. (quoted as ref. (130)).
- VI E. Rostrup, I. Law, F. Pott, K. Ide, and G. M. Knudsen. Cerebral hemodynamics measured with simultaneous PET and near-infrared spectroscopy in humans. *Brain Res*, 954:183 93, 2002.(quoted as ref. (131)).
- VII E. Rostrup, G.M. Knudsen, I. Law, S. Holm, H.B. W. Larsson, and O.B. Paulson. The relationship between cerebral blood flow and volume in humans. *Neuroimage*, 24:1 11, 2005. (quoted as ref. (125)).
- VIII E. Rostrup, H.B.W. Larsson, G.M. Knudsen, A.P. Born, and O.B. Paulson. Changes in BOLD and ADC weighted imaging in acute hypoxia and altitude adaptation. *Neuroimage*, 28:947-955, 2005. (quoted as ref. (129)).

2 Introduction

The concept of blood oxygenation level dependent (BOLD) signal changes in MRI was originally described in the context of cerebral blood vessels around which a signal decrease was seen when the oxygenation of venous blood was altered (109; 110). These original observations from 1990 were made in highly experimental settings, in anesthetized rats at a very high magnetic field strength of 7 T, and it was therefore to take a number of years before the technique was commonly accepted and applied. Soon after the initial reports, however, followed studies in cats, conducted at lower field strength, in which large global cerebral signal changes were observed in response to respiratory challenges (147).

The initial studies in human volunteers that appeared during the following years, focused on the ability to detect functional activation in the primary visual and motor cortices (87; 112). These studies relied on, and confirmed earlier observations from positron emission tomography (PET) studies, that the oxygen content of venous blood increases during functional activation of the brain. This effect is due to an increase in the delivery of oxygen that outweighs the smaller increase in oxygen metabolism, when neurons in a particular region of the brain are engaged in a specific task. As a consequence of this inequality in response the concentration of venous deoxy-hemoglobin decreases, and since deoxy-hemoglobin — as opposed to oxy-hemoglobin — is paramagnetic, the result is an increase in magnetic field homogeneity, with a concomitant increase in the measured MRI signal.

Several early studies described the basic mechanisms of the BOLD response (42; 111), mostly from a biophysical point of view, i.e. regarding the relationship between venous oxygenation and the resulting change in transversal relaxation rate of the tissue.

However, a rapidly increasing fraction of studies have dealt purely with functional activation in the context of brain mapping, and this led to the development of the term functional magnetic resonance imaging (fMRI) as opposed to the more classical structural imaging methods. Functional MRI may be defined as MR imaging with the purpose of mapping the location of activated brain areas, or following changes in such areas over shorter or longer time periods. During the last decade this technique has been developed to become probably the most important tool to detect and map functional activation of the brain, and BOLD imaging is the most commonly applied technique to obtain functional contrast. Other MR techniques are available, but apart from spin labeling techniques, which measure flow changes more directly than BOLD techniques, none of these have so far gained widespread use.

Technical advances that made the development of BOLD possible include the dissemination of echo-planar imaging (EPI) in many MR research facilities, a process that has taken place simultaneously with the rapid and continued rise in the number of fMRI publications during the last 10 years. Although the feasibility of fMRI using more conventional multi-shot techniques was demonstrated early (55), the high-speed acquisition made possible with EPI has proved essential to reach the current standard for fMRI studies.

Brain-mapping using fMRI is now a well-established and reliable technique, that continues to contribute important knowledge within several areas such as functional neuroanatomy, basic neuropsychology, as well as neuropsychiatry and clinical neurology. The technique nevertheless depends on the assumptions that the BOLD response faithfully reflects neural activation across

different brain regions and baseline states, and is relatively uniform between subjects. In order to further examine such assumptions, it is crucial to have as detailed an understanding of the mechanisms of the BOLD response as possible, including biophysical, physiological and neurophysiological factors. In the present work only the physiological factors, i.e. factors determining the magnitude of oxygenation change for a given activation, will be treated in depth. The biophysical factors, those relating oxygenation to BOLD signal change, have been described in numerous earlier reports, and these results will be used in the present work. The neurophysiological factors relate neuronal activation, resulting from a given stimulus, to increases in flow, and metabolism, and have been treated in some recent reviews (89; 98).

The importance of physiological factors lies in their role as potential sources of intra- and inter-individual variation, which is notoriously high in fMRI. Furthermore, systematic differences may easily arise between groups of patients or selected subjects, due to differences in underlying physiology, such as baseline flow or hematocrit. Finally, when fMRI is used to determine the magnitude of parameters, such as the cerebral metabolic rate of O₂ (CMRO₂), a quantitative understanding of the response is crucial.

Some early studies by Rostrup et al. confirmed the initial observations regarding the importance of respiratory conditions, and demonstrated that both alterations of arterial oxygen- and carbon dioxide tensions elicited changes in BOLD signal in human subjects. (126; 128). This has subsequently been followed up by many studies, dealing with the basic mechanisms producing the BOLD response. Notably, since the demonstration by Bandettini et al. that the BOLD response to functional activation was inhibited in states of high baseline blood flow (7), several reports have emerged dealing with the importance of various physiological baseline parameters for the BOLD response during functional activation. In some of these studies partially conflicting results have been reached regarding the interaction of BOLD with baseline parameters; examples are whether the functional BOLD response increases or decreases during hypercapnia (23; 116), as well as whether it is constant or decreased in hypoxia (7; 129).

When describing these types of interactions, the interpretation can be based on two general types of mechanisms. One class is the biophysical mechanisms, such as the change in venous oxygenation for a given change in flow, the relationship between tissue oxygenation and metabolism at constant flow, or the influence of hemoglobin properties. The other includes more specific physiological mechanisms, such as changes in vascular reactivity due to a pharmacologically active substance, or the suggested increase in reactivity during hypoxia that would counteract a decrease in oxygen delivery (104). Another example is the baseline hematocrit which may influence the BOLD response both directly by altering the amount of deoxy-hemoglobin, and indirectly by its effect on cerebral blood flow. In principle the first class of mechanisms can be completely described using biophysical models. The prerequisite for this is that adequate knowledge about the relevant physiological constants can be obtained, and in practice this may certainly be a limiting factor. Clearly, it becomes of great importance to apply a comprehensive biophysical BOLD model, including as much of the experimentally available information as possible. This should make it possible to interpret direct effects and interactions involving various global stimuli, and to judge whether they are expected from biophysical BOLD theory, or whether they represent specific physiological interactions.

Several models have been presented to account for the magnitude of BOLD response taking

the cerebral oxygen balance into account. The majority of these original publications are based on the application, by Ogawa et al. (111), of Ficks principle to express cerebral metabolic rate for oxygen as the product of CBF, arterial hemoglobin concentration and saturation. Later publications derived expressions for the interrelationship of the relative values of cerebral blood flow and volume (CBF and CBV), as well as O_2 metabolism during activation. This was done by simple division with the baseline values (85; 86). Further developments were presented by Davis et al. (28) by including the baseline values into a signal scaling factor, so that BOLD signal changes could be directly related to the relative $CMRO_2$ and CBF, and this form of the equations has become a standard expression for BOLD (21; 57).

A conceptually important parameter appearing from this derivation is a scaling factor expressing the maximal BOLD signal increase that is obtainable if all deoxy-hemoglobin were to be removed from the cerebral circulation. This parameter therefore expresses the signal attenuation caused by deoxy-hemoglobin in the resting state, and it is dependent on absolute $CMRO_2$, CBF and CBV (28). Because models of this type contain only a small number of parameters, they are limited in their ability to predict the consequences of changes in other than the most basic parameters. Furthermore, they are mostly suited to the investigation of relative parameter values, and are therefore rarely applied to study the effect of absolute magnitudes of parameters, such as vascular permeability, or oxygen metabolic rate.

One of the first studies to present a more detailed approach to modeling cerebral oxygen metabolism in the context of BOLD imaging was that of Hathout et al. (52). In this study a quantitative model for venous oxygenation, based on Ficks principle, was presented; a potential influence of the arterial compartment, or of the oxygen dissociation curve was not considered.

A later very influential study demonstrated the importance of oxygen transport efficiency for the relationship between flow and oxygen metabolism, and between flow and BOLD signal change (19). Two different models are conceivable: in one oxygen is freely diffusible and the extra-vascular oxygen tension (P_tO_2) is so high that oxygen metabolism can increase without the need for increased arterial oxygen delivery. In the other model oxygen transport is so slow that the tissue oxygen tension approaches zero, and $CMRO_2$ can only be increased by increasing flow, whereby the trans-endothelial O_2 -gradient increases. Conversely, $CMRO_2$ is seen as limited by flow, and is expected to increase as a direct consequence of any flow increase. This is the so called oxygen limitation model, the concept of which has also been presented by other authors (45).

Although there are some recent exceptions (e.g. (151)) many conventional models do not directly take important factors such as hemoglobin properties and oxygen availability into account. It is also a common feature that there are many approximations, of unknown quantitative importance, and that the models are limited to certain physiological standard conditions, such as an arterial oxygen saturation close to 100%.

The purpose of the present study is to review the part of BOLD literature that pertains to the effect of basic physiological factors. Where possible both *main effects* and *interactions* of these factors will be described: The former (described in section 4) concern the direct effects of physiological changes on the baseline signal in fMRI, and the latter the way these changes may influence the neurally elicited BOLD signal (section 5). The review will be concerned primarily with studies in human subjects involving respiratory (CO_2 or O_2 modulations) or similar

interventions, designed to change oxygen delivery and the BOLD signal.

The term BOLD signal will be used to describe the magnitude of the MR-signal in the absence of any specific experimental manipulation. The MR-signal of most relevance for BOLD imaging is the signal arising from susceptibility weighted measurements, i.e. those that are sensitive to changes in the apparent transversal relaxation rate (T_2^*).

The BOLD signal will be thought of as the normalised signal relative to the signal when no deoxy-hemoglobin is present (i.e. in the theoretical situation of no oxygen metabolism, the signal will be 1). Generally the term *baseline* will be used for the resting period preceding (or following) a period in which a particular stimulus expected to elicit neural activation is given. Signal changes elicited by experimental effects or manipulation will be referred to as BOLD responses. When these are related to neural activation they will be referred to as $BOLD_A$, whereas BOLD changes that are related to baseline conditions, such as varying CBF, CBV or the arterial CO_2 -tension (P_aCO_2), will be referred to as $BOLD_B$.

From the point of view of BOLD theory these two types of response are very similar, since they are both caused by decreases in total deoxy-hemoglobin content, and it is therefore mainly for the sake of clarity that the distinction is made. However, it should be noted that while $BOLD_A$ is associated with changes, mainly decreases, in oxygen extraction fraction (OEF) (119), $BOLD_B$ may (e.g., during CO_2 -inhalation) or may not (e.g., during changes in arterial oxygen content or hematocrit) be associated with such changes.

A large part of the more recent literature concerns the dynamics of the $BOLD_A$ response, rather than the factors determining the general magnitude of the response. Notably, one very central concept is a difference in time constants for the various constituents of the BOLD response. According to the Balloon Model (20) the normalisation of CBV occurs slower than that of CBF following a neural stimulus. This leads to the post-stimulus undershoot, which is often observed experimentally. However, the dynamic features, and the modeling approaches, are outside of the scope of the present work, which will be concerned predominantly with the response magnitude in the stable, or semi-steady state situation. Dynamic models have been integrated and reviewed in a recent paper (21).

In order to aid the interpretation of experimental BOLD results, a numerical compartment model will be presented. This model includes several known features of oxygen transport in relation to the BOLD response, and enables free adjustment of parameters, and sampling of physiological quantities during the course of a simulated experiment. No assumptions of physiological relationships (e.g., oxygen limitation) are inherent in the model, but the parameters can be varied to simulate different degrees of diffusion barriers, or other. The model will be used to compare biophysical arguments to more physiological arguments in the interpretation of experimental findings, and to resolve factors that will enhance or decrease the $BOLD_N$ response. The following sections will further describe the background and implementation of the model.

3 Theory

In general terms the cerebral oxygen balance can be described using a mass-balance approach, and considering that oxygen is supplied by the arterial blood flow, and removed by venous out-

flow or by cerebral metabolism. Furthermore, the content of O_2 in a unit volume of tissue (C_tO_2) can be calculated as the weighted sum of concentrations in the different compartments. As shown previously by the present author (131) this leads to an expression of the form:

$$C_tO_2 = rCBV_{tot} \cdot C_aO_2 - rCBV_v \cdot \frac{CMRO_2}{CBF} \quad (1)$$

where $rCBV_{tot}$ is the total volume of all vascular compartments, and $rCBV_v$ the volume of the venous compartment. $CMRO_2$ is the cerebral metabolic rate for O_2 , and C_aO_2 the arterial O_2 content. In this derivation it is assumed that the blood volume can be described by only an arterial and a venous compartment, and no other reserves of oxygen are assumed.

The oxygen extraction fraction, OEF, is the fraction of O_2 that is taken up and converted metabolically by the brain:

$$OEF = \frac{CMRO_2}{CBF \cdot C_aO_2} \quad (2)$$

By combining eqs. 1 and 2 the following expression can be obtained

$$C_tO_2 = C_aO_2 \cdot (rCBV_{tot} - rCBV_v \cdot OEF) \quad (3)$$

which is conceptually useful in relating the key determinants of cerebral oxygen content. The amount of deoxy-hemoglobin, which is the parameter that BOLD techniques are sensitive to, can be obtained by subtraction from the total amount hemoglobin pr. unit volume of tissue.

Simple analytical models such as the above do not take several potentially important aspects of cerebral oxygen balance into account. These include hemoglobin properties (parametrised by the oxygen dissociation curve, ODC), capillary O_2 exchange and diffusibility (as quantified by the PS-product, PS_cO_2), and physically dissolved O_2 in blood and tissue. They also do not allow estimation of these and other parameters as a function of time, which may be useful during the simulation of an experiment. Several more detailed analytical models have been proposed, but in general several mathematical and physiological assumptions are necessary to derive the models.

In the present work a more comprehensive model will therefore be presented. The model is novel by explicitly including three vascular compartments, by directly describing the convective and diffusive transport of O_2 between the compartments, and by performing all estimations in absolute rather than normalised units. A sketch of the model is shown in figure 1, and details will be presented in the following sections.

3.1 Mathematical model

The transport of oxygen to and from the capillary compartment takes place due to flow and diffusion over the blood-brain barrier, and can be described by the equation:

$$\frac{dC_cO_2}{dt} = \frac{F \cdot (C_aO_2 - C_cO_2^{out}) + PS_cO_2 \cdot ([O_2]_t - [O_2]_c)}{V_c} \quad (4)$$

where C_aO_2 is the capillary concentration of O_2 , and $C_cO_2^{out}$ is the concentration in the venous end of the capillary. In both cases “total concentration” refers to the sum of physically dissolved

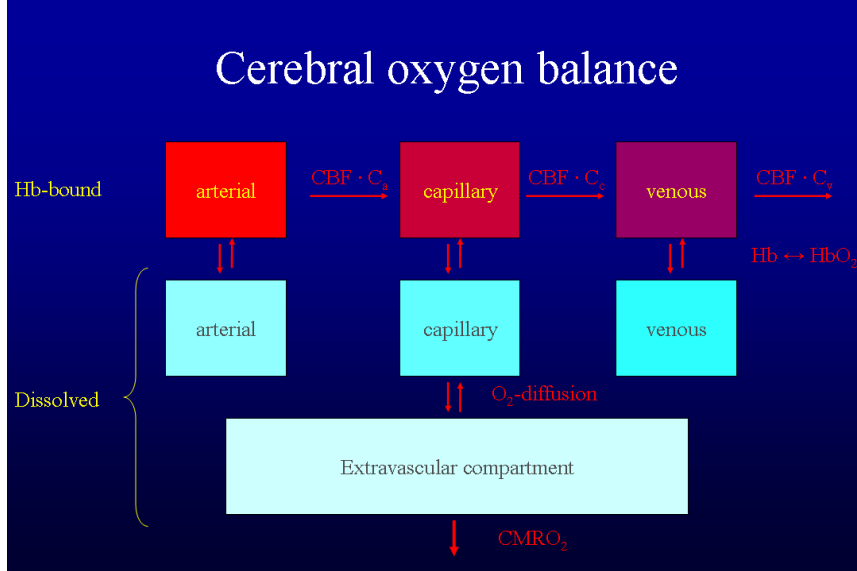


Figure 1: Basic structure of the numerical model, showing the main compartments between which oxygen is transported. The upper row shows hemoglobin bound oxygen in the intravascular compartments, with decreasing oxygen saturation along the vascular path. Arrows indicate convective transport. The middle row shows physically dissolved oxygen; the exchange with oxy-hemoglobin is assumed to be in fast equilibrium, determined by the oxygen dissociation curve (ODC). From the capillary compartment oxygen diffusion into tissue (limited by PS_cO_2), where it is eventually enters oxidative metabolism in the mitochondria.

($[O_2]_c$) and hemoglobin bound O_2 . PS_cO_2 is the permeability-surface product ($\text{ml}\cdot\text{hg}^{-1}\cdot\text{min}^{-1}$), V_c is the capillary volume ($\text{ml}\cdot\text{hg}^{-1}$), and F is the blood flow into the capillary compartment ($\text{ml}\cdot\text{hg}^{-1}\cdot\text{min}^{-1}$).

In the blood the total concentration of oxygen is related to the concentration of free O_2 as

$$C_cO_2 = [O_2]_c + C_{c,hb} \cdot Sat(P_tO_2) \quad (5)$$

where $Sat(P_tO_2)$ is the sigmoid function linking the fractional occupation of O_2 -binding sites to the oxygen tension. Several mathematical expression for the oxygen dissociation curve has been proposed, but here the one published by Winslow et al. (157) will be used, as it incorporates the influences of PCO_2 , pH as well as the concentration of 2,3-diphosphoglycerate (DPG).

The total concentration of oxygen in the compartment (C_tO_2 , assumed equal to the concentration, $[O_2]_t$, of physically dissolved O_2) can be described by

$$\frac{dC_tO_2}{dt} = \frac{PS_cO_2 \cdot ([O_2]_c - [O_2]_t) - M_{O_2}}{V_t} \quad (6)$$

where V_t is the compartment volume. The effective cerebral metabolic rate for O_2 is denoted by M_{O_2} ($\text{mmol}\cdot\text{hg}^{-1}\cdot\text{min}^{-1}$), and is influenced by the specific metabolic requirements, as well as by

the availability of O_2 . Following Valabregue et al. (151) we assume that M_{O_2} can be described by a set-point value $M_{O_2}^*$ through a Michaelis-Menten expression:

$$M_{O_2} = M_{O_2}^* \cdot \frac{[O_2]_t}{K_m + [O_2]_t} \quad (7)$$

under conditions of normal oxygen delivery M_{O_2} is very close to $M_{O_2}^*$. This is because the magnitude of the constant K_m is considered to be very small ($K_m = 0.13 \mu\text{M}$ (69)), compared to measured average tissue O_2 concentrations, $[O_2]_t$, of 10–20 μM (60; 124).

The venous concentration of O_2 is simply described by

$$\frac{dC_v O_2}{dt} = \frac{F \cdot (C_c O_2^{\text{out}} - C_v O_2)}{V_v} \quad (8)$$

During the capillary passage oxygen is progressively extracted from the blood and the saturation will drop from arterial to end-capillary levels ($C_c O_2^{\text{out}}$). Under a set of assumptions, including zero back-diffusion, this longitudinal gradient $\frac{dC_c}{dx}$ (along the capillary) can be assumed to be an exponential function with a decay constant that depends on flow and capillary permeability (19; 151). In the general case the exact form of the decay profile cannot be derived, but it may still be assumed that the longitudinal gradient can be approximated by a simple exponential function (60). This means that the average capillary concentration can be expressed as:

$$C_c O_2 = \int_0^1 C_a O_2 \cdot e^{-k \cdot x} dx \quad (9)$$

where x is the position along the capillary length, normalised to a maximum value of 1. According to this model the capillary outflow concentration is given by

$$C_c O_2^{\text{out}} = C_a O_2 \cdot e^{-k} \quad (10)$$

in which k can be determined using equation 9 since $C_c O_2$ and $C_a O_2$ are known at each iteration step.

The transport of hemoglobin into the capillary compartment is described by the equation:

$$\frac{dC_{c, hb}}{dt} = \frac{F \cdot (C_{a, hb} - C_{c, hb})}{V_c} \quad (11)$$

For the venous compartment the equation is quite similar.

In order to estimate the influence on transversal relaxation and the MR signal, the change in magnetic susceptibility of blood relative to tissue has to be calculated as a function of oxy- and deoxy-hemoglobin concentrations. Weisskoff and Kihne presented a relationship between blood susceptibility and saturation (156). The relationship between hematocrit and saturation can be expressed as $Hct \cdot Sat = C_{ohb}/mchc$, where $mchc$ is the mean erythrocyte concentration of hemoglobin, so the susceptibility shift due to hemoglobin can be calculated as

$$\Delta\chi_{i, blood} = \frac{C_{i, ohb} \cdot \Delta\chi_{ohb} + C_{i, dhb} \cdot \Delta\chi_{dhb}}{mchc} \quad (12)$$

where $\Delta\chi$ is the difference in susceptibility relative to plasma. It will be assumed that the susceptibility of fully oxygenated blood equals that of tissue, so that $\Delta\chi_{blood}$ relative to tissue can be calculated by using $\Delta\chi_{ohb} = 0$ and $\Delta\chi_{dhh} = 1.83 \cdot 10^{-6}$ (156).

In the fundamental paper by Ogawa et al. (111) the change in relaxation rate relative to tissue with fully oxygenated blood was described as

$$\Delta R_{2,i}^* = k_{lv} \cdot \nu_i \cdot v_i \quad (13)$$

for large vessels (i.e. $i = a, v$) and

$$\Delta R_{2,i}^* = k_{sv} \cdot \nu_i^2 \cdot v_i \quad (14)$$

for small vessels, i.e. $i = c$. The parameter v_i is the volume fraction of the i 'th compartment ($v_i = V_i / (100 \cdot ml \cdot hg^{-1})$), and the values of the large and small vessel constants are $k_{lv} = 4.3$, $k_{sv} = 0.04$ (111). The resonance shift for the i 'th compartment, ν_i is calculated as $\Delta\chi_{i,blood} \cdot \omega_0$, where ω_0 is the resonance frequency at the given field strength.

The total change in relaxation rate can be calculated by summation

$$\Delta R_2^* = \sum_{i=a,c,v} \Delta R_{2,i}^* \quad (15)$$

and the corresponding T_2^* -weighted MR-signal at echo time TE, relative to the fully oxygenated state, is given by:

$$S = e^{-\Delta R_2^* \cdot TE} \quad (16)$$

The general approach described above is similar to that used in previous modeling studies (13; 19; 57).

Table 1: Parameters of compartment model. The subscript x indicates the compartment, and can be a , c or v corresponding to the arterial, capillary, venous compartment. Variables referring to the tissue compartment have subscript t , but usually have different units. Note that hemoglobin concentrations are expressed in terms of O_2 binding sites. For general abbreviations please refer to the list on page 3

Symbol	Definition	Units	Type	Typical value
C_{x,O_2}	Total concentration of O_2 in compartment x	$\text{mmol}\cdot\text{ml}^{-1}$	state	$8\cdot 10^{-3}$
$C_{x,hb}$	Concentration of hemoglobin	$\text{mmol}\cdot\text{ml}^{-1}$	state	
$C_{x,dhb}$	Concentration of deoxyhemoglobin	$\text{mmol}\cdot\text{ml}^{-1}$	derived	
$C_{x,ohb}$	Concentration of oxyhemoglobin	$\text{mmol}\cdot\text{ml}^{-1}$	derived	
$C_{t,hb}$	Total tissue content of hemoglobin	$\mu\text{mol}\cdot\text{hg}^{-1}$	derived	40
C_{t,O_2}	Total tissue content of O_2	$\mu\text{mol}\cdot\text{hg}^{-1}$	derived	35-40
F_x	Blood flow out of compartment x	$\text{ml}\cdot\text{hg}^{-1}\cdot\text{min}^{-1}$	input	
K_m	Michaelis Menten constant for O_2 metabolism	$\text{mmol}\cdot\text{ml}^{-1}$	input	$0.13\cdot 10^{-6}$
Hct	Volume fraction of erythrocytes		input	0.48
M_{O_2}	Actual metabolic rate for O_2	$\mu\text{mol}\cdot\text{hg}^{-1}\cdot\text{min}^{-1}$	input	150
$M_{O_2}^*$	M_{O_2} when $P_t O_2 \gg K_m$	$\mu\text{mol}\cdot\text{hg}^{-1}\cdot\text{min}^{-1}$	input	150
$mchc$	Erythrocyte hemoglobin concentration	$\text{mmol}\cdot\text{ml}^{-1}$	constant	$16.5\cdot 10^{-3}$
$[O_2]_x$	Concentration of physically dissolved O_2	$\text{mmol}\cdot\text{ml}^{-1}$	derived	
P_{50}	O_2 tension for 50% hemoglobin saturation	kPa	derived	3.54
$P_x O_2$	Partial pressure of O_2	kPa	derived	
PS_{x,O_2}	Permeability-Surface product for O_2	$\text{ml}\cdot\text{hg}^{-1}\cdot\text{min}^{-1}$	constant	7000
R_2^*	Transversal relaxation rate	sec^{-1}	constant	16.7
T_2^*	Transversal relaxation time ($=1/R_2^*$)	ms	constant	60
$V(O_2)$	Oxygen delivery	$\mu\text{mol}\cdot\text{hg}^{-1}\cdot\text{min}^{-1}$	derived	450
V_x	Compartment volume	$\text{ml}\cdot\text{hg}^{-1}$	input	

3.2 Assumptions

There is a number of assumptions underlying the model, some of which will be commented in the following.

1. At the time scales considered here, the blood flow out of each of the arterial, capillary and venous compartments (F_a, F_c, F_v) is equal, and can be expressed by a common value F . This may not be true at shorter time scales, giving rise to transient changes in compartment volumes (20). Given the appropriate values of the time constants involved, the model should be able to accommodate dynamic oxygenation changes, but this will not be included in the present work.
2. The capillary longitudinal concentration gradient for O_2 is well-described by a mono exponential function, and capillary passage can be described with a single transit time. The possibility of effects related to capillary heterogeneity are discussed further in section 4.2.
3. The time constants for the O_2 - hemoglobin reaction are so short that the reaction can always be considered in equilibrium. Non-equilibrium states, with higher venous than capillary PO_2 have been described theoretically (139), but apparently not empirically.
4. The net diffusion of oxygen from the capillary is driven by the concentration difference $[O_2]_t - [O_2]_c$, where $[O_2]_t$ is the average tissue concentration of molecular O_2 , and $[O_2]_c$ is the capillary concentration averaged along the capillary length. In spite of the longitudinal concentration gradient, this is likely to hold for an ensemble of capillaries. Valabregue et al. (151) showed that a model including capillary sub-compartments yielded very similar results to a simpler model.
5. The average tissue oxygen concentration is a valid description of the concentration in the mitochondria. If this is not the case oxygen metabolism will be limited by oxygen delivery at higher flow values than predicted here.
6. Flow increases occurs without significant capillary recruitment, so PS_cO_2 can be considered constant during physiological flow changes.
7. The cerebrovascular system can be modeled as two non-exchanging compartments (labeled arteries and veins) and one compartment in which O_2 exchange takes place (capillaries). Anatomically it is known that some exchange may take place in arterioles (67), although some investigators argue that this is not enough to significantly change oxygen content (139).

3.3 Implementation of model

The differential equations are solved numerically using ordinary differential equation tools in Matlab (Mathworks Inc.). At each time step during the process the balance between physically and hemoglobin bound O_2 (eq. 5), using the current values of PO_2 , PCO_2 and pH. Furthermore

the longitudinal capillary O_2 gradient are recalculated according to eq. 9. The model contains five state variables, for which differential equations are given. As shown in table 1 the state variables are the concentrations of capillary, venous and tissue O_2 , as well as of capillary and venous hemoglobin. Other parameters are treated as input variables, i.e., their values are assumed to change during the course of a simulated experiment including neural activation, or unrelated changes in physiological conditions. Typical values for some of these parameters are given in table 1. Other values are $P_aCO_2 = 5.5$ kPa, arterial pH 7.41, molar ratio of DPG to oxygen binding sites 0.6 (5). These values will be used, if not otherwise stated. Some parameters are constrained by being tied together by known physiological relationships, notably that between CBF and CBV (see section 3.4). For other parameters, e.g., CBF and M_{O_2} , the dynamic relationships are less well known, as discussed later. To the extent that reliable estimates of the time constants for each input parameter are known, the model could be used to estimate rapidly varying time courses. However, since such estimates are a matter of debate, the current work will be mostly concerned with the estimation of tissue oxygenation and BOLD effects in steady state conditions. As shown in table 1 a third group of parameters are derived by expressions relating physiological constants, input and state variables.

The model is generally used for 'forward' calculation, i.e. the calculation of blood and tissue oxygenation given specific values of the input parameters and constants. However, it is also available for parameter estimation, such as the calculation of the minimal flow value required to sustain a given $V(O_2)$, in section 4.4.

3.4 Determination of constants

A quantitative understanding of the relationship between CBF and CBV is crucial due the opposed effects of these two parameters on the BOLD signal. Surprisingly, there have been very few studies of this relationship in human subjects, and most modeling studies refer to the classical work of Grubb et al. (49), who investigated it in animals, using single crystal detection of flow tracers. This work describes the relationship using a power function, apparently as a purely empirical choice. In a recent study, Rostrup et al. investigated this relationship with PET scanning in human subjects, and found no significant difference in the goodness of fit, whether a linear or non-linear function was employed (125); a similar observation was made by Lee et al. (92). In the work by Rostrup et al. it was further shown that a power function is mathematically sensible during CO_2 -induced changes, because both CBF and CBV are generally assumed to display an exponential dependency on P_aCO_2 (125). As has been argued by van Zijl et al. the power function may be expected on theoretical grounds, assuming validity of Poiseuille's law in cerebral hemodynamics (125; 152). In the present work the following expression will therefore be employed

$$rCBV = B \cdot rCBF^A \quad (17)$$

with parameters $A=0.4$, and $B=0.8$, within the experimental accuracy of the mentioned experimental work (units of B correspond to those of rCBV divided by $rCBF^A$). A similar relationship has been found between rCBV and rCBF increases during visual stimulation, suggesting that this relationship may be governed by general hemodynamic principles rather than by the nature of

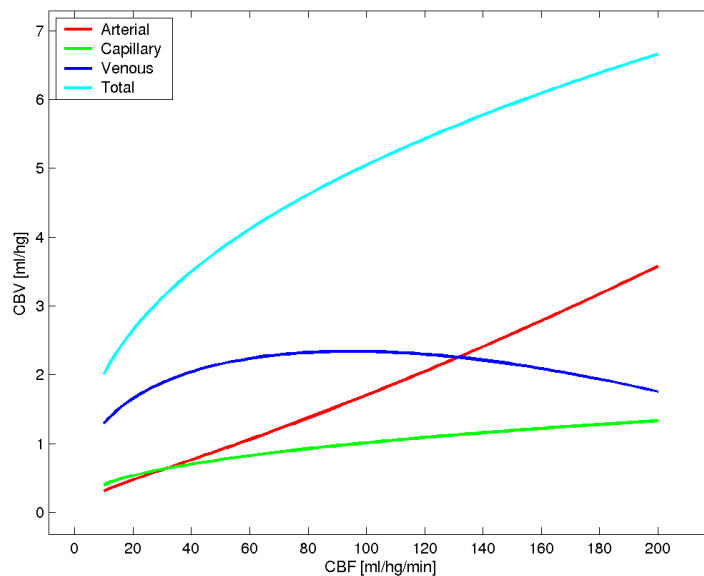


Figure 2: Compartmental and total CBV as a function of CBF, using the general equation $CBV = 0.8 \cdot CBF^{0.4}$ and the results from Lee et al. (92) regarding the dependency of arterial volume fraction on CBF.

the flow increasing stimulus (65).

Data stemming from external detection of radiotracers only provide an estimate of total CBV. Unfortunately, this is not detailed enough for comprehensive modeling, because the different vascular compartments contribute in significantly different ways to the BOLD response. An estimate, based on anatomical observation of the relative compartmental volumes is given by Sharan et al. (139) who finds 21, 34 and 45% for the arterial, capillary and venous volumes. A somewhat lower estimate of venous CBV (29%) was found by Duong et al. (32), elegantly applying an oxygenation sensitive perfluorocarbon to distinguish between arterial and venous volumes. Using the same method Lee et al. found that the majority (2/3) of the increase in CBV during increased CBF is arterial (92). Using PET scanning and compartmental modeling, Ito et al. found that only arterial blood volume contributes to the CBV increase during hypercapnia (63). In the present compartmental volumes were calculated from eq. 17, in combination with the principles of Lee et al. (92). This is illustrated in figure 2.

Normal values of gray matter CBF are assumed to vary from $50\text{-}60 \text{ ml}\cdot\text{hg}^{-1}\cdot\text{min}^{-1}$, and in accordance with eq.17, the corresponding total CBV values are $3\text{-}4 \text{ ml}\cdot\text{hg}^{-1}$. The value of M_{O_2} is assumed to lie in the range $150\text{-}250 \mu\text{mol}\cdot\text{hg}^{-1}\cdot\text{min}^{-1}$ (123).

4 Baseline BOLD signal

4.1 Effect of baseline parameters

In this section the direct effects and interactions of basic physiological variables on tissue oxygenation will be evaluated using the model approach described above. Speculations on the effects of isolated changes in e.g., CBF or CBV are somewhat hypothetical since in most clinical and experimental situations there will be a coupling between several physiological variables, which makes it difficult to observe the isolated effects. Observing the behavior of the model predictions during such changes nevertheless gives insight into the scope of the model, and its implications. In later sections the effect of composite physiological changes will be evaluated.

Tissue oxygenation is expected to depend on the balance between the consumption of oxygen and its delivery by convection as well as diffusion, and this balance is therefore influenced by the value of the capillary permeability-surface product for O₂ (PS_cO₂). Figure 3 shows model predictions regarding tissue PO₂, oxygen-metabolism and relative MRI signal when CBF is varied in isolation. The calculation is performed for logarithmically spaced values of PS_cO₂

The upper left panel shows that the oxygen-tension in tissue increases in a non-linear fashion with CBF. The oxygen-tension is much larger than the O₂ affinity of the cytochrome system for values of PS_cO₂ larger than 2–3000 ml·hg⁻¹·min⁻¹. For the higher values of PS_cO₂ there is a very steep decrease in P_tO₂ when CBF decreases below 20 ml·hg⁻¹·min⁻¹. The absolute values of P_tO₂ as well as the general sigmoid shape of the curves are in good agreement with the measurements of Duong et al., who reported values of about 4 kPa under control conditions in rats (31). A similar magnitude of P_tO₂ was found by Ances et al. (4) and values of about 3.5 kPa have been measured at the surface of small, directly post-capillary, venules (67). One study has questioned the relevance of reporting a mean tissue PO₂ by demonstrating a large regional variability in P_tO₂ with values ranging from 1.5 to 5.9 kPa (100), and in comparison the lowest or critical P_tO₂ that is compatible with normal energy metabolism has been estimated to be about 1 kPa (124).

The predicted CBF - P_tO₂ relationship is similar to that reported from *in vivo* measurements in human brain (29), in showing a critical CBF of about 20 ml·hg⁻¹·min⁻¹, below which the tissue PO₂ drops rapidly. At low P_aO₂ the predicted curve drops more rapidly than the experimental data suggest, but this could be related to cessation of oxidative metabolism during extreme ischemia.

The upper right panel shows that tissue PO₂ increases about linearly with venous PO₂. For a PS-product of about 7000 ml·hg⁻¹·min⁻¹, which is the value found by Kassissia et al. (74), the oxygen tensions are nearly equal, and only at even higher values does the PO₂ of tissue slightly exceed that of veins. This occurs in the situation where the O₂ diffusion is so fast that P_tO₂ approaches the mean capillary PO₂, which is by definition always higher than the venous. There are few direct measurements of PS_cO₂. Menzel et al (103) found that P_tO₂ was 30% lower than P_vO₂ (3.9 vs. 5.8 kPa), and given the validity of the present model this would point to a PS_cO₂ in the range of 4000–6000 ml·hg⁻¹·min⁻¹.

The kinetics of O₂-transport in the brain have been investigated by the multiple indicator technique in a number of studies. Both Grieb et al. (47) and Kassissia et al. (74) used ⁵¹Cr-labeled

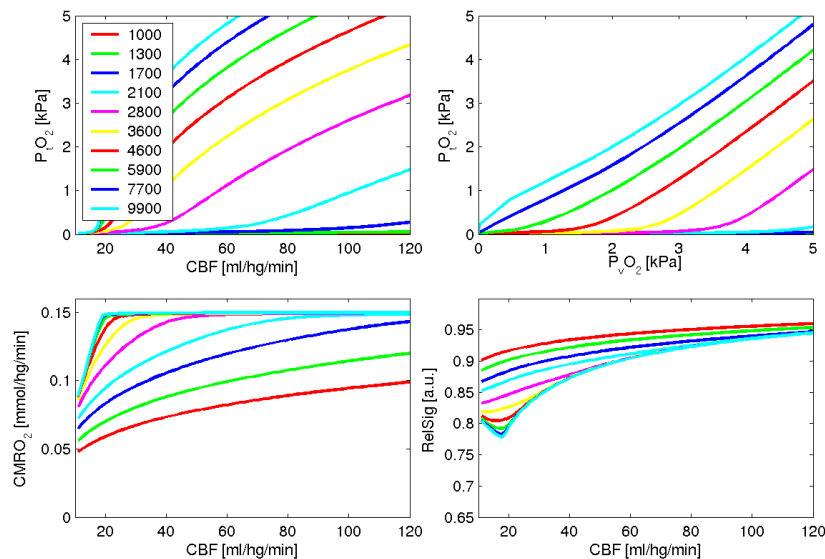


Figure 3: Oxygenation as a function of flow and PS_cO_2 . Simulations are made for $P_aO_2 = 16$ kPa, $Hb = 8$ mM, $M_{O_2}^* = 0.15$ mmol·hg⁻¹min⁻¹. Upper panels show tissue oxygenation as a function of CBF and venous oxygenation, respectively. Lower left panel shows M_{O_2} as a function of CBF; a non-linear relation is seen for low PS_cO_2 values, for high values the M_{O_2} is independent of CBF as long as oxygen delivery exceeds $M_{O_2}^*$. The lower right panel shows the relative MR signal as a function of CBF: note that highest signal is obtained for lowest PS_cO_2 products, where the extraction of O_2 is limited.

erythrocytes and $^{18}O_2$ to study oxygen exchange, and both studies find that the outflow curve of O_2 is quite similar to that of the intra-vascular tracer. However, slightly different results and conclusions are reached, in that the former study finds that the transit time for $^{18}O_2$ is significantly longer than that for erythrocytes, and that the fractional outflow tapers out more slowly than for the intra-vascular tracer; this allows for the calculation of extra-vascular distribution volume, and a mean tissue PO_2 . Grieb et al. reported a linear relation between P_tO_2 and P_vO_2 , under slightly hyperoxic conditions that resulted in P_tO_2 values of about 2–7 kPa. In the study of Kassissia no significant difference in transit time is found and it is concluded that in spite of a very high endothelial oxygen permeability, tissue O_2 levels are probably so low that back-diffusion does not take place to any significant degree. It is unclear what the cause of this discrepancy may be, but it could be partly related to the high arterial O_2 tensions used in Grieb’s study.

In another study (137) O_2 kinetics were investigated by the use of $^{15}O_2$ labeled hemoglobin, which was compared to $H_2^{15}O$. If O_2 , as it enters the tissue compartment, is instantaneously converted into metabolic water, then it is expected that the outflow curves from the two tracers are identical. The outflow curves however, were found to be significantly steeper following

injection of $^{15}\text{O}_2$ and the difference was attributed to non-metabolized oxygen. While this result points to a $P_t\text{O}_2$ significantly above zero, it only pertains to a tissue average, rather than the PO_2 at the exact location of oxygen metabolism.

The lower left panel of figure 3 shows the relationship between CBF and M_{O_2} as predicted by the model. It is seen that M_{O_2} is independent of CBF when flow and permeability are sufficiently high (e.g., $\text{PS}_c\text{O}_2 > 3000$, $\text{CBF} > 50 \text{ ml}\cdot\text{hg}^{-1}\cdot\text{min}^{-1}$), but drops quickly when CBF is decreased below a critical value of $15\text{--}20 \text{ ml}\cdot\text{hg}^{-1}\cdot\text{min}^{-1}$. For lower values of PS_cO_2 there is a non-linear relation between flow and O_2 -metabolism, which becomes flow limited at the normal level of CBF. When choosing a higher value of $M_{\text{O}_2}^*$, $250 \mu\text{mol}\cdot\text{hg}^{-1}\cdot\text{min}^{-1}$ metabolism becomes flow limited in the normal range already for $\text{PS}_c\text{O}_2 < 5000 \text{ ml}\cdot\text{hg}^{-1}\cdot\text{min}^{-1}$ (data not shown).

This relation has been studied theoretically by several authors, and a similar figure is present in e.g., the work of Valabregue et al. (151). In that work however, a constant $P_t\text{O}_2$ is assumed and this forces CBF and M_{O_2} to be non-linearly related. The consequences of assuming a constant $P_t\text{O}_2$ close to zero have been explored extensively by the group of Gjedde et al. (44; 45; 149), who accordingly finds a non-linear relationship where M_{O_2} is predicted to vary continuously in the range from $140\text{--}200 \mu\text{mol}\cdot\text{hg}^{-1}\cdot\text{min}^{-1}$ as CBF varies from e.g., $40\text{--}100 \text{ ml}\cdot\text{hg}^{-1}\cdot\text{min}^{-1}$ (149). In those studies an oxygen diffusibility is calculated which corresponds (when corrected for O_2 -solubility) to a PS_cO_2 of about $3000 \text{ ml}\cdot\text{hg}^{-1}\cdot\text{min}^{-1}$. According to the present calculations this value should cause independence of CBF and M_{O_2} at normal CBF and an M_{O_2} value of $150 \mu\text{mol}\cdot\text{hg}^{-1}\cdot\text{min}^{-1}$; when M_{O_2} is assumed to be higher ($250 \mu\text{mol}\cdot\text{hg}^{-1}\cdot\text{min}^{-1}$) flow and metabolism are non-linearly coupled over the full range of physiological CBF variation.

There are however few or no experimental results that demonstrate a direct relation between M_{O_2} and CBF. In the classical work of Kety and Schmidt (83) both parameters were measured under hyper- and hypocapnia that changed CBF and oxygen delivery, but under these conditions there were no significant changes in M_{O_2} , and no detectable correlation between the parameters (see figure 4).

In that study as well as in a study of Shimojyo et al. (141) the cerebral metabolism was also investigated during altered inspiratory oxygen tension. No changes in M_{O_2} were seen in any of the studies, and this can be confirmed by calculating and plotting oxygen delivery from the data (see figure 5). This shows no intra-subject correlation between M_{O_2} and CBF or oxygen-delivery. It is an interesting additional observation that there is a much stronger general (i.e. inter-subject) correlation between oxygen-delivery and M_{O_2} than between CBF and M_{O_2} . This correlation, however, is more likely to reflect structural differences, such as variations in neuronal density, than a dynamic relationship between oxygen supply and use. It is well known that M_{O_2} and CBF are rather closely correlated when comparing regions in the brain (123), but this again does not necessarily imply that a dynamic coupling is also present.

By demonstrating that the flow response to activation is unchanged during hypoxia, Mintun et al. (104) argued that cerebral metabolism cannot be limited by oxygen delivery across the blood brain barrier, since in that case a larger flow response would have been expected to support the metabolic demand in the hypoxic than in the normoxic condition. This expectation is based on the assumption that oxygen delivery, and consequently also capillary and tissue PO_2 are significantly decreased in the hypoxic baseline condition (44), and this may not always be the case due to the compensatory increase in blood flow seen in hypoxia. However, even though

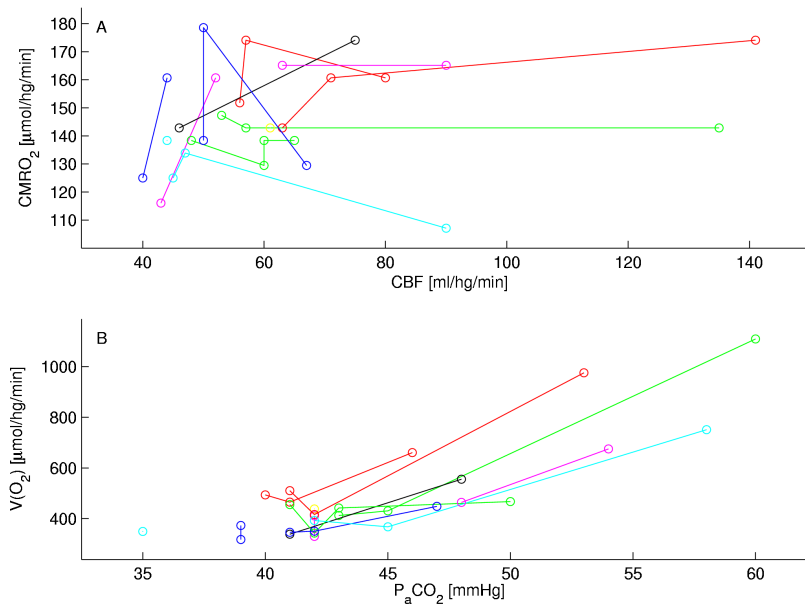


Figure 4: Cerebral metabolism, flow and oxygen delivery during hypercapnia, data replotted from Kety and Schmidt (83). Upper panel illustrates that no significant correlation between M_{O_2} and CBF is present during hypercapnia, in spite of pronounced increase in flow and oxygen delivery (lower panel) when $P_a\text{CO}_2$ increases. Points from same volunteer connected with lines

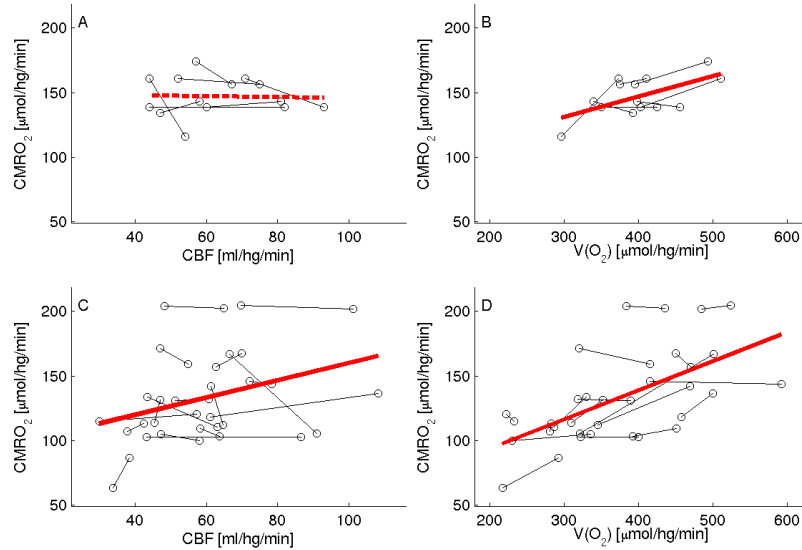


Figure 5: Cerebral metabolism, CBF and oxygen delivery, during altered oxygen inhalation. Upper row shows data replotted from Kety and Schmidt (83), all measurements under control, hypo- or hyperoxic conditions. Lower row shows data from Shimojyo et al. (141), control and hypoxic conditions. Points from same volunteer connected with lines, and whole-brain data from (141) were adjusted using, arbitrarily, a brain weight of 1200g. Inter-subject regression lines are shown in red. In both datasets there is significant inter-subject correlation between M_{O_2} and O_2 delivery ($p < 0.01$), but a significant correlation between M_{O_2} and CBF ($p = 0.047$) is only present in the data from Shimojyo et al. There is a trend towards a significant intra-subject correlation in the lower right panel, ($p = 0.050$)

oxygen delivery may be almost unchanged in moderate hypoxia, it is remarkable that a flow response of not just similar, but actually significantly lower magnitude was found during hypoxia, and this may speak against a strong coupling of CBF and M_{O_2} .

In other theoretical work (60; 104), the oxygen transport is modeled using a cylindrical tissue model with a central capillary. This results in P_tO_2 values ranging from about 0.7–3.3 kPa (as in figure 3), and no strict coupling between M_{O_2} and CBF. The basic difference between these results and those of other groups seems to be the assumption of a much higher oxygen diffusibility, and a variable tissue oxygen tension. The lower right panel of figure 3 shows the relative MR signal predicted from the compartment model and eq. 15. In the modeling CBV is assumed to increase with CBF as described by eq. 17. As expected the signal generally increases with CBF, due to increased oxygenation, and in spite of increased blood volume; the slope of the curves represent the magnitude of the predicted $BOLD_B$ signal. Higher values of PS_cO_2 leads to lower signal, due to the higher extraction, and consequently lower blood oxygenation. However, when CBF (and oxygen delivery) is high enough to maintain oxygen metabolism at its maximum rate, $M_{O_2}^*$, the signal is independent of PS_cO_2 . In this situation the predicted $BOLD_B$ signal change is -7% and +5% when CBF changes from a reference value of 60 to 30 or 120 $ml \cdot hg^{-1} \cdot min^{-1}$, respectively. For high permeabilities the signal is predicted to increase slightly as flow decreases below 20 $ml \cdot hg^{-1} \cdot min^{-1}$. This is due to the associated decrease in blood volume. *In vivo*, however, the power law relation between CBF and CBV probably will not hold under severely ischemic conditions.

Hoge et al. (57) estimates the fractional baseline signal to about 0.8, thus somewhat smaller than here, whereas other studies have estimated the maximal obtainable BOLD signal to be 8–9%, i.e. a baseline signal of about 0.92 (28; 77). Discrepancies may be due to the dependency on CBV and M_{O_2} , which may have differed between their measurements, as well as in comparison to the present model assumptions.

The cerebral blood volume has an important influence on the BOLD signal. In a previous work of the present author a correlation was found empirically between the magnitude of hypercapnic $BOLD_B$ response and baseline CBV (127). The importance of CBV, and other vascular factors such as vessel orientation has also been emphasised in other studies, and hypercapnic normalisation of the BOLD signal has been used to counteract the influence of local blood volume variation (7). In this technique hypercapnia is used to produce a $BOLD_B$ signal of which the spatial variation is thought to be due mainly to CBV, and this can be used to remove the blood volume weighting in $BOLD_A$ maps from activation studies (see also section 6.1).

Another parameter, the oxygen extraction fraction (OEF, eq. 2) is clearly also of major importance, since oxygen extraction is what produces the endogenous contrast agent underlying the BOLD response. As will be discussed below the OEF has been suggested to be closely linked to the concept of activated versus non-activated or default states of the brain. Raichle et al. proposed that a value of 0.4 is maintained generally in the non-activated state, and that it is the deviations from this value during activation or deactivation, that makes the BOLD response possible (119). To what extent activation may occur without changes in OEF is probably not quite clear at present, but it should be noted that there are examples of the opposite. During hypoxia, for instance, a negative $BOLD_B$ response is seen, although there is no change in OEF; both arterial and venous O_2 -content are reduced by the same fraction (e.g., 60% in (83)).

4.2 Capillary heterogeneity

At the capillary level the perfusion of the brain is heterogeneous in the sense that some capillaries have higher flow velocities than others. Flow increases are thought to occur due to an increase in mean velocity rather than by recruitment of previously unperfused capillaries at constant velocity. Additionally, there is a large variability in hematocrit between capillaries, and increases in oxygen delivery may therefore also occur by functional recruitment, i.e. through homogenisation of the hematocrit. The relative importance of these mechanisms is not known quantitatively, and may vary between regions.

Possible effects of heterogeneity can be explored using model calculation, and assuming that the brain can be modeled hemodynamically as an ensemble of tissue units each containing a single vessel with a characteristic flow value.

Figure 6 shows the results of a simulation where CBF is assumed to follow a gamma-variate distribution with a mean of $50 \text{ ml}\cdot\text{hg}^{-1}\cdot\text{min}^{-1}$ (upper row), which increases to $70 \text{ ml}\cdot\text{hg}^{-1}\cdot\text{min}^{-1}$ (lower row) due to a shift in the velocities, so that fewer capillaries with slow flow are present (compare 6, A and D). This results in a more narrow distribution of transit times and a lower mean transit time (1; 115). The content of deoxy-hemoglobin in the tissue units (fig. 6, B and E) turns out to show a very similar distribution, as is also expected from eq. 1, predicting proportionality between tissue oxygen content, and (venous) mean transit time ($MTT = \frac{CBV}{CBF}$).

The resulting distribution of tissue signals is shown in fig. 6, C and F, using a normalised signal, where a value of 1 refers to the expected signal with all deoxy-hemoglobin removed. The distribution is skew, and has a mean value that is slightly lower than if the same mean CBF had been obtained by vessels with identical flow velocity. The discrepancy between the mean values is reduced at high flow due to the decrease in heterogeneity. This suggests that heterogeneity may influence the baseline signal as well as the BOLD response to flow changes.

The effect on the BOLD response will be even stronger if heterogeneity is so pronounced that some vessels approach full deoxygenation in the baseline state, but are oxygenated during activation with flow increase. It should be noted that similar effects are not seen with a model where heterogeneity is assumed to affect hematocrit rather than flow in each tissue unit.

Buxton and Frank (19) considered different distributions of transit times, and found a negligible effect when the mean extraction fraction was expressed as a weighted sum of extraction fractions corresponding to different transit times. In this approach the mean transit time was held constant between different shapes of the transit time distribution function, and this minimises the effect because the OEF (and consequently deoxy-hemoglobin and baseline signal) are so closely related to the mean transit time. In the present approach the mean values for a non-heterogeneous (single transit time) and a heterogeneous distribution with same mean CBF are compared (red and green lines in fig. 6).

However, the model of Buxton and Frank, as well as the present model, only captures one aspect of capillary heterogeneity, namely the variation in mean extraction fraction. A possible effect on the relation between tissue deoxy-hemoglobin and MR signal has not been included. To fully describe such an effect of heterogeneity, where some capillaries have high and others relatively low oxygen saturation, a spatially resolved model is required, and such investigations seem not to have been performed so far.

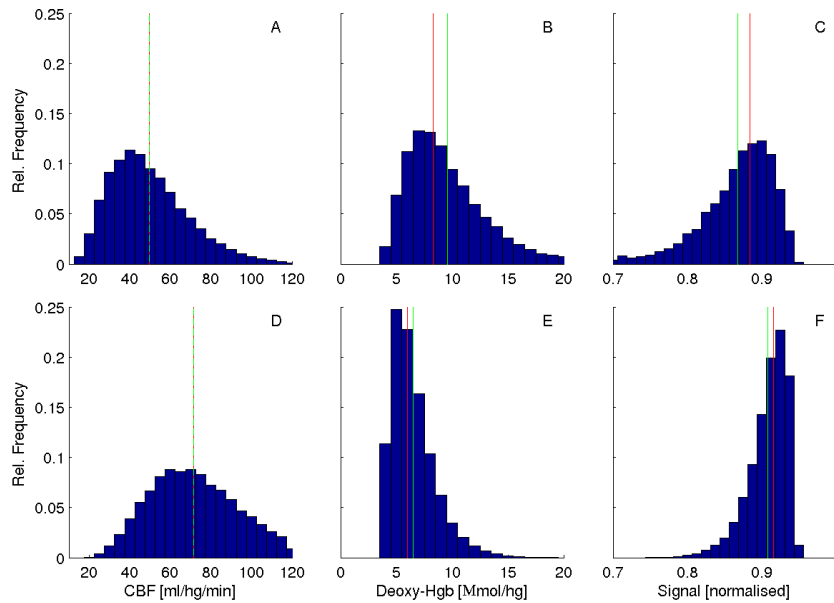


Figure 6: Predicted effect of capillary heterogeneity on the distribution of flow values (A and D), tissue deoxy-hemoglobin content (B and E) and normalised baseline signal (C and F). The upper row shows the distributions for a mean flow of 50, the lower for a mean flow of 70 $\text{ml}\cdot\text{hg}^{-1}\cdot\text{min}^{-1}$. The green lines show the location of the mean for each distribution, while the red lines show the values corresponding to a non-heterogeneous distribution with same mean CBF. Heterogeneity causes a slightly lower mean baseline signal, due to the skewness of the distributions. This is less pronounced at high flow, where transit times, deoxy-hemoglobin and signal values are more homogeneous.

4.3 Arterial CO₂ tension

Of any substance with a pronounced influence on the cerebral circulation, carbon dioxide is probably the best and most often described. That CBF increases during hypercapnia has been known for a long time, but was first quantified using modern methods by Kety and Schmidt (83). The vasodilatory effect of CO₂ is thought to be mediated through its influence on pH predominantly in the space surrounding arterioles (34; 138). The response is known to be inhibited by the cyclooxygenase inhibitor indomethacin (75), but the details of its mechanism of action have not been fully elucidated. Furthermore, inhibition of nitric oxide (NO) synthase also seems to diminish the response leading to the hypothesis that NO is an important mediator, but this has been questioned (62). From a clinical point of view carbon dioxide is interesting due to the often debated use of hyperventilation in the treatment of intra-cranial hypertension (122), as well as to its assumed role in conditions such as acute mountain sickness (51).

It is generally recognised that the relation between CBF and P_aCO₂ can be described as an exponential function, with modest CBF changes during hypocapnia, and pronounced changes during hypercapnia (83). One of the first studies to employ the exponential function to model this was that of Olesen et al. (114) but several authors have found a similar relationship (84; 146). Olesen et al. found global CBF to increase by a factor of $e^{0.041}$, or about 4%, pr. mmHg increase in P_aCO₂ (corresponding to about 34% pr. kPa). It is known from animal studies that the slope of the curve decreases at extreme P_aCO₂ values (e.g., below than 2 or above 8 kPa), so that its true shape may be sigmoid rather than exponential (34); human data, however, do not allow for such a distinction (125).

Probably because global CO₂-reactivity was considered well-studied with the classical whole-brain methods, only a few studies have tried to confirm the findings with newer imaging methods, and it has been unclear to what degree e.g., white matter regions responded to hypercapnia. The regional variation in CBF response to hypercapnia was investigated by Rostrup et al. using PET scanning in normal volunteers. In this study the response was found to be homogeneous in grey matter structures but much lower in white than in grey matter (130). Using a linear model the reactivity was found to be 19–24 and 7 ml·hg⁻¹min⁻¹kPa⁻¹ in grey and white matter, respectively. In the same study BOLD imaging was used to study the temporal course of the CO₂ response, which was found to increase to half its maximal response in about 30 seconds in grey matter, whereas the response in white matter was 2–3 times slower. This difference may be due to a slower build-up of pH changes in white matter due to the lower blood supply.

While difference in BOLD_B magnitude between grey and white matter is obviously the most conspicuous, other regional differences have also been reported. Resulting from a PET study Ito et al. reports significantly higher reactivity in the pons, cerebellum and deep grey matter structures than in cortex (66). In BOLD studies high reactivity is found in temporal and occipital cortical areas, whereas in deeper brain structures, the response is found to be high in the thalamus, but low in the basal ganglia (76; 127; 130). Some of these regional differences may well be due to differences in partial volume effects, such as inclusion of larger vascular structures (e.g., in the insular area), and may thus be less specific for a given grey matter area. However, since large flow changes and low BOLD is found in the putamen, this seems to reflect a more specific mechanism, resulting in a region-specific decrease in CBF-BOLD coupling.

In a recent PET study both hypo- and hypercapnia were investigated and a significantly lower response to P_aCO₂ changes was found during hypo- than during hypercapnia, consistent with the expectation that the full range can be modeled by an exponential function (Rostrup et al. (125)). The exponential reactivity constants for CBF were quite similar for all regions, ranging from 0.22 for white to 0.28 kPa⁻¹ for grey matter (corresponding to about 25–32% change pr. kPa P_aCO₂). Similar reactivities were obtained in a different study (64), although quantitative comparison is complicated by the reactivities being reported in % pr. mmHg, even though they are based on fitting a linear relation. Furthermore, results are only reported for grey matter.

The reactivity of the cerebral blood volume to CO₂ has been studied less frequently than that of blood flow. There are several studies using non-spatially resolved methods, but only a few imaging studies that would allow for investigation of regional differences. As with CBF there is some disagreement about whether the relation should be modeled in a linear or non-linear way. Grubb et al. model both parameters as linear functions of P_aCO₂, and finds a slope of 0.31 ml·hg⁻¹·kPa⁻¹ for global CBV (49). However, replotting the data from each individual shows that the relation is not clearly linear, and an exponential function is actually marginally better (125). Using an early SPECT system, Greenberg et al. was able to measure CBV in grey and white matter separately during hyper- and hypocapnia, and reported linear reactivities slightly higher than those of Grubb et al. From the graphical representation these results are very suggestive of a 2–3 fold higher reactivity during hypercapnia (46). This would be consistent with the 31% CBV increase during hypercapnia (P_aCO₂ increase of 1.2 kPa) as measured with PET scanning in normal subjects (127). Rostrup et al. found significantly higher hyper- than hypocapnic reactivity for CBV, and estimated exponential reactivities of 0.13–0.16 kPa⁻¹ (125). Interestingly, when reactivities are expressed in this way, there seemed to be no significant difference in the values for grey and white matter (for an illustration of the spatial distribution of reactivities for both CBF and CBV see figure 7).

It has been known from the earliest studies that hypercapnia - due to the pronounced flow increases, unaccompanied by any changes in metabolism - results in a reduction in the cerebral oxygen extraction fraction, which decreased from 36% to 23% in the the Kety and Schmidt study (83). Similarly, an increase to 58% was observed during hyperventilation. Because this leads to changes in venous oxygenation, these findings form the basis for the use of CO₂ in BOLD studies. Soon after the introduction of the concept of BOLD signal changes, the technique was applied to human volunteers during hypercapnia by Rostrup et al. (128). This study, which was performed at 1.5 T using a FLASH sequence, showed an apparently linear relation between BOLD_B and global CBF, with signal increases for deep grey matter of 3.2% and 4.8% during inhalation of 5 and 7% CO₂, respectively. Higher signal changes (up to 9%) were found in cortical regions, probably due to a higher blood volume, and possibly also to inflow-phenomena when using this multi-shot sequence. In a later study a single-shot EPI sequence was used, giving lower BOLD_B signal changes of about 2 and 3.5% during 5 and 7% CO₂ (130).

Similar results have been found by others, with BOLD_B increases ranging from the equivalent of 1.8% to 2.8% during inhalation of 5% CO₂ (23; 78). A signal decrease has been demonstrated in hyperventilation, corresponding to the decrease in P_aCO₂ and CBF, and resulting decrease in blood oxygenation. In the hypocapnic range Posse et al. described a linear relation between signal change and P_aCO₂, with much smaller signal decreases in white than in grey matter (117).

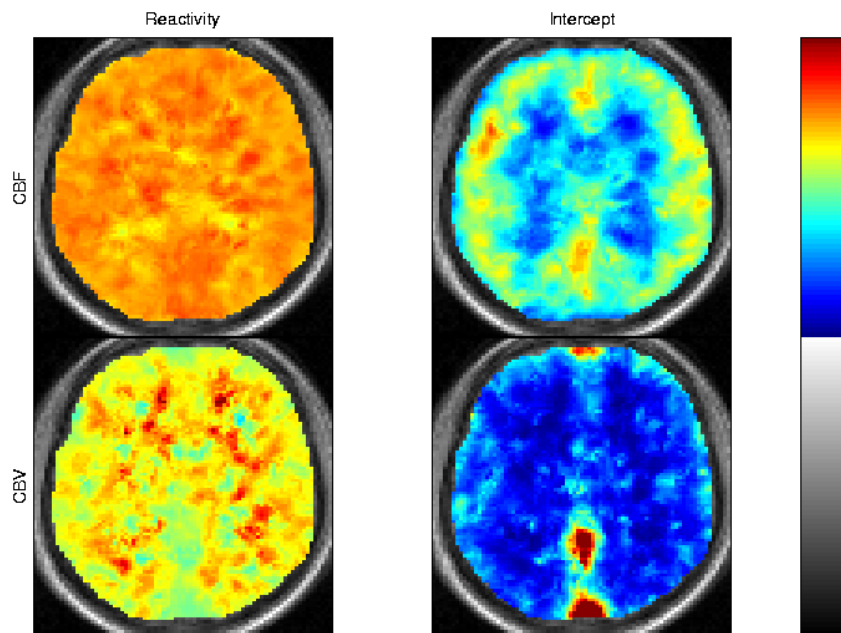


Figure 7: Voxelwise estimation of the parameters of an exponential CO₂ reactivity model according to eq. 18. The two upper images are for CBF and the two lower for CBV. The images show the median value of the parameters estimated for each subject. The left column shows the distribution of the reactivity (R in eq. 18), while the right shows the intercept (I in eq. 18). Color-coding is from -0.5 to 0.5 kPa⁻¹ for rCBF and rCBV reactivity, from 0 to 30 ml·hg⁻¹·min⁻¹ for rCBF intercept and from 0 to 10 ml·hg⁻¹ for rCBV intercept. From ref. (125)

In a later study the full range of P_aCO₂ values from 2.7–9.3 kPa was investigated, and it was found that T₂^{*} and BOLD_B were non-linearly dependent on P_aCO₂ with values ranging from 62 to 72 ms (116).

By contrast, in the study of Cohen et al. (23), which also investigated both hypo- and hypercapnia, a linear relation between BOLD_B response and P_aCO₂ was reported, with response magnitudes ranging from -3 to 6% in the P_aCO₂ range 3–7 kPa. While it cannot be ruled out that this discrepancy could be due to experimental differences (T₂^{*}-measurement at 1.5 T (116) vs. T₂^{*}-weighted EPI at 7 T (23)), the most obvious difference is the range of P_aCO₂. The study by Posse et al. is unique in using inspiratory fractions higher than 7%, and P_aCO₂-values significantly exceeding 7 kPa. This may have increased the detectability of a non-linear relationship.

As mentioned above the primary cerebrovascular effect of CO₂ is a flow increase caused by arterial and arteriolar dilation, with an accompanying effect on blood volume. This will influence blood oxygenation and the BOLD response, but the response is further complicated by the associated changes in blood gases. Hypercapnia causes an increase in P_aCO₂, and as a consequence a decrease in blood pH, and both of these effects influence hemoglobin properties, by decreasing the O₂-affinity and right-shifting the ODC. During hypocapnia a respiratory alkalosis (and lowered P_aCO₂) will occur, with the opposite effect on the ODC. Contrary to what is often assumed, P_aO₂ may furthermore increase during both hyper- and hypocapnia. This is because both situations, in spontaneously breathing subjects, are associated with an considerable increase in respiratory minute volume. These factors need to be considered when modeling the influence of altered P_aCO₂ on blood oxygenation.

In the present study the following relation between CBF and P_aCO₂ will be used

$$CBF = I \cdot e^{R \cdot P_a CO_2} \quad (18)$$

with I=15 ml·hg⁻¹·min⁻¹ and R=0.25 kPa⁻¹, corresponding to values measured for central grey matter (125). The relationship between CBF and CBV will be assumed to follow 17. The relationship between P_aCO₂ and pH and P_aO₂ is determined by interpolation from values compiled from the studies of Rostrup et al. and Ito et al. (64; 125; 128). These reports show a P_aO₂ increase of 4–6 kPa in both voluntary hyperventilation and moderate hypercapnia; a linear function is used in the hypocapnic range, combined with a quadratic function in the hypercapnic range. Based on these studies a linear function is also used to express the dependency of pH on P_aCO₂. Using these parameters, and an M_{O₂}^{*} of 250 μmol·hg⁻¹·min⁻¹ reveals a relation between the baseline signal and P_aCO₂ in good agreement with experimental data (23). This is shown in figure 8A, where the BOLD_B signal has been calculated by normalisation with the signal during normocapnia (P_aCO₂ = 5.5 kPa, CBF = 59 ml·hg⁻¹·min⁻¹). The green curve shows the signal changes predicted when only the hemodynamic effects (CBF and CBV) of altered P_aCO₂ are included in the model. The downward convex shape of the curve in the hypercapnic range is due to oxygen delivery being decreased to a level where tissue oxygenation (P_tO₂) approaches zero, and where venous saturation cannot be decreased substantially by further lowering of the flow. This non-linearity therefore disappears when the curve is plotted for a lower value of M_{O₂}^{*}.

From figure 8A it is seen that including pH and P_aCO₂ changes in the modeling results in a slight shift of the BOLD_B curve toward less signal change (blue vs. green curve), which is

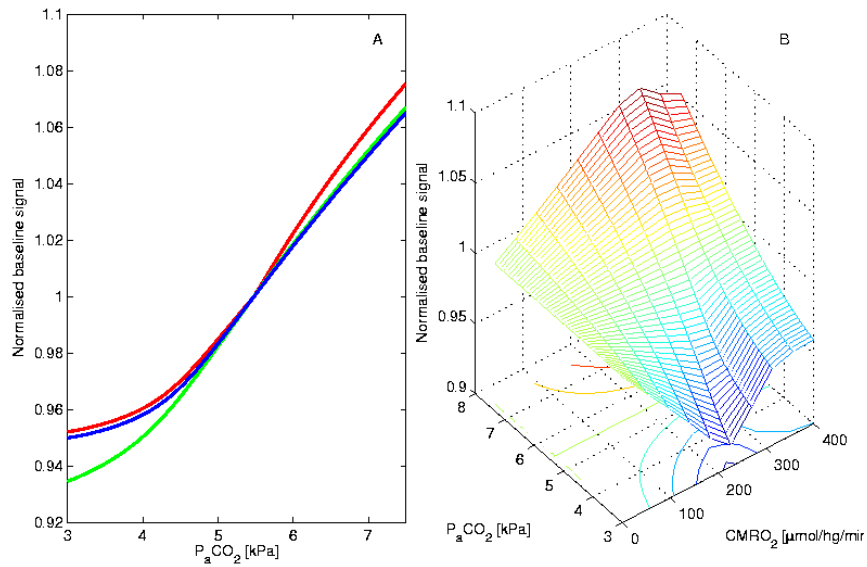


Figure 8: Normalised baseline signal (BOLD_B) vs. $P_a\text{CO}_2$. The signal is normalised to a reference state at $P_a\text{CO}_2 = 5.5$ kPa, $\text{CBF} = 59$ $\text{ml}\cdot\text{hg}^{-1}\cdot\text{min}^{-1}$. Panel A shows the response for an $M_{\text{O}_2}^*$ of 250 $\mu\text{mol}\cdot\text{hg}^{-1}\cdot\text{min}^{-1}$ with all factors taken into account (hemodynamic, $P_a\text{O}_2$, pH and $P_a\text{CO}_2$: red curve), with only hemodynamic (green), or with hemodynamic as well as pH and $P_a\text{CO}_2$ included (blue). Panel B shows the predicted relationship between BOLD_B and $P_a\text{CO}_2$ at various values of $M_{\text{O}_2}^*$ (all factors included).

most pronounced during hypocapnia. The blue curve should represent the result obtained from an experiment where P_aO_2 is fixed.

The relative small changes may be surprising given the well known Bohr effect, whereby pH decrease causes a right shift in the ODC. When oxygen supply is ample, as in hypercapnia, and P_tO_2 is high, changes in pH probably have little effect on hemoglobin saturation due to the limited distribution space for O₂. Instead PO_2 is expected to change. Conversely, when tissue oxygen tension is close to zero, as in hypocapnia, changes in pH will be able to exert an effect on hemoglobin saturation, as excess O₂ can escape from the capillaries. The respiratory alkalosis of hypocapnia therefore causes oxygen saturation to be higher than it would have been at a fixed pH.

The effect of relative hyperoxia is more pronounced than the pH effect in the hypercapnic range, and causes an increased signal at both high and low P_aCO_2 values (compare red and blue curves in fig. 8A). At $P_aCO_2 = 7$ kPa, the signal is increased by 14% relative to the level at a constant P_aO_2 ($M_{O_2}^* = 250 \mu\text{mol}\cdot\text{hg}^{-1}\text{min}^{-1}$). This effect was found to increase at lower $M_{O_2}^*$ values, reaching about 30% for $M_{O_2}^* = 150 \mu\text{mol}\cdot\text{hg}^{-1}\text{min}^{-1}$.

The conclusion that pH and P_aO_2 changes may significantly contribute to $BOLD_B$ responses was also made in a previous study by the present author, using an earlier version of the model (131). In that study it was also suggested that part of the reason why the $BOLD_B$ response to hypercapnia is so high, may be that a significant fraction the measured CBV increases take place in the arterial compartment, which do not contribute much to the BOLD signal under these circumstances.

Figure 8B shows that the $BOLD_B$ response is strongest for $M_{O_2}^*$ -values in the range of 100–200 $\mu\text{mol}\cdot\text{hg}^{-1}\text{min}^{-1}$. At very low oxygen consumption rates the oxygen extraction fraction remains low, and venous and the venous saturation changes relatively little as a function of CBF. At high oxygen consumption rates, on the other hand, M_{O_2} decreases progressively with flow in hypocapnia, and this limits any further deoxygenation of the blood, and keeps the BOLD signal more constant than it would have been otherwise.

Across the full range of P_aCO_2 values oxygen delivery was found to increase from 260 to 790 $\mu\text{mol}\cdot\text{hg}^{-1}\text{min}^{-1}$. For an M_{O_2} of 150 $\mu\text{mol}\cdot\text{hg}^{-1}\text{min}^{-1}$ the corresponding values of P_tO_2 were found to be 2.3 to 7.4 kPa, whereas for a higher M_{O_2} of 250 $\mu\text{mol}\cdot\text{hg}^{-1}\text{min}^{-1}$ P_tO_2 decreased to 0.15 kPa during hypocapnia, and increased to 3.25 during hypercapnia. It is the last set of values that best fit the results of Schneider et al. who reported a change in P_tO_2 during hyperventilation from 3.28 to 2.92 kPa (133). Given large experimental variability of P_tO_2 and the dependency on M_{O_2} which may also vary, these results do not appear to be incompatible.

The general relation between P_aCO_2 and cerebral hemoglobin oxygenation has been verified by Rostrup et al. by direct measurements of oxy- and deoxy-hemoglobin using near infrared spectroscopy, NIRS (131). This technique allows both oxy- and deoxy-hemoglobin levels to be measured, by detecting the transmission of near infrared light through the tissue. The light is emitted and detected by optodes placed near each other on the surface of the head, see figure 9. With knowledge of the hematocrit, the CBV in the region below the optodes can be estimated. In this study a change in total tissue deoxy-hemoglobin of $-0.13 \mu\text{mol}\cdot\text{hg}^{-1}$ was found during hypercapnia, but since the NIRS method is severely affected by partial volume effects and the true value is probably much higher. The present simulation leads to normocapnic values for total

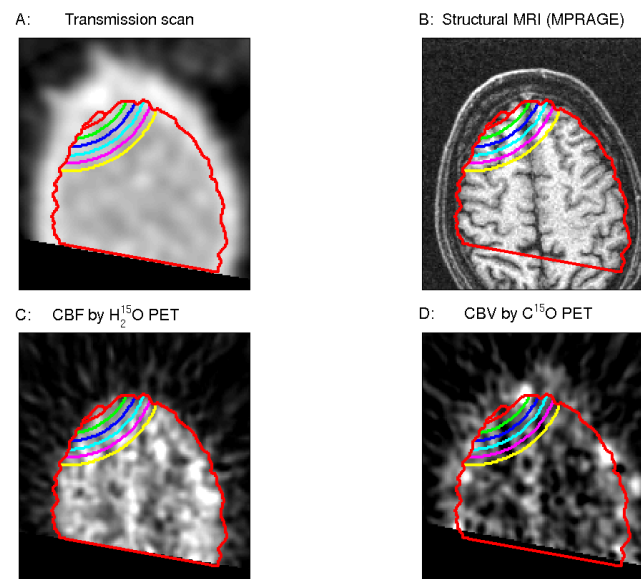


Figure 9: A PET and NIRS study of cerebral oxygenation (131). Optodes were placed on the head during PET measurements of CBF and CBV. The optodes are visible in the upper left part of the transmission scan in panel A. The red line marks the outline of the brain, and the concentric lines indicate the regions indicate the intracerebral field of view of the optodes. Panel B. shows the corresponding structural MR scan to which the PET images have been resliced. Panel C and D. shows the CBF and CBV images from the same slice position.

tissue deoxy-hemoglobin of $6.8 \mu\text{mol}\cdot\text{hg}^{-1}$ with changes $-2.6 \mu\text{mol}\cdot\text{hg}^{-1}$ during hypercapnia (at $M_{\text{O}_2}^* = 150 \mu\text{mol}\cdot\text{hg}^{-1}\text{min}^{-1}$).

In the above discussion the effect of CO₂ has been considered a direct vascular effect, rather than an effect caused by neuronal activation. Some studies, however, have raised the question of whether hypercapnia might cause widespread perfusion changes through neural effects due to increased arousal, as well as sensory and emotional changes associated with breathing CO₂. This has been investigated in a number of PET studies, e.g., (14), and a complex pattern of activations was revealed, including mesencephalic, limbic and cerebellar structures. The generalisability of these studies is uncertain because they employed very high CO₂ concentrations (8%), and they may furthermore be influenced by the problem of detecting regional activations on a background of pronounced global CBF changes. It is therefore interesting to compare with the work of another group, that focused more specifically on the sensation of air hunger and used BOLD imaging (38). Air hunger was induced by varying the tidal volume in mechanically ventilated subjects, while keeping P_{ET}CO₂ constant; activations were seen in the insular area, the anterior cingulate as well as in midline cerebellum. In summary these findings indicate that regional variation may be partly due to specific neural activation patterns, at least during very high P_{ET}CO₂, and when air hunger is experienced. The implications of this at moderate hypercapnia, e.g., P_aCO₂ < 6 kPa, is less clear, since this situation induces very little discomfort in many subjects.

4.4 Arterial O₂ tension

The arterial oxygen tension is the main determinant of cerebral tissue and venous oxygenation and was also crucial to the early investigation of the BOLD response. Ogawa et al. first described the BOLD mechanism by demonstrating that vascular contrast in T₂^{*} weighted images correlated with the venous oxygenation during various physiological states (109). Soon after Turner et al. was able to demonstrate global signal decreases in cat brain during apnea, and even more pronounced changes during anoxic ventilation (147).

The effect of hypoxia and hyperoxia on cerebral perfusion and metabolism has been the subject of numerous studies. It is well known that the decrease in oxygen delivery caused by low P_aO₂ is counteracted by an increase in cerebral perfusion, but the influence of P_aO₂ on CBF is less well described in mathematical terms than that of P_aCO₂. Contrary to the CO₂ response the result of varying P_aO₂ has been described by some authors as a threshold phenomenon, with virtually no CBF changes occurring in the normoxic range (62), but with an exponential increase occurring below a P_aO₂ of 4–5 kPa in humans (141), or 6–8 kPa in rats (31; 143). This is consistent with the view that CBF is primarily responsive to oxygen delivery, which does not change much in normo- and moderate hyperoxia. However, it seems that P_aO₂ cannot be ruled out as an important regulator as well (71). Other studies have also shown increases at moderate hypoxia in humans (9% increase at P_aO₂ of 8.7 kPa, (35)), and during hyperoxia the flow has been shown to decrease by up to about 30% (126).

The issue of whether oxygen delivery (V(O₂)) is maintained during hypoxia is not clearly resolved in the literature. Recent PET studies suggest a decrease in V(O₂), but the absolute magnitude is quite variable (90; 104). Other studies fail to show a decrease in V(O₂) (17; 126)

during moderate hypoxia. During severe hypoxia it has been reported that the maximal vasodilation is less than the one obtained during hypercapnia, and this limitation will further contribute to a rapid decline in oxygen delivery (70).

Few studies directly report $V(O_2)$ during hyperoxia, but there seems to be agreement that any increase in oxygen delivery is very small, because hemoglobin is almost saturated already in normoxia, and because of the associated decrease in CBF. Some studies are actually compatible with a decrease in oxygen delivery during hyperoxia (83; 126). However, the fraction of oxidative metabolism covered by O₂ in physical solution may increase from 3% to more than 15% during hyperoxia, and this will contribute to the increase in venous saturation that causes a positive BOLD_B signal.

For the purpose of the present study the data of Kety and Schmidt (83), and Shimojyo et al. (141) have been used, showing a modest but significant decrease in $V(O_2)$, as expressed by the relation:

$$V(O_2) = 200 \cdot (S_a O_2) + 270 \quad (19)$$

where the constants have units of $\mu\text{mol}\cdot\text{hg}^{-1}\cdot\text{min}^{-1}$. During hyperoxia (arbitrarily defined as $P_a O_2 > 14$ kPa, $S_a O_2 > 0.97$) it is assumed that $V(O_2)$ stays constant at the value obtained at $S_a O_2 = 0.97$. Cerebral perfusion over the full range can then be estimated as $\text{CBF} = V(O_2)/C_a O_2$.

It should be noted that the hemodynamic effect of oxygen has been shown to be modulated by $P_a \text{CO}_2$, with higher reactivity to both hypo- and hyperoxia when $P_a \text{CO}_2$ is elevated. This is included only implicitly in the above equation, which may therefore represent a reactivity slightly different from the response seen during experiments where $P_a \text{CO}_2$ has been controlled. The CBF response to hypoxia can be modeled by calculating the smallest value required to maintain an M_{O_2} that is 50% of the maximal value $M_{O_2}^*$. The result of this simulation (see Fig. 10) is very dependent on the values of $\text{PS}_c O_2$ and indicates that a value of $\text{PS}_c O_2 = 3000 \text{ ml}\cdot\text{hg}^{-1}\cdot\text{min}^{-1}$ is consistent with a very steep flow increase at a $P_a O_2$ of about 5 kPa, as seen experimentally. At this value of $\text{PS}_c O_2$ the oxygen metabolism is flow limited at an $M_{O_2}^*$ of 250 but not at 150 $\mu\text{mol}\cdot\text{hg}^{-1}\cdot\text{min}^{-1}$ (see fig. 3).

Several studies have shown that cerebral energy metabolism may be maintained in spite of pronounced hypoxia, e.g., down to a $P_a O_2$ of 4 kPa (102). Constant M_{O_2} in humans has been reported down to a mean $P_a O_2$ of 3.3 kPa. However, at this level both cognitive symptoms and loss of consciousness occurred (141). No increase in brain lactate was detected with MR spectroscopy during hypoxemia with $P_a O_2$ down to 4.5 kPa (43). As long as CBF regulation is intact, the brain metabolism therefore seems to be well protected against hypoxemia. Cognitive symptoms, however, may occur before manifest disruption of energy metabolism.

The mediators of hypoxic and hyperoxic flow changes are not fully known, but a number of mechanisms have been proposed. Under severe hypoxia the response is probably dominated by increases in extracellular ions such as H⁺ and K⁺, and decrease in Ca⁺⁺. Under moderate hypoxia other mechanisms such as release of adenosine (105) and possibly increased activation of oxygen sensitive medullary neurons may be effective (62). The mechanism of hyperoxic flow decrease is also not quite well-known, but one proposed mechanism is that it is related to arterial

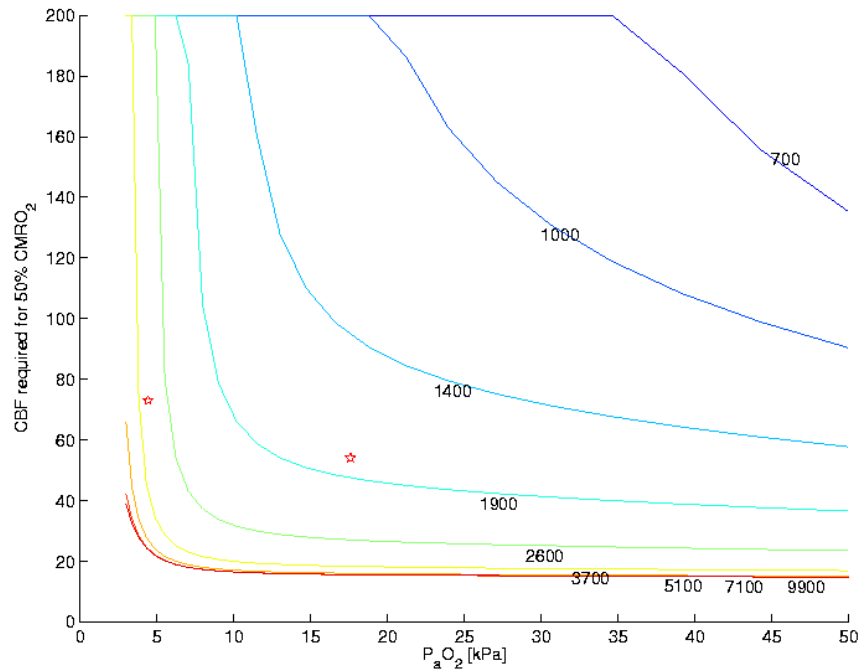


Figure 10: Minimal CBF ($\text{ml}\cdot\text{hg}^{-1}\cdot\text{min}^{-1}$) required to sustain oxidative metabolism at 50% activity (i.e. 50% of $M_{O_2}^* = 250 \mu\text{mol}\cdot\text{hg}^{-1}\cdot\text{min}^{-1}$) as a function of P_aO_2 and calculated for different PS_cO_2 -products (inserted numbers). The red symbols are average normoxic and hypoxic data from (83), where M_{O_2} was found unchanged during hypoxia. They illustrate typical experimental findings, and suggest that the correct value of PS_cO_2 is probably not less than 3000 $\text{ml}\cdot\text{hg}^{-1}\cdot\text{min}^{-1}$.

hypocapnia, caused by central effects of the reduced CO₂-carrying capacity caused by hyperoxia (Haldane effect). However, this mechanism has been shown to be of minor importance since flow decreases also occur when inspiratory CO₂ is adjusted to maintain a constant P_aCO₂ (39). It has also been proposed that the flow decrease is related to specific gene activation (71) or inactivation of NO related mechanisms (62).

Contrary to the situation under hyper- or hypocapnia, the oxygen extraction fraction changes only very little during moderate hypoxia, because arterial and venous oxygen contents are decreased to a similar extent (83). In spite of this, hypoxia causes a pronounced negative BOLD_B response, due to the overall increase in deoxy-hemoglobin levels. Rostrup et al. investigated hypoxemia in human volunteers (mean P_aO₂ of 6.0 kPa, S_aO₂ 81%) and found signal decreases of about 2.2% in central grey matter, and about twice that value in cortical grey matter, probably due to differences in blood volume (126). In comparison inhalation of 100% oxygen (mean P_aO₂ 68.8 kPa) resulted in signal increases of 0.84% in central grey matter. During the hypoxic condition a linear relation between S_aO₂ and ΔR₂^{*} was described (126).

This is confirmed by model calculation which shows an approximately linear relation between S_aO₂ and ΔR₂^{*} (or BOLD_B response). The response is lower for higher values of M_{O₂}^{*} and the slope decreases when oxygen metabolism becomes limited by oxygen delivery. The magnitude of the response also depends on blood volume, and the results shown in figure 11 have been calculated for a standard CBV of 3.7 ml·hg⁻¹ at normoxia, and following the CBV-CBF relation as described by eq. 17. In an animal study Prielmeier et al. (118) described a decrease in the slope, i.e. a smaller ΔR₂^{*} response, below a S_aO₂ of 0.6-0.7. They suggested that this could be due to flow increases, although CBF was not measured directly in the study.

Calculations using the present model predicts a linear relation between ΔR₂^{*} and S_aO₂, provided that the CBF increases are assumed to match decreases in C_aO₂ (i.e. at constant oxygen delivery) and blood volume effects are ignored. This is illustrated in the upper right panel of fig. 11. However, when the CBV increases are considered, the rate of ΔR₂^{*} change becomes progressively more pronounced as hypoxia deepens (fig. 11A).

If a constant CBF is assumed, M_{O₂} will quickly become limited by oxygen delivery, and smaller ΔR₂^{*}-values will result, due to decreased production of deoxy-hemoglobin (fig. 11C). Any limitations in hypoxic flow increase, or any specific decreases in brain tissue metabolism during hypoxia, will therefore result in a non-linear relation, as in the study of Prielmeier et al. It should be noted that other studies have showed a linear rather than a non-linear relation (96; 126). In a very detailed theoretical and experimental analysis van Zijl et al. (152) present relaxation rate vs. O₂-saturation curves that are similar to those in figure 11A, although they seem more linear. A major difference in the modeling approaches is that the van Zijl study deals with R₂ effects, which are considered to be purely intra-vascular, and dominated by erythrocyte water exchange. In contrast the present study employs the biophysical equations for R₂^{*} developed by Ogawa et al. which concerns a general tissue average (111). Another possible reason for a discrepancy is the distribution of blood volume changes which is assumed to be equally distributed in (152), while in the present study the arterial compartment is assumed to show the largest increase. To further resolve the issue, direct measurements of CBF, CBV and possibly M_{O₂} would have to be conducted at different levels of hypoxia.

During hyperoxia a flow decrease of about 10% occurs under the assumption of constant

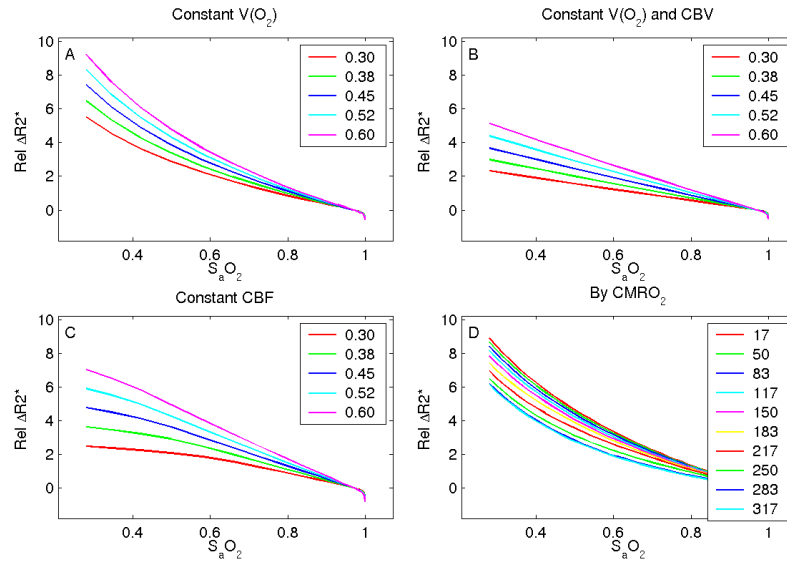


Figure 11: $BOLD_B$ effect of hypo- and hyperoxia, with various values of the arterial hematocrit, ranging from 0.3-0.6 ($PS_c O_2 = 7000$, $M_{O_2}^* = 150 \mu\text{mol}\cdot\text{hg}^{-1}\text{min}^{-1}$). The value of ΔR_2^* is calculated relative to R_2^* at normoxia ($P_a O_2 = 14 \text{ kPa}$). Simulation was performed under different assumptions of the hemodynamic effects of hypoxia: A. Oxygen delivery is kept constant at $375 \mu\text{mol}\cdot\text{hg}^{-1}\text{min}^{-1}$ ($OEf = 0.4$), across $P_a O_2$ and hematocrit values, resulting in a non-linear relation between ΔR_2^* and $S_a O_2$. B. To show the influence of CBV this parameter is kept constant, resulting in linear relationship. C. When CBF is also constant, oxygen delivery is insufficient in severe hypoxia, resulting in decreased M_{O_2} and smaller changes in ΔR_2^* . D. Predicted effect at a range of $M_{O_2}^*$ -values, as listed in the insert box. Hematocrit = 0.48, oxygen delivery $375 \mu\text{mol}\cdot\text{hg}^{-1}\text{min}^{-1}$ (OEf assumed to vary as function of M_{O_2} but not of $P_a O_2$).

$V(O_2)$, and the resulting $BOLD_B$ signal is positive, as observed experimentally (126). This response is also quite dependent on the flow change, and if the flow decrease is more pronounced a decrease in $V(O_2)$ and $BOLD_B$ signal is predicted.

In figure 11D the $BOLD_B$ response has been calculated for a range of $M_{O_2}^*$ values (listed in insert), and oxygen delivery (as in figure 11A) as well as constant hematocrit. Small values of $M_{O_2}^*$ (high OEF values) are seen to lead to higher $BOLD_B$ changes in hypoxia; this seems to be due a progressive inhibition of M_{O_2} , limiting the increase in venous deoxy-hemoglobin levels.

In the above mentioned study by the present author (126) there was a pronounced regional variability in the response to O_2 , which was attributed to regional variation in blood volume, consistent with findings during hypercapnia. However, a higher flow response to hypoxia has been demonstrated specifically for the hypothalamus (17), while in animal studies a lower BOLD response has been demonstrated in the hippocampus (30). The result of the latter study may well have been due to the effect of regional blood volume, and therefore rather unspecific. Otherwise, the mechanisms behind these findings, or their clinical significance, are not clear presently.

4.5 Breath-holding

Breath-holding is a respiratory challenge, that combines the effects of hypoxia and hypercapnia, and has been investigated in several BOLD imaging studies. In one of the earliest BOLD studies Turner et al. investigated apnea in anesthetized cats (147), and found a small signal increase during apnea, followed by a pronounced enhancement of image signal when respiration was restored. Interestingly, when anoxia, instead of apnea, was induced by ventilation with N_2 , a strong signal decrease was seen, which was also followed by a signal increase when normal ventilation was resumed. It is possible that the difference between anoxia and apnea was caused by a more rapid arterial deoxygenation, and less compensatory CBF increase, in the latter situation than under conditions of apnea. In human subjects only a few results point to $BOLD_B$ decreases during breath-hold (144), and some to a more complex pattern of increases and decreases, possibly influenced by respiratory movements (107). In general, however, human studies have shown a BOLD signal increase during breath-holding (78; 94; 140).

Clearly, breath-holding therefore represents a complex situation that is characterised by the gradual development of both arterial hypoxia, leading to a decreased baseline signal, and hypercapnia which will lead to hyperperfusion, and increases in the baseline signal (94). The balance between these factors determines the magnitude and direction of the $BOLD_B$ response, and this may be the reason for apparently discrepant results between animal and human experiments, and between human experiments performed with different breath-hold paradigms.

Kannurpatti et al. showed in an animal study, that the response magnitude and direction is very dependent on pre breath-hold conditions. While no response was seen with carbogen breathing (95% O_2 , 5% CO_2), a positive response was seen after pre-breathing with 100% O_2 , and a negative after atmospheric air (72).

Breath-holding performed after normal expiration in humans usually results in a rapid increase in both CBF and $BOLD_B$ signal, due to increases in P_aCO_2 and decreases in P_aO_2 . When normal respiration is resumed, an undershoot in both signals occurs, probably due to a reactive hyperventilation with decreased P_aCO_2 (94). In contrast, when breath-hold is initiated after a

deep inspiration, there may be increases in P_aO_2 , and decreases in P_aCO_2 that will lead to an initial $BOLD_B$ signal decrease of 20-30 sec duration, followed by a strong increase as P_aCO_2 and CBF eventually rises.

A biphasic response with decreases in signal intensity during short (24 seconds) periods of breath-hold and increases immediately after, have been reported by Shiino et al. (140). In this study breath-hold was performed after normal expiration, and the causes of the initial signal decrease are therefore not quite clear. It may have been caused by rapid deoxygenation, but was also seen after prebreathing with 100% oxygen. Prebreathing was shown to very strongly enhance the $BOLD_B$ response, probably due to the absence of arterial hypoxia during short periods of breath-hold when they are preceded by hyperoxia.

In modeling breath-hold experiments precise knowledge of time constants for the individual parameters would be of great importance due to the relatively short duration of the paradigm. The rate of P_aCO_2 and P_aO_2 change may be of importance and could explain the observed differences in temporal dynamics of the $BOLD_B$ response. Similarly, a slow increase in CBV relative to CBF will enhance the early response caused by CBF increase. Since precise estimates of these constants are not available, modeling has not been performed here.

4.6 Hematocrit

The hematocrit is expected to have a substantial influence on the baseline MR signal due to its direct relation to the brain vascular concentration of oxy- and deoxy-hemoglobin. In general the effect of hematocrit will be similar to that of cerebral blood volume, in that a lower hematocrit will reduce the amount of deoxy-hemoglobin, and thus lead to a higher baseline signal. However, if both CBF and M_{O_2} are constant, a higher OEF will result from hemodilution, counteracting a decrease in deoxy-hemoglobin.

In modeling the effect of hemodilution on BOLD signals, the concomitant adjustments of CBF should therefore be considered. Experimental evidence suggests that the dependency of CBF on arterial hemoglobin concentration is similar to the relationship to P_aO_2 , in that a regulation takes place in order to maintain a constant oxygen delivery (54). In situations of high hematocrit the elevated blood viscosity may be a separate, CBF-decreasing factor, but this has not been included in the present modeling. Another special situation arises in individuals with increased oxygen affinity variants of hemoglobin; in these individuals CBF may be increased in spite of elevated hematocrit (153).

While a number of studies have described the relation between $BOLD_A$ and baseline hematocrit (see section 5.4), very few studies have directly investigated the influence of hematocrit on baseline signal. Lin et al. measured decreases in R_2^* of 0.2 and 0.4 Hz when the hematocrit was reduced acutely by 20 or 40%, respectively (97). This corresponded to a positive $BOLD_B$ signal of 1.5% and 2.5%.

Modeling with the present approach suggests that changes in baseline signal due to hemodilution are critically dependent on concomitant CBF adjustments. When CBF is kept constant, hemodilution does not result in R_2^* change. In the absence of any changes in O_2 -metabolism, the extraction fraction must increase in proportion to the decrease in hemoglobin delivery, and this results in a constant venous deoxy-hemoglobin concentration. By contrast when CBF is as-

sumed to increase to maintain a constant oxygen delivery, the OEF and venous saturation will also remain unchanged (54), and hemodilution will result in a smaller venous deoxy-hemoglobin concentration (results not illustrated). A hypothetical decrease in hematocrit from 0.6 to 0.3 would then lead to a 1 Hz decrease in R_2^* , not too different from the results of Lin et al.

The arterial hematocrit interacts with other physiological parameters. In a different study Lin et al. showed that the effect of arterial hypoxemia was significantly attenuated by hemodilution (96), as expected from a simple consideration of the relationship between arterial and venous oxygen content:

$$C_vO_2 = S_aO_2 \cdot Hct \cdot (1 - OEF) \quad (20)$$

When $V(O_2)$ and M_{O_2} are constant, the OEF is also constant, and a linear relationship between R_2^* and S_aO_2 is predicted (ignoring blood volume effects, so that R_2^* can be considered linearly dependent upon the sum of C_aO_2 and C_vO_2). This linearity and its dependency on arterial hematocrit is confirmed by model calculations as shown in figure 11B. However, the data of Lin et al. showed a decrease in slope with hematocrit which was more pronounced than predicted from the above relationship, and they suggested that this could be due to difference between large and small vessel hematocrit. This aspect has not been included into the present modeling due to the relative lack of quantitative data concerning the relative distribution of vascular compartment sizes and their hematocrits.

4.7 Clinical use

4.7.1 Vascular reserve capacity

The use of BOLD MRI as a clinical test of vascular reserve capacity in the setting of carotid stenosis has been proposed by several authors. Lythgoe et al. investigated the use of CO_2 inhalation to test cerebrovascular reactivity in carotid stenosis. While in this study a qualitative evaluation of decreased reactivity was possible, there was no significant correlation between quantitative measures of vascular reactivity determined from BOLD and transcranial Doppler (101). By contrast, in a more recent study a relatively close correlation between $BOLD_B$ changes in T_2^* and transcranial Doppler reactivity measurements was found (159); the improved correlation found in the latter study may have been due to the use of a higher inspired CO_2 fraction (7 vs 6%), as well as a high number of acquisitions to increase signal to noise ratio.

As a clinical technique, CO_2 -inhalation may sometimes cause patient discomfort, because elevated P_aCO_2 may lead to sensation of air-hunger, in spite of high P_aO_2 . Breath-hold techniques have therefore been suggested as a possible replacement technique, requiring less equipment and enabling more control by the patient. Studies have shown a high correlation between the magnitude and spatial pattern of signal increases during 5% CO_2 -inhalation and short (36 seconds) breath-hold periods (78). This is in itself an interesting finding, since the stimuli are quite different, with one leading to hyper-perfusion with hyperoxia, the other one to hypoxic hyper-perfusion. Further studies of these related stimuli may lead to a more detailed description of similarities and dissimilarities in the response.

Compromised arterial blood supply is associated with a decreased CBF/CBV ratio and an increase in OEF and resting deoxy-hemoglobin levels (56). According to the modeling results

in figure 12 this should in itself lead to higher $BOLD_B$ responses to hypercapnia. A theoretical caveat is therefore that moderately decreased CBF responses may be masked by enhancement of $BOLD_B$ due to increased baseline CBV and deoxy-hemoglobin. However, Shiino et al. (140) found a good correlation between breath-hold BOLD measurements and SPECT imaging of patients with internal carotid occlusions, suggesting the clinical utility of the method, in spite of possible theoretical limitations.

4.7.2 Tumor vascularity

An interest in measuring tumor oxygenation and vascular reactivity stems from the observation that hypoxic tumor tissue is less sensitive to radiation than normoxic tissue. Various means of increasing tumor oxygenation prior to radiation therapy have been proposed, but there seems to be a large variation in the ability of tumor tissue to respond to this due to abnormalities in vascularity and metabolism (40).

On this background it has been proposed to use BOLD imaging to investigate increases in tissue oxygenation due to inhalation of hyperoxic gasses (48). Using carbogen breathing large signal increases could be demonstrated in a range of tumor types (145), and pronounced variability in the response was found, both between and within individual tumors. In that study an MR sequence with some T_1 -weighting was used, making it difficult to distinguish between flow and oxygenation effects. However, similar results have been obtained for intracerebral tumors, with a presumably less flow sensitive EPI sequence (59), suggesting that oxygenation is the major source of signal change during respiratory interventions. Hsu et al. used a breath-holding paradigm and saw generally no $BOLD_B$ response in low-grade tumors, which was interpreted as a consequence of low vascular CO_2 -reactivity in abnormal vessels, or a very high resting oxygen extraction fraction (59). In some tumors a negative $BOLD_B$ response occurred, possibly reflecting a vascular steal phenomenon.

In conclusion the BOLD method seems to provide interesting results on tumor oxygenation and vascular reactivity, with minimal patient discomfort. However, the response is variable and should probably be interpreted carefully, if used for diagnostic purposes.

5 The BOLD_A response

5.1 Basic determinants of the BOLD_A response

As described in the introduction the BOLD response elicited by neural activation results from a balance between the changes in CBF, CBV and M_{O_2} . The magnitude of these parameters before, as well as during activation is therefore important for the magnitude of the BOLD signal. Equation 3 expresses the cerebral oxygen content (and indirectly the content of deoxy-hemoglobin and R_2^*) in terms of the oxygen extraction fraction, which is clearly a crucial parameter. In fact, an operational definition of the resting or default state, vs. activated or deactivated states of the brain, has been suggested based on the value of this parameter (119). This suggestion is based on the observation that brain regions, that are not known to be directly engaged in an imposed task or stimulus generally exhibit an OEF of about 0.4. Conversely, when a region is recruited for a specific task-related activity, a decrease in the OEF is observed.

An approximate model for the magnitude of deoxy-hemoglobin change during activation can be derived by considering the change in OEF during activation. By using the expression for OEF (eq. 2) and assuming a constant C_aO_2 , the fractional increase in OEF during activation can be expressed as

$$f_{act}(OEF) = \frac{f_{act}(CMRO_2)}{f_{act}(CBF)} \quad (21)$$

where $f_{act}(x)$ refers to the relative value of a parameter during activation, $f_{act}(x) = \frac{x_{activated}}{x_{baseline}}$. During activation in normoxia, the total amount of deoxy-hemoglobin can be approximated as

$$C_{t,dhb} \approx f_{act}(OEF) \cdot f_{act}(V_v) \cdot [C_aO_2 \cdot OEF \cdot V_v] \quad (22)$$

where the terms in brackets approximates the baseline or resting value of $C_{t,dhb}$, which for small changes is linearly related to the change in BOLD signal (eqs. 12–15).

Several studies have demonstrated that, in general, OEF decreases during activation, i.e. $f_{act}(OEF)$ has a magnitude less than 1. Because CBV changes are modest, this leads to an overall decrease in $C_{t,dhb}$, and a resultant positive BOLD_A effect. In their classical paper Fox and Raichle (41) found that sensory stimulation elicited a 29% increase in CBF, 5% increase in M_{O_2} , a corresponding 19% decrease in OEF and a 7% increase in CBV. According to eq. 22 this will result in a 13% increase in average tissue deoxy-hemoglobin content. Although other studies have found larger M_{O_2} -increases during activation (85; 150), there is general agreement that they do not exceed or match the increase in CBF (19). The M_{O_2} response, and its relation to CBF, has also been shown to be highly variant between regions, (150). A high variability, spatially and across paradigms may be the key to the apparent discrepancy in the literature.

Equation 22 predicts a linear relation between the change in $C_{t,dhb}$, and its value in the resting state, meaning that the BOLD_A response should be smaller when less deoxy-hemoglobin is present, such as in e.g., hypercapnic hyperperfusion. Due to the definition of OEF 2 a dependency on M_{O_2} and CBF^{-1} is also expected. However, these predictions are based on assuming independence of the parameters, such that arbitrary combinations of $f_{act}(OEF)$, M_{O_2} and CBF

can be selected, and this may not always be justified. When comparing across regions, for instance, M_{O_2} and CBF are known not to be independent, but to vary in proportionality, keeping OEF almost constant (41; 123). Another important issue is whether a proportional or an additive model for CBF change is valid, i.e. whether the fractional ($f_{act}(\text{CBF})$) or the absolute change of CBF is constant during activation . .

This has been investigated by several authors. Ramsay et al. (120) found no significant interaction between global and regional CBF during visual stimulation, and therefore concluded that the absolute CBF increase in visual cortex is independent of global CBF, corresponding to an additive model. Similar results were later reached by voxel based analysis (24) of BOLD data. Using a spin labeling technique Kastrup et al. (79) found a negative correlation between the fractional change in CBF during activation and the spontaneously varying baseline value, as well as a constant absolute CBF change, also in support of an additive model. A later study from the same group confirmed this by showing the same absolute response to visual stimulation under normal conditions, as during breath-hold (95).

A number of other studies have reached the opposite conclusion, i.e. that it is a constant fractional increase that best describes the CBF changes during activation. Using very similar experimental paradigms as in the above studies Shimosegawa et al. found significantly lower visually evoked CBF increase during hypocapnia than during normocapnia, and a constant fractional increase of 30% independent of baseline CBF (142). Similar results were found by Kemna et al. (82), as discussed below (section 5.2).

In general, a majority of studies seem to point toward an additive model, but the issue is probably not finally resolved. Methodological difficulties include the ability to measure the rather small difference in absolute CBF that would be expected during activation, under each of the two hypotheses. It should be noted also that of the studies cited above in support of the additive model, those two that use CO₂ stimulation (PET and MRI, (24; 120)) both investigate very small groups of subjects and rely on negative findings (lack of interaction) to reach their conclusion. Studies with better statistical power could have reached different conclusions. Furthermore, one may speculate that the situation may differ for different conditions, such as states of high vs. low baseline flow. For example, a ceiling effect occurs when baseline flow is sufficiently high to prevent any further flow increase during activation, and this will tend to create less than proportional flow increases.

An additional type of ceiling effect must be considered when measuring the BOLD_A response as opposed to direct flow responses. This is because the BOLD_A response is due to decreases in the amount of deoxy-hemoglobin during activation, and only a limited amount is present in the baseline condition. Thus, when baseline flow is high (at a constant M_{O_2}), the deoxy-hemoglobin level is low, and the possibility for further decrease due to activation is limited.

These issues and the effect of various assumptions on the BOLD_A response can be explored further using model calculations. Figure 12 shows the predicted BOLD_A response as a function of CBF and $M_{O_2}^*$, for a proportional and an additive model, respectively. Under the proportional model (fig. 12, A–B) the magnitude of physiological changes during neural activation is assumed to be as quoted above from the study of Fox et al. (41), i.e. a 29% increase in CBF and a 5% increase in M_{O_2} . However, the CBV increase was calculated from eq. 17, and therefore is slightly larger (10%). For the additive model (fig. 12, C–D), the increase in CBF was assumed to be 17

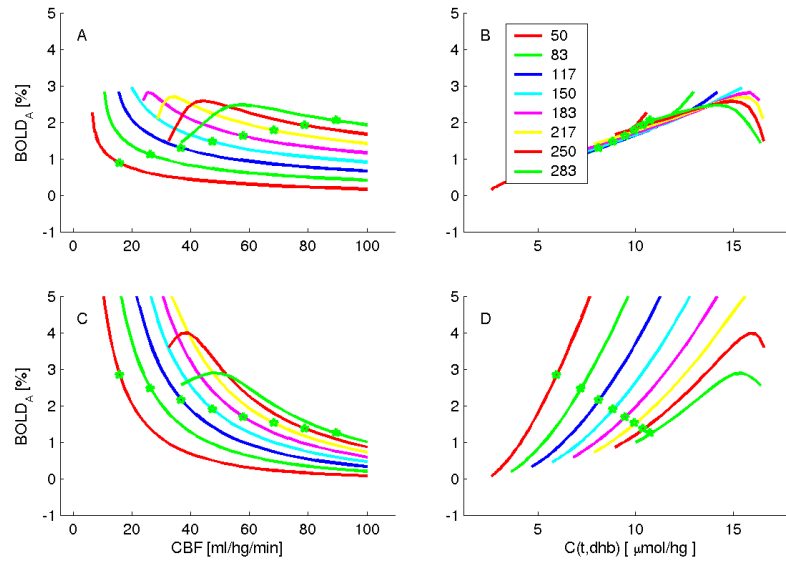


Figure 12: BOLD_A response vs baseline CBF and deoxy-hemoglobin ($C_{t,dhb}$), respectively, at various values of $M_{O_2}^*$. The upper row (panel A–B) shows BOLD_A under the *proportional model* of activation related flow change. The lower row (C–D) shows the results for an *additive model*. For the proportional model the BOLD_A signal was calculated for a fixed set of response parameters during neural activation: 5% increase in $M_{O_2}^*$, 29% increase in CBF (41). In the additive model a constant absolute flow change was assumed ($17 \text{ ml}\cdot\text{hg}^{-1}\cdot\text{min}^{-1}$). In both cases the corresponding CBV increases was calculated from eq. 17. Assuming higher M_{O_2} -changes (57) will shift the curves downward, but will not change the overall configuration. Points of constant OEF = 0.4 have been marked with green stars, see text for details.

ml·hg⁻¹·min⁻¹ at all baseline flows (corresponding to 29% increase at a baseline flow of 60 ml·hg⁻¹·min⁻¹), while the M_{O_2} is assumed to increase by 5% as in the proportional model. The relation between BOLD_A and baseline CBF is plotted for values of $M_{O_2}^*$ ranging from 50–283 $\mu\text{mol}\cdot\text{hg}^{-1}\cdot\text{min}^{-1}$. It is of note that both the proportional and the additive model predict a decrease in BOLD_A response with increasing flow. However, the decrease is much more pronounced under the additive model, where the fractional flow change gets progressively smaller as baseline flow increases. The relation is monotonic except for the highest values of $M_{O_2}^*$, which cannot be sustained at low flow values. In the present model this leads to a decrease in BOLD_A, because M_{O_2} is limited by CBF, and therefore is able to increase more during activation with its associated increase in perfusion.

When the response is plotted against the baseline value of total deoxy-hemoglobin content in the tissue ($C_{t,\text{dhh}}$), a significant difference between the two models become evident. For the proportional model (fig. 12B) there is an almost perfect linearity, as expected from eq. 22, and previous reports (21). By contrast, with the additive model the relation between BOLD_A and resting $C_{t,\text{dhh}}$ is non-linear, and highly dependent on M_{O_2} (fig. 12D). It can therefore be concluded that BOLD_A depends on resting M_{O_2} , but for the proportional model this is only due to a dependency on resting $C_{t,\text{dhh}}$. For the additive model the response depends on both M_{O_2} and $C_{t,\text{dhh}}$. This reason for this is to be sought in the fact that a constant flow corresponds to a constant increase in oxygen delivery. When the increase in oxygen delivery is large compared to M_{O_2} , it may create a large BOLD_A response, whereas it will have less impact when M_{O_2} is large, and the oxygen delivery change comparatively small.

The lines plotted in fig. 12 refer to independent changes in baseline CBF. However, a more likely situation is some degree of coupling between baseline CBF and M_{O_2} , especially when comparing between different regions. In the figure those CBF- M_{O_2} combinations that lead to a constant OEF of 0.4 have therefore been highlighted (green stars). Interestingly, it seems that for the proportional model, regions with high CBF will display a larger, rather than a smaller, response than low-flow regions. Due to CBV effects, and in spite of a constant venous saturation, the high-flow regions have a larger baseline $C_{t,\text{dhh}}$, leading to the higher response (fig. 12B). For the additive model (fig. 12D), the effect of baseline $C_{t,\text{dhh}}$ is canceled by the dependency on M_{O_2} : in regions with more intensive O₂-metabolism the BOLD_A response is generally lower. This is because the CBF change is assumed to be constant, and therefore of decreasing relative importance as baseline CBF and M_{O_2} gets larger.

In conclusion, BOLD_A is shown to depend on both baseline CBF and M_{O_2} , and especially so under the assumption of additive flow increases. Baseline levels of deoxyhemoglobin are good predictor of the BOLD_A response under the proportional model.

Another factor of major importance for the magnitude of the BOLD_A response is the baseline CBV. This is evident from eq. 3 as well as from eqs. 13–14, where blood volume is a direct determinant of the tissue content of oxygenated hemoglobin, and of R_2^* . Generally, therefore it is assumed that BOLD is linearly related to baseline CBV. However, as previously noted (85), in normoxia the BOLD_A response depends not on the total change in blood volume per se, but rather on the change in the BOLD-visible fraction, i.e. the venous fraction in which changes in oxygenation can take place. The present study utilizes estimates from the literature regarding both the distribution of total blood volume in rest and the fractional changes for each compart-

ment during activation (92).

In the following sections experimental results regarding the influence of baseline conditions on the BOLD_A response will be reviewed, and compared to model predictions.

5.2 Effect of hypo- and hypercapnia

The characteristics of the BOLD_A response during altered P_aCO₂ conditions have been investigated in several studies. Although most studies show a significant influence of CO₂-related changes in baseline condition, there is some disagreement about the precise nature of this interaction.

The first study to apply simultaneous CO₂- and visual stimulation probably was the one by Bandettini et al. (7). In this study a pronounced attenuation of the BOLD_A response was demonstrated in subjects inhaling 5% CO₂. This decrease was attributed to the hyperperfusion caused by CO₂, but was not analysed quantitatively.

In an important study by Hoge et al. (57) graded hypercapnia and visual stimulation were applied simultaneously, and the BOLD responses were described as additive, i.e. apparently there was no decrease in BOLD_A during hypercapnia. The induced hypercapnia was modest, however, with perfusion changes < 20%. Based on the model calculations, the authors predicted higher BOLD_A responses during hypocapnia, and — presumably — lower responses during more pronounced hypercapnia. This was based on the assumption of a constant absolute CBF change (additive model) which would lead to a higher relative CBF change during hypocapnia.

Increased BOLD_A response during hypocapnia has been directly demonstrated in an animal study conducted at very high field (7T (58)), and was thought to be a consequence of the widened arterio-venous oxygenation difference due to decreased flow.

Another group of publications (81; 116; 155) describes a more complex relation between the prevailing P_aCO₂ and the BOLD_A response, which is found to increase with P_aCO₂ in the range 4–6.7 kPa. Above and below these values the response decreases. Notably, the maximum BOLD_A is found at moderate hypercapnia (P_aCO₂ = 6.7 kPa), but it is not stated whether the response at this value is significantly different from the normocapnic response (116). The decrease at extreme hypercapnia is interpreted as a result of maximal vasodilation in the baseline state. The decrease in hypocapnia is ascribed to the low baseline flow, which, according to the proportional model, gives a smaller absolute flow increase during activation. Additionally, the influence of blood volume increases could be enhanced in hypocapnia, due to a higher OEF and a lower venous saturation (155).

As mentioned above, one BOLD study (24), employing voxel-based analysis, found no interaction between BOLD_A magnitude and P_aCO₂, and concluded that the absolute signal increase was constant during hypercapnia. However, both the degree of hypercapnia (4% CO₂) and the number of subjects in this study were modest.

Finally, in a more recent study Cohen et al. found a significant negative correlation between BOLD_A (visual stimulation) and the baseline signal, when the latter is modified by changes in venous saturation (23). This is in agreement with the above prediction of a positive relation between baseline deoxy-hemoglobin levels (C_{t,dhb}) and BOLD_A magnitude (sec. 5.1); Correspondingly, a significant decrease of the response was found during hypercapnia (5% CO₂), and

a near-significant increase during hypocapnia.

In summary, there seems to be some consensus that the BOLD_A response decreases in hypercapnia. However, at what level of P_aCO₂ at which this becomes apparent is not reported consistently, and the effect is interpreted either as being inherent to the BOLD mechanism, or as a physiological consequence of maximal vasodilation. During hypocapnia some report an increased while others a decreased BOLD_A response. Regarding the temporal dynamics of the response there does seem to be agreement that the response gets slower and more prolonged during hypercapnia (23; 81). This finding is somewhat contrary to what would be expected in consideration of the shortened transit time, and has not yet been fully explained.

An understanding of the BOLD response is dependent on understanding primarily the underlying hemodynamic changes, and secondly the deoxy-hemoglobin response to these changes. It is therefore of interest to consider direct measurements of changes in CBF response during hypercapnia.

Apart from the above mentioned PET studies (120; 142), which used ¹⁵O-labeled water, one important study used ¹⁵O-labeled butanol to investigate the interaction between CBF increases caused by CO₂-inhalation and visual stimulation (82). This tracer has the advantage of being more diffusible than water, and may therefore reflect high flow values more reliably. In this latter study the activation related flow-increase is shown to increase with increasing baseline flow. In fact even the relative flow increase is reported to be significantly higher during hypercapnia, but the changes are small, and the values could probably be regarded as approximately constant, in agreement with the proportional model (81). During very severe hypercapnia, probably some of the highest flow values measured in man are reported (> 200 ml·hg⁻¹·min⁻¹), and not surprisingly, no further CBF increase during activation is seen in this condition.

Additional information, guiding the interpretation of these partially conflicting results may be gained from modeling. Figure 13 shows the results of modeling the BOLD_A response with a 50% flow increase (proportional model), as reported in several studies of visual activation, and a small M_{O₂} increase of 5% (41). The values of pH and P_aO₂ are assumed to covary with P_aCO₂ as described in section 4.3. A general decrease of BOLD_A is found with increasing P_aCO₂ and CBF (fig. 13A), corresponding to the findings for isolated CBF and CBV changes in fig. 12.

However, combinations of high M_{O₂}^{*}, and low CBF (hypocapnia) constitute a region of flow-limited metabolism, in which the responses are different. In this region (values for P_aCO₂ <4 kPa in fig. 13A, and right side of fig 13B) the BOLD_A response is predicted to increase with P_aCO₂, rather than decrease as seen in the normo- and hypercapnic range. This is because M_{O₂} under these circumstances becomes limited by CBF. During activation oxygen delivery increases, enabling an M_{O₂} increase in excess of the 5% increase in M_{O₂}^{*} due to activation.

Furthermore, in the flow-limited region there is a pronounced influence of blood composition on the BOLD_A response. Specifically, a reduction in the response is predicted due to the increase in pH that occurs with hypocapnia (blue vs green curve in fig. 13A). A higher pH value increases the O₂-affinity of hemoglobin, which further limits oxygen metabolism, and leads to a higher venous saturation. Because this effect is more pronounced in baseline than in the activated state the BOLD_A response becomes dependent on pH. The induced changes in P_aO₂ *per se* seems to have only a minor influence on BOLD_A magnitude (red vs blue curve).

As mentioned above an increased effect of CBV changes during activation may also con-

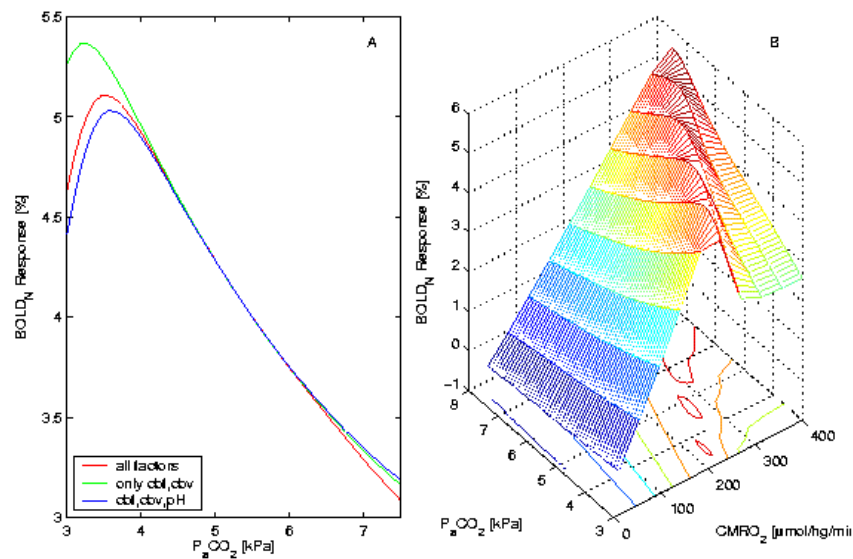


Figure 13: The relation between BOLD_A magnitude and P_aCO₂. The BOLD_A response is modeled as a 50% increase in CBF (with corresponding CBV increase), and a 5% increase in M_{O₂}^{*}. Panel A shows the response for an M_{O₂}^{*} of 250 μmol·hg⁻¹·min⁻¹ with all factors taken into account (hemodynamic, P_aO₂, pH and P_aCO₂: red curve), with only hemodynamic (green), or with hemodynamic as well as pH and P_aCO₂ included (blue). Panel B shows the predicted relationship between BOLD_A and P_aCO₂ at various values of M_{O₂}^{*} (all factors included).

tribute to a smaller response in hypocapnia. However, the venous saturation shows the same dependency on $P_a\text{CO}_2$ as the BOLD response, and saturation may therefore be responsible for a major part of the effect.

To the author's knowledge the effect of pH (or other changes in oxygen affinity) on the BOLD_A response has not been investigated experimentally, and the modeling results should therefore be interpreted with some caution. However, they do provide a potential explanation for the variability in experimental results, because the behavior of the BOLD_A response under different levels of $P_a\text{CO}_2$ may be dependent on resting M_{O_2} and oxygen extraction fraction.

It should be noted that transient hypercapnia has been reported to increase the flow response but not the BOLD_A response during subsequent normocapnia (8). A later study reproduced this finding in the same type of experiments (animals studies using α -chloralose anaesthesia) (33), and it was suggested that CO_2 might have a stimulating effect on M_{O_2} ; presumably also the M_{O_2} response to activation would be increased in order to keep the BOLD_A response constant in spite of higher flow response. However, it has not been possible to reproduce these findings in human subjects. Kim et al. investigated healthy volunteers during visual stimulation and hypercapnia, respectively, and found no significant difference in the BOLD or perfusion responses before and after hypercapnia (85). Schwarzbauer and Hoehn, using a slightly different stimulation paradigm, also investigated this and were not able to detect any change in BOLD_A or perfusion responses after a period of hypercapnia (135). It was concluded that the most likely reason for the difference between animal and human results was the use of anesthesia in the animal studies, and the difference was therefore possibly associated with the state of awokeness. No direct investigations of this hypothesis seem to be available in human subjects.

5.3 Effect of hypo- and hyperoxia

Relatively few studies have directly described the magnitude of BOLD_A response as a function of arterial oxygen tension. Bandettini et al. (7) reported only a slight decrease in activation response during hypoxia caused by inhalation of 12% O_2 . This was attributed to a lack of flow increase at this mild level of hypoxia. Rostrup et al. recently investigated visual stimulation in normal subjects during normoxia, as well as during inhalation of 10% O_2 , and found that the BOLD_A response was reduced to about 1/3 at a mean $S_a\text{O}_2$ of about 0.75 (129). This is illustrated in figure 14, which shows that the response to visual stimulation in some subjects was almost completely abolished during hypoxia.

Conversely, during hyperoxia, a small but significant increase in BOLD_A response to visual stimulation has been demonstrated by Kashikura et al. (73). The authors had previously found that the CBF response is also higher during hyperoxia, and interpreted the increased BOLD_A effect as a consequence of this.

The magnitude of the BOLD_A response is critically dependent on the magnitude of blood volume change taking place during activation. During hypoxia the effect of CBV increases is enhanced due to the higher overall blood content of deoxy-hemoglobin. As shown in figure 16B when neural activation during normoxia elicits a 5% increase in M_{O_2} , a concomitant 20% increase in blood volume will attenuate the response to a magnitude of 2% signal increase. During hypoxia (16A), with an $S_a\text{O}_2 = 0.75$, the same blood volume increase will eliminate the

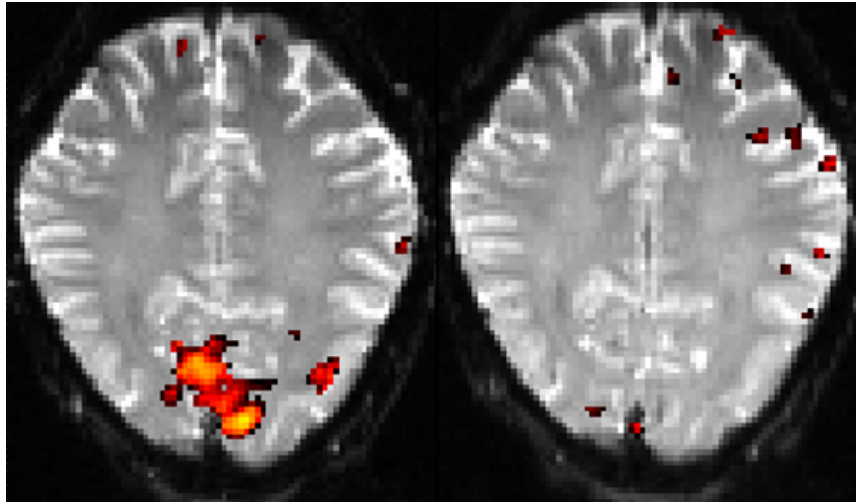


Figure 14: Effect of hypoxia on visual stimulation, from ref. (129). On average the BOLD_A response to visual stimulation (8 Hz flickering checkerboard) was reduced to about 1/3 at S_aO_2 of 0.75. In some subjects the response was almost completely abolished. Colored pixels show voxels with significant paradigm correlation ($p < 0.01$).

BOLD_A response, in agreement with experimental findings (129).

Another possible explanation for changes in the BOLD_A response is specific effects of hypoxia upon the hemodynamic response. E.g., a lower CBF response could be expected, if it is assumed that hypoxia leads to near-maximal dilation in the baseline state. Alternatively, if O₂-delivery is severely limited by diffusion restriction, some authors have hypothesised that a higher activation related flow increase would be needed to sustain neuronal activity in hypoxia (104).

However, two separate studies have found a constant CBF increase during activation in spite of decreases in oxygen delivery of 11-28% during hypoxia (90; 104). From these data it seems that baseline or activated CBF are not tightly regulated to maintain a constant oxygen delivery, and in the present model calculation a constant CBF increase of 50% has been used.

The influence of blood volume changes was also discussed by van Zijl et al. who showed that if blood T₂ is longer than tissue T₂ a positive BOLD_A response may be obtained even in a situation of equal increases in CBF and M_{O₂} (matching of the responses, (152)). Most likely, and as assumed in the present work, this effect is not large during normoxia. However, it may influence the responses seen during altered oxygenation.

During hyperoxia, the effect of blood volume increase is attenuated, and as shown in figure 16C for a 5% increase in M_{O₂}, even a 50% increase in CBV during activation would still cause a positive BOLD_A response. It therefore seems that the results of Kashikura et al. (73) may be explained by BOLD biophysics, without assuming specific effects of hyperoxia on neural or hemodynamic reactivity.

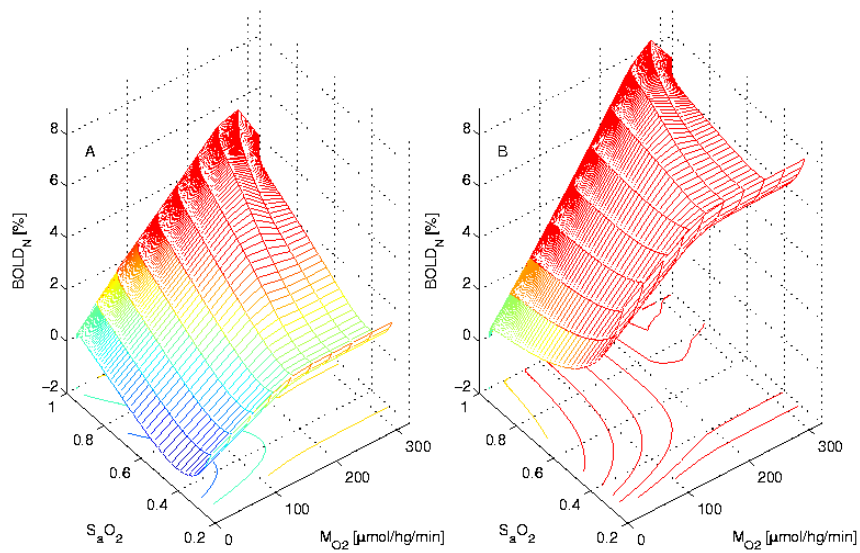


Figure 15: Predicted BOLD_A response as a function of arterial oxygen saturation, S_aO_2 and $M_{O_2}^*$ during activation. The effect of blood volume increase during activation is included in panel A, but not in B. The CBF increase was 50% , and the $M_{O_2}^*$ increase 5% during activation. Blood volume increases cause a general decrease of BOLD_A magnitude, and negative values are actually predicted for very low saturations and $M_{O_2}^*$ values.

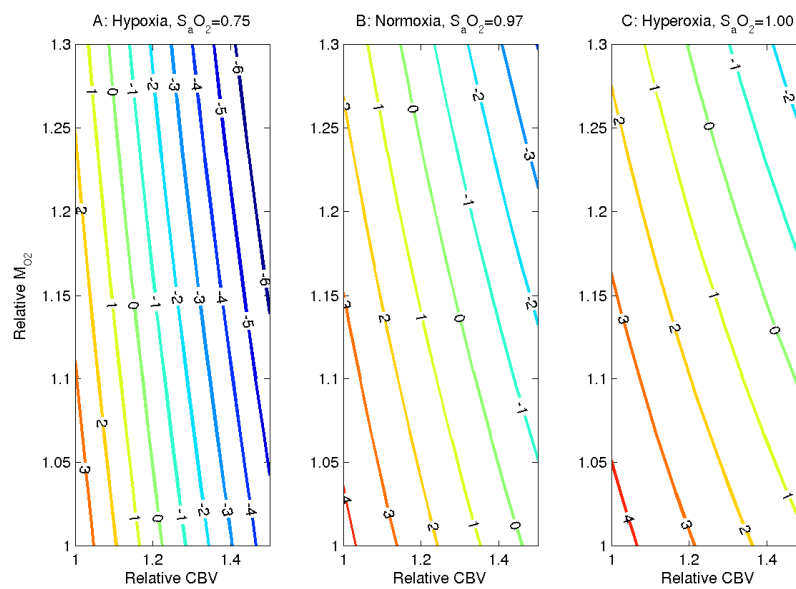


Figure 16: Predicted BOLD_A response as a function of the fractional change in blood volume and M_{O₂} during activation in hypoxia (A), normoxia (B) and hyperoxia (C). The magnitude of the response is marked in % on each contour line. Baseline M_{O₂}^{*} was 200 μmol·hg⁻¹min⁻¹, and a CBF increase of 50% was assumed under all conditions.

5.4 Hematocrit

The hematocrit has been implicated as an important factor determining individual differences in BOLD_A response. In particular Levin et al. demonstrated a significant relation between baseline hematocrit and BOLD_A response to visual stimulation. This relation partly explained the smaller magnitude of BOLD_A response found in female subjects, but within groups, it was only significant for men (93). A similar relation was found for BOLD_A in motor cortex activation vs. baseline hemoglobin concentration (50), although gender effects were not reported. Levin et al. interpreted their results based on a model of cerebral oxygenation, which predicts increased BOLD_A in response to increased hematocrit. However, the validity of the model is difficult to judge, as neither changes in CBV, M_{O₂} or OEF during activation are explicitly included. All of these parameters are important and should be taken into account.

In the absence of flow increases a decrease in hematocrit would be expected to lead to an increase in OEF of the same magnitude. As can be shown from eq. 20, this will result in a downward shift in C_vO₂, but will not change the slope of the relationship between OEF and venous oxygenation, and should therefore lead to only very small, if any changes in BOLD_A. This is confirmed by modeling, which shows that the activation related ΔR_2^* increases by only 0.03 Hz when hematocrit is augmented from 0.3 to 0.6 at constant CBF. However, under conditions of a constant V(O₂), i.e., when a physiologically more plausible decrease in CBF is taken into account, a decrease in ΔR_2^* of 0.15 Hz is seen (corresponding to a BOLD_A increase from e.g. 2.4 to 3.4%).

If V(O₂) is the significant factor being regulated during activation, then fractional CBF change should be higher in anemia. However, in line with studies showing the same activation response in hypoxia, an unchanged CBF response has also been assumed for the above model calculations. To the author's knowledge the magnitude of CBF response as a function of hemoglobin concentration has not been studied experimentally.

Another issue of potential importance is the oxygen affinity of hemoglobin as expressed by the P₅₀ value. This value can be altered by several factors such as pH and 2,3-diphosphoglycerate, or in some cases be constitutionally different due to genetically determined unusual hemoglobin forms. In normoxia modeling suggests that there would be only very small changes in baseline signal or BOLD_A in a range of P₅₀ from 1.7 to 5 kPa (normal value about 3.5 kPa). Below this range the M_{O₂} is compromised due to impaired O₂ release and vanishing P_tO₂, resulting in baseline signal increases, and decreases in BOLD_A. When a P_{S_cO₂} value of 3000 ml·hg⁻¹·min⁻¹ is assumed (rather than 7000) the limitation in M_{O₂} starts already at P₅₀ of 2.5 kPa, much closer to the normal value of P₅₀. Depending on the assumed magnitude of P_{S_cO₂} it therefore seems that high-affinity subjects (low P₅₀) should have deviant BOLD responses. On the other hand, low-affinity variants (high P₅₀) should be more sensitive to hypoxia than normal subjects, due to the rapidly declining oxygen delivery in this situation, with large decreases in both baseline and BOLD_A signal. No experimental data seems to be available regarding these issues, and it should also be noted that longstanding changes in oxygen affinity may create compensatory changes in, above all, hemoglobin concentration, which will further complicate prediction and interpretation of BOLD responses as a function of hemoglobin properties.

5.5 Pharmacological perturbation

Several drugs have been reported to influence the hemodynamic, or specifically the BOLD response to activation, with a wide range of putative mechanisms of action. Some of these will be discussed here, either because they are directly related to BOLD mechanisms, as discussed above, or because they are relatively common, and so should be considered possible confounds in e.g., studies of selected patient groups.

Acetazolamide is a drug that inhibits the carbonic anhydrase mediated reaction between CO₂ and H₂O, and mimics the effect of hypercapnia by creating tissue hypercapnia and acidosis. This causes an increase in baseline CBF, and acetazolamide, in similarity with CO₂ has been shown to decrease the BOLD_A response (16). Its mechanism of action on the BOLD_A response is thought to be a general consequence of hyperperfusion and increased venous saturation, rather than a specific effect on coupling.

Among the non-steroidal anti-inflammatory drugs, the cyclooxygenase inhibitor indomethacin has a special role, due to its vasoactive properties. Although its precise mechanism of action remains unknown, indomethacin is known to decrease baseline CBF with up to about 40% (18). Since M_{O₂} is unchanged this leads to a pronounced increase in arterio-venous O₂-difference, and a decrease in venous oxygenation. Accordingly, a pronounced decrease in baseline BOLD signal have been demonstrated by Bruhn et al. (15). Furthermore indomethacin reduces the flow response to both hypercapnia and acetazolamide, which underlines the assumed similarity of the mechanisms behind these two responses (154). In the study of Bruhn et al. (15) indomethacin was also shown to reduce the BOLD_A response to visual stimulation to about half the magnitude seen under control conditions.

Cyclooxygenase exists in two isoforms (COX-1 and 2), with different distributions, and pharmacological inhibitors differ in their selectivity to these two types. While indomethacin is a non-specific cyclooxygenase inhibitor, it has been shown that specific inhibition of COX-1 reduces both the baseline CBF and the CO₂ response, but not the functional response (108). Conversely, specific COX-2 inhibition, reduces the magnitude of the functional CBF response as well as changes its temporal characteristics (6). Specific COX-2 inhibition is brought about by drugs such as Rofecoxib (Vioxx) that until recently have been in very common use. These findings indicate that the actions of indomethacin may be due to its influence on cyclooxygenase products. However, other common cyclooxygenase inhibitors, such as aspirin, have no effect on cerebral circulation, and it is currently unclear whether this discrepancy is due to failure of these agents to reach high intra-cerebral concentrations, or to the fact that pharmacological properties other than COX inhibition contribute to the effect.

Another group of commonly occurring drugs, of which the effect on cerebrovascular reactivity has been investigated, are the ones influencing the adrenergic system, and especially beta-receptor blocking agents. The background for this is that stimulation of beta receptors located in cerebral vessels is known to cause vasodilation. Some results indicate that beta-blockade with propranolol will reduce the hemodynamic response to hypercapnia (53). In this study an increase in M_{O₂} was also seen during hypercapnia and it was thought that propranolol only acted on the part of the flow increase that was due to neural, probably stress related activation. A later study showed that propranolol almost abolished the activation related decrease in arterio-venous

O₂ difference, probably by diminishing the flow response (132). This study only provided global measures of brain function and the stimulus probably included a large arousal, and possibly stress-related component. It is therefore difficult to judge how much of the effect are due to direct vascular or metabolic mechanisms, and although intriguing these effects seem not to have been investigated further.

Pharmacological agents in very common, although not medical use include nicotine, ethanol and caffeine, which all have vasoactive properties.

Cholinergic agents, such as nicotine, generally have a vasodilatory effect on the cerebral vessels, and produce CBF increases (26), possibly as an indirect effect through stimulation of cholinergic neurons. In the case of a purely hemodynamic effect, a decreased BOLD_A response could therefore be expected after nicotine administration. However, Jacobsen et al. found an unchanged response magnitude to visual stimulation in a group of 9 subjects, and concluded that previously observed flow changes were more likely to be caused by neuronal than vascular effects (68). The expected effect of nicotine on CBF is not equally pronounced in all brain regions, and since direct CBF measures were not obtained in the study mentioned, it is uncertain whether a CBF effect could actually be observed in visual cortex.

The effects of ethanol on fMRI have been investigated and reviewed by Seifritz et al. (136). A modest reduction in BOLD_A response to auditory stimulation was seen. This was qualitatively in agreement with the known vasodilatory effect of ethanol, producing a CBF increase. No direct measures of CBF was obtained in this study, and the quantitative importance of baseline CBF increases, as opposed to cognitive or attentional effects of ethanol, could not be established.

Caffeine is an adenosine receptor antagonist with interesting properties of decreasing CBF and increasing M_{O₂} (26). These effects are due to the combined effect on two types of adenosine receptors that are involved in vascular dilation and neural inhibition, respectively. In subjects that are not regular caffeine users, the effect has been shown to be pronounced enough to cause a detectable increase in brain lactate (27). Furthermore, caffeine was shown to increase BOLD_A contrast in visual stimulation experiments by more than 20%, and its use as a general BOLD enhancer was even suggested by Mulderink et al. (106). The enhancing effect is consistent with the lowered CBF seen after caffeine ingestion, but could also be due to increased neuronal activity. In the study of Mulderink et al. CBF was measured only in the baseline, and it was therefore not clear whether flow (and presumably neuronal activation) responses to functional activation were altered by the drug. In another study the BOLD_A response enhancing effect of caffeine was shown to be very dependent on the subjects daily intake of caffeine; high users displayed a large enhancement, and this was thought to be due to up-regulation of adenosine receptors (88). The complexity of the mechanisms, as well as the dependency on daily intake limits the usefulness of caffeine as a BOLD_A booster. But caffeine remains a substance with high relevance for BOLD imaging, because it is likely to account for a significant amount of the inter-subject variability of response magnitude of many populations.

5.6 Other conditions

5.6.1 Effects of aging

A number of studies have shown that the BOLD_A response may not be constant with age. This has important implications for the ability to compare between groups of different age, which is a common procedure in studies of aging and development, but the underlying causes for the such an age effect have not be clarified completely. When the total volume of activation is reported as a measure of the intensity of activation, it should be kept in mind that this depends just as much on BOLD magnitude as on the magnitude of signal noise, and it is therefore important to distinguish between decreases in BOLD magnitude, and increases in background noise.

A recent study found decreases in the amplitude of both BOLD_B (hypercapnia) and BOLD_A-response (finger tapping) in elderly subjects, while there seemed to be no difference in noise magnitude (121). This finding was interpreted as a result of decreased vascular reactivity in elderly subjects, and as such partially in agreement with the earlier finding, using Doppler flow measurements, that vascular CO₂ reactivity decreases within age, at least in women (80).

Other groups have found that the hemodynamic response to activation has the same amplitude and form in young and elderly subjects, but that a higher noise-level in the latter group causes the number of activated voxels to be lower on average (36; 61). The causes of this predominantly low-frequency noise (37) are not obvious, and should probably be explored further with sampling of physiological noise signals.

It has been suggested that the variability in results regarding whether higher or similar responses are found in elderly could be related to regional differences, with visual cortex display a larger propensity to age-related changes. This is partially corroborated by Aizenstein et al. (2) who find a higher fraction of negatively activated voxels in visual, but not in motor cortex. In this study the negative signal deviations are thought to represent true neuronal deactivations, due to unconstrained activity in the baseline conditions. Alternatively, they could be due to a vascular steal phenomenon, but no direct evidence in favor that mechanism has been found.

There are a number of possible reasons for lower response in elderly subjects (36). First of all lower vascular reactivity has been demonstrated, and could be due to thickening of vascular walls due to arteriosclerotic changes. General age-related decreased in CBF and M_{O₂} have also been demonstrated, but should, however, only influence BOLD if they lead to an altered OEF and venous hemoglobin. There seems to be no direct investigations of age-related changes in the physiological activation response, including the evoked changes in CBF, CBV and M_{O₂}. Interestingly, there are also age-related changes in parameters such as arterial saturation (5), but these are modest, and probably too small to have an influence on BOLD.

Looking at the other end of the age spectrum, it should be noted that very different responses have been found in infants (10). While there may be specific causes, related to developmental stage, there are experimental results indicating that a major part of this difference may be related to the sleeping state in which infants are usually investigated (9; 11). This will be discussed in the subsequent section.

5.6.2 Investigations during sleep

Probably the first occasion on which $BOLD_A$ responses were investigated in sleeping subjects was the study by Born et al (12). In this study young infants were studied with visual stimulation, and due to their age they they were necessarily sleeping either spontaneously or due to sedation. In both cases a negative $BOLD_A$ response was noted, but it the underlying causes of this surprising finding were unclear. Later studies showed that the negative $BOLD_A$ response was associated with flow decreases as measured using a spin labeling technique (11). Furthermore, a similar negative response was found in adult sleeping subjects, using BOLD MRI, as well as PET measurements of CBF (9). This lead to the conclusion that the negative $BOLD_A$ was associated with sleep rather than age or anesthesia, and probably was caused by deactivation, rather than an alteration of the BOLD mechanism. Generally, are more anterior location of the responding areas in visual cortex were seen during sleep than in the awake state.

Similar findings have been done using auditory stimulation, in which case the areas showing BOLD signal decreases during sleep were shown to be much more widespread than those activated positively in the awake state. An important recent study (25) demonstrates that $BOLD_A$ decreases during sleep are correlated with simultaneously obtained electro-physiological recordings, showing signs of neuronal deactivation. This has lead to the hypothesis that the specific response pattern seen during sleep is due altered functional connectivity, and deactivation which may be part of a protective response during certain sleep stages. Currently, no evidence seems to speak for a different coupling between neuronal activity and flow changes, or between flow and BOLD changes.

6 Using BOLD for quantification

6.1 Cerebral blood volume

Cerebral blood volume is directly proportional to the content of deoxy-hemoglobin in the brain, and is therefore a main determinant of the baseline signal as well as of BOLD responses. This was exploited by van Zijl et al. who showed that CBV can be calculated from BOLD R_2 measurements during varying degrees of arterial hypoxemia (152). The method rests on two assumptions, namely that oxygen delivery remains constant during mild hypoxia, and that relative CBV is related to relative CBF as described by the Grubb equation. CBV can then be expressed in terms of the measurable quantities S_aO_2 and hemoglobin concentration, and this enables the calculation of normoxia blood volume from the slope between R_2 and S_aO_2 . A similar method was proposed by the same group, using CO_2 instead of hypoxia to create changes in cerebral oxygenation (148). Hypercapnia, as opposed to during hypoxia, causes the OEF to change, and CBV can therefore no longer be estimated based on arterial saturation values only. When the OEF is known from invasive measurements of arterio-venous differences, the resting CBV can be calculated from the slope of the R_2 vs OEF curve.

A high correlation between the BOLD response magnitudes due to hypercapnia and neural activation, has been demonstrated. This is due to the variation of CBV, or blood volume fraction, across voxels, with high-CBV voxels showing both higher $BOLD_A$ and $BOLD_B$ responses. It

has therefore been proposed to correct BOLD_A maps for the CBV related modulation, thereby obtaining a more direct picture of the distribution of neural-vascular activity, rather than vascular volume fraction. This method was originally proposed by Bandettini and Wong (7), who demonstrated that the apparent activation in large vascular structures during neural stimulation could be diminished by correction for the spatial variation in the hypercapnic response. More recently this method — hypercapnic normalisation — has been shown not only to reduce the variation between subjects but also between experiments obtained at different field strength (22). Whether this translates to an increased sensitivity in brain mapping group studies has not yet been shown directly, and currently the method is not used routinely in that context.

6.2 Regional O₂ saturation

As discussed in the previous sections, the oxygen extraction fraction and thereby the venous oxygen saturation, are major determinants of the BOLD part of the baseline signal, as well as of BOLD responses. However, the derivation of an analytical expression of the relationship between blood oxygenation and tissue transversal relaxation rate is not trivial. One reason for this - from a physiological point of view - is that the signal measured from a region of interest depends just as much on blood volume as on blood oxygen saturation, and that these parameters most often will change together. Technically, one also has to consider that the effect of intravascular deoxy-hemoglobin is different in the intra- and compartments, and also depends strongly on the size of the vessels, relative to typical proton diffusion distances, as well as on their orientation relative to the main magnetic field. The sensitivity to oxygenation changes, and the compartmental selectivity are therefore also quite dependent on the type of MRI sequence used for the experiments.

Gradient-echo sequences are sensitive to intravascular effects, but also highly sensitive to the effects of deoxy-hemoglobin. This is because static inhomogeneities around vessels are not refocused. For practical purposes this mechanism is usually seen as an advantage, because it amplifies the signal, and provides more sensitivity towards the oxygenation changes. However, it emphasises larger vessels more than small, because the large vessels creates larger areas of inhomogeneity, and this is unfortunate since it confers less spatial selectivity towards the potentially small region in which neurons are activated. Spin-echo sequences on the other hand are insensitive to spatial inhomogeneities that are large compared to the average proton diffusion distance. Furthermore, the non-refocusable signal loss, due to diffusion in the inhomogeneous magnetic field caused by deoxy-hemoglobin in the erythrocytes, is much larger within vessel than outside. At the cost of a lower sensitivity spin-echo sequences therefore primarily detect intra-vascular effects, and supply results that are more weighted towards the oxygenation changes within smaller vessels.

Various approaches to quantifying oxygen saturation have been proposed, based either on spin-echo or gradient-echo measurements. An and Lin (3) describe a method based on a signal for MR signal behavior in the static dephasing regime, i.e., when pure T₂ or spin-spin relaxation effects can be ignored. This method uses gradient-echo (T₂*-weighted) data, and primarily deals with the effects of intra-vascular oxygenation change. A multi gradient-echo sequence is used to provide data from which venous blood volume and the static inhomogeneity contribution to

R_2^* can be estimated. The venous oxygenation may then be inferred following a relationship between intra-vascular resonance frequency and oxygenation, originally due to (158). In accordance with other literature OEF values of 0.4 were found for normal volunteers. The technique has later been applied in combination with perfusion imaging to obtain estimates of M_{O_2} in stroke patients (91); in this case only relative values are reported (by comparison with the unaffected hemisphere), most likely because of the problems associated with absolute blood flow determination using non-invasive MR techniques.

Another technique was presented by the group of van Zijl et al. The approach is based on a comprehensive theory for the intra-vascular relaxation rate changes due to exchange between protons in plasma and erythrocytes, and is therefore directed towards the results obtained with spin-echo measurements (113; 152). This technique provided resting state OEF values of 0.3, with a decrease to 0.2 during in the occipital cortices during visual stimulation; this latter finding directly supports the view that BOLD responses are due to disproportionate changes of CBF and M_{O_2} , rather than other effects such as CBV changes (113). Because only intravascular effects are included in the signal expressions, the vascular structures must be delineated using thresholding of T_2 maps, and this may represent a practical problem due to partial volume effects, and the small separation between tissue and venous T_2 . The technique was later extended to gradient-echo based data, by combination with a recent method for suppression of intravascular signals. This allows the absolute determination of changes in blood volume as well as ΔR_2^* , from which the average oxygen saturation can be estimated (99; 158).

6.3 Oxygen metabolism

A number of reports have described methods to estimate changes in M_{O_2} based on the BOLD technique. The central observation forming the basis for these methods is that for a given flow change the BOLD response to hypercapnia is much larger than that to functional activation. This difference is ascribed to the increase in oxygen metabolism that is assumed to take place during functional activation.

Specifically, it has been shown that the BOLD response to visual stimulation is reduced by 50–75% relative to the hypercapnic response when conditions are adjusted to give the same flow change (57; 85). For an illustration of these results see figure 4-5 in the study by Kim et al. (85). When conditions are adjusted to give the same BOLD response much higher flow changes have been found during visual than during hypercapnic stimulation (about 1.8% BOLD at 45 vs 18% flow increase (28)).

Although the formalism differs slightly between these studies, they have in common the derivation of an expression for the BOLD magnitude (relative to the baseline signal (28; 57), or as ΔR_2^* (85)), as a function of CBF and M_{O_2} . Important parameters are α , which is the exponent in the CBV-CBF relation (eq. 17), and β , which indicate the degree of non-linearity in the dependency of tissue ΔR_2^* on the susceptibility shift caused by deoxy-hemoglobin (in the present study assumed to be 1 for large and 2 for small vessels, eqs. 13–14). In all models a subject and region specific constant, usually labeled M , is calculated from BOLD and CBF data obtained under graded hypercapnia. This constant describes the relationship between relative BOLD and CBF change. The physiological determinants for M are the baseline blood volume, and the

baseline deoxy-hemoglobin concentration. It is the determination of this calibration constant that enables the relative M_{O_2} during functional activation to be calculated from measured values of CBF and BOLD response.

In the study by Kim et al. (85), the values of the calibration constants are determined using data from an earlier study with two levels of hypercapnia (128). An extra parameter κ is introduced to describe the relation between total fractional blood volume change, and the change in BOLD-visible, i.e. venous blood volume. Depending on whether this volume is assumed to be significant or not ($\kappa=1$ or 0, i.e. all or none of the blood volume change affects the BOLD signal), the relative change in M_{O_2} is determined to be 16 and 30%, respectively. The reason for this is that both blood volume and M_{O_2} increases are assumed to decrease the $BOLD_A$ response, and when the blood volume changes are assumed to be large, a smaller fraction of the decrease (relative to $BOLD_B$) is attributed to M_{O_2} effects. In the study by Hoge et al. (57) both graded hypercapnia and graded visual stimulation are employed, and a linear relation between relative CBF- and relative M_{O_2} -changes during activation is determined with the ratio being 2:1. This corresponds quite well to the model obtained with blood volume contribution by Kim et al, where the average functional flow increase was 44%.

In a study performed at 3 T the BOLD responses during hypercapnic and visual stimulation are more similar in magnitude, and the estimated M_{O_2} changes were only 5% (134). This work differs from the studies cited above in using 3 vs. 1.5 T field strength, and by not adjusting for potential differences in CBF and CBV during the two conditions. It is unclear to which degree these factors may have contributed to the quantitative difference between the results.

It may be speculated that the difference in results between the original studies of Fox et al. and several newer estimates of M_{O_2} could be caused by regional differences between primary motor and primary visual cortex. However, a recent calibrated fMRI study has also shown high (16%) M_{O_2} increases in primary motor cortex during a graded activation paradigm (77).

As seen from the discussion above, the calibrated fMRI method rests on the assumption that the responses to hypercapnia and neural activation are similar in all respects, except for the change in M_{O_2} . At least one additional factor should be taken into account, namely the increase in arterial oxygenation (P_aO_2) that accompanies hypercapnia (83; 126). As shown in fig. 8A this is an independent factor that causes an up to 20% enhancement in the $BOLD_B$ response. The consequence of this would probably be an overestimation of the calibration factors, as derived from graded hypercapnia experiments. Using the data and procedure of Kim et al. (85) and assuming that 20% of the hypercapnic $BOLD_B$ response is due to hyperoxia, only leads to a 10% decrease in the estimated relative M_{O_2} during activation. The data of Davis et al. seems somewhat more susceptible to this effect, in that a 20% overestimation of the calibration factor leads to a 40% reduction of the average relative M_{O_2} estimate during activation. In conclusion hyperoxia does not fully explain the observed BOLD difference between hypercapnic and neural activation, but may have lead to some overestimation of the M_{O_2} -contribution during activation.

Potentially a difference in vascular dilation pattern could also explain the difference between the two types of BOLD responses. Due to the global nature of the hypercapnic response, it could be weighted more toward superficial and possibly larger veins than the functional response, causing the effectively contributing blood volume to be larger (larger value of the κ parameter of (85)). This would cause an enhancement of the hypercapnic response. An effect of such

structural differences has not been addressed directly in any of the calibrated fMRI studies, but could possibly be investigated with high-resolution imaging.

7 Conclusion

In present work several aspects of the BOLD mechanism have been reviewed and results from previous studies by the present author, as well as others, have been compared to those of a numerical compartment model of cerebral O_2 and oxy-/deoxy-hemoglobin balance. The model approach is based on approaches described in the literature but some aspects are novel. This includes the direct inclusion of both arterial, capillary and venous compartments, the presence of PS_cO_2 as an adjustable parameter, and the application of the model to various physiological situations such as arterial hypoxemia.

For the sake of clarity effects related to functional neural activation and those that are not are described separately, using the abbreviations $BOLD_A$ and $BOLD_B$. In the following, some general observations will be emphasised.

The literature provides few quantitative estimates of the oxygen O_2 diffusibility, PS_cO_2 , but many assumptions. In the present study it shown that this parameters is indeed of great importance for the magnitude of BOLD responses, because it determines whether independence of CBF and M_{O_2} changes can be assumed. However, there is no experimental evidence Many studies seem to be compatible with a PS_cO_2 value of 3–5000 ml·hg⁻¹·min⁻¹. In this range the present results indicate that CBF and M_{O_2} are independent when a low (150 $\mu\text{mol}\cdot\text{hg}^{-1}\text{min}^{-1}$) value of $M_{O_2}^*$ is assumed but non-linearly related for higher values (250 $\mu\text{mol}\cdot\text{hg}^{-1}\text{min}^{-1}$). In other words, the existence of an oxygen limitation regime may be assumed for states of relatively high metabolism and low flow, but the precise values of CBF and M_{O_2} at which the transition to this regime occurs, are not well known.

Hypercapnia has often been shown to cause an increase in baseline BOLD signal, and the present modeling confirms that this is due mainly to the increase in flow and the associated decrease in oxygen extraction fraction. Only during pronounced hypocapnia is the pH change (decrease) expected to exert some influence. Hyperoxia on the other hand accompanies both hyper- and hypocapnia, and according to the modeling results has a non-negligible effect on the BOLD signal. It should also be noted that the response is not independent of baseline $M_{O_2}^*$, and is smaller in the oxygen limitation regime (i.e. for high $M_{O_2}^*$ -values).

The BOLD response to functional activation has also been shown in several reports to be dependent on baseline P_aCO_2 , and it is a general finding that it is decreased in hypercapnia. During hypocapnia both increases and decreases have been described. The present modeling results predict a decrease in hypercapnia which is mainly due to the increase in baseline flow, and which is seen even when the flow functional flow response is assumed to be unlimited by an elevated baseline value. However, at extreme hypercapnia exhausting of the vasodilatory capacity may be an additional factor limiting the $BOLD_A$ response. Generally an increase in $BOLD_A$ responsivity during hypocapnia is predicted, but under the oxygen limitation regime (high $M_{O_2}^*$ values, and hypocapnia) a decrease in the response, partly due to pH effects, is predicted.

Hypoxia and hyperoxia was shown early to cause reciprocal changes in BOLD signal. Hy-

poxia cause a negative $BOLD_B$ response, in spite of CBF increase. In contrast to the flow increase caused by hypercapnia, the hypoxic flow increase is associated no or only minor changes in the oxygen extraction fraction. In this sense the mechanism of the BOLD responses caused by changes in P_aCO_2 and P_aO_2 are different, and in the case of hypoxia it is caused by an increase in deoxy-hemoglobin in all of the vascular compartments.

Recently hypoxia has been shown to decrease the magnitude of the $BOLD_A$ response (to visual stimulation). The present modeling results suggest that this may be due to blood volume effects, but limitations of the vascular response to activation may also play a role in severe hypoxia.

The hematocrit, or more precisely the hemoglobin concentration, is another physiological factor of known importance for BOLD mechanisms. Changes in hematocrit are generally accompanied by changes in flow, and the effect on the BOLD signal seems to be tightly linked to these flow changes. Changes in the oxygen carrying capacity for other reasons may influence BOLD mechanisms in a similar way, but these effects have not been investigated experimentally.

In general many different factors may contribute to a substantial intra- and inter-individual variation in BOLD magnitude. Precisely how large a fraction of the this variation that could be explained by variations in measurable physiological variables, is currently unknown, and future studies should seek to address this issue. Measurements of these parameters in combination with a modeling approach such as the present one, is expected to add significantly to the quantitative understanding of BOLD signals, as well as of brain oxygenation.

Apart from its widespread use for brain mapping, BOLD imaging has a number of potentially interesting applications. Some regard clinical conditions such as diseases with altered perfusion or vascularity, others the investigation of pharmacological effects. The recent rapid development in modeling the BOLD response holds promise that such investigations will be possible, with appropriate control for covariation in baseline physiological factors.

Practical issues include the availability of measurements of BOLD and related hemodynamic factors, that are accurate enough to provide the necessary information for modeling. However, this area continues to develop due to continued improvements and innovation in technology for CBF and CBV measurements, as well as the more widespread availability of high-field scanners.

It may therefore be concluded that the understanding of BOLD imaging has progressed rapidly during the later years, and now offers a theoretical basis that will allow the development of the technique in new areas.

References

- [1] R. Abounader, J. Vogel, and W. Kuschinsky. Patterns of capillary plasma perfusion in brains in conscious rats during normocapnia and hypercapnia. *Circ Res*, 76:120–6, 1995. 25
- [2] H.J. Aizenstein, K.A. Clark, M.A. Butters, J. Cochran, V.A. Stenger, C.C. Meltzer, C.F. Reynolds, and C.S. Carter. The BOLD hemodynamic response in healthy aging. *J Cogn Neurosci*, 16:786–93, 2004. 56
- [3] H. An and W. Lin. Quantitative measurements of cerebral blood oxygen saturation using magnetic resonance imaging. *J Cereb Blood Flow Metab*, 20:1225–36, 2000. 58
- [4] B.M. Ances, D.G. Buerk, J.H. Greenberg, and J.A. Detre. Temporal dynamics of the partial pressure of brain tissue oxygen during functional forepaw stimulation in rats. *Neurosci Lett*, 306:106–10, 2001. 19
- [5] O. Andersen, P.D. Wimberley, N. Andersen, and I.H. Gothgen. Arterial oxygen status determined with routine ph/blood gas equipment and multi-wavelength hemoximetry: reference values, precision, and accuracy. *Scand J Clin Lab Invest Suppl*, 203:57–66, 1990. 17, 56
- [6] R. Bakalova, T. Matsuura, and I. Kanno. The cyclooxygenase inhibitors indomethacin and rofecoxib reduce regional cerebral blood flow evoked by somatosensory stimulation in rats. *Exp Biol Med*, 227:465–73, 2002. 54
- [7] P. A. Bandettini and E. C. Wong. A hypercapnia-based normalization method for improved spatial localization of human brain activation with fMRI. *NMR Biomed*, 10:197–203, 1997. 8, 24, 46, 49, 58
- [8] C. Bock, B. Schmitz, C.M. Kerskens, M.L. Gyngell, K.A. Hossmann, and M. Berlage. Functional MRI of somatosensory activation in rat: effect of hypercapnic up-regulation on perfusion- and BOLD-imaging. *Magn Reson Med*, 39:457–61, 1998. 49
- [9] A.P. Born, I. Law, T.E. Lund, E. Rostrup, L.G. Hanson, G. Wildschiodtz, H.C. Lou, and O.B. Paulson. Cortical deactivation induced by visual stimulation in human slow-wave sleep. *Neuroimage*, 17:1325–35, 2002. 56, 57
- [10] A.P. Born, M.J. Miranda, E. Rostrup, P.B. Toft, B. Peitersen, H.B. Larsson, and H.C. Lou. Functional magnetic resonance imaging of the normal and abnormal visual system in early life. *Neuropediatrics*, 31:24–32, 2000. 56
- [11] A.P. Born, E. Rostrup, M.J. Miranda, H.B. Larsson, and H.C. Lou. Visual cortex reactivity in sedated children examined with perfusion MRI (FAIR). *Magn Reson Imaging*, 20:199–205, 2002. 56, 57

- [12] P. Born, E. Rostrup, H. Leth, B. Peitersen, and H. Lou. Change of visually induced cortical activation patterns during development. *Lancet*, 347:543–543, 1996. 57
- [13] J. L. Boxerman, P. A. Bandettini, K. K. Kwong, J. R. Baker, T. L. Davis, B. R. Rosen, and R. M. Weisskoff. The intravascular contribution to fMRI signal change: Monte Carlo modeling and diffusion-weighted studies in vivo. *Magn Reson Med*, 34:4–10, 1995. 14
- [14] S. Brannan, M. Liotti, G. Egan, R. Shade, L. Madden, R. Robillard, B. Abplanalp, K. Stofer, D. Denton, and P.T. Fox. Neuroimaging of cerebral activations and deactivations associated with hypercapnia and hunger for air. *Proc Natl Acad Sci U S A*, 98:2029–34, 2001. 33
- [15] H. Bruhn, P. Fransson, and J. Frahm. Modulation of cerebral blood oxygenation by indomethacin: MRI at rest and functional brain activation. *J Magn Reson Imaging*, 13:325–34, 2001. 54
- [16] H. Bruhn, A. Kleinschmidt, H. Boecker, K. D. Merboldt, W. Hanicke, and J. Frahm. The effect of acetazolamide on regional cerebral blood oxygenation at rest and under stimulation as assessed by MRI. *J Cereb Blood Flow Metab*, 14:742–748, 1994. 54
- [17] A. Buck, C. Schirlo, V. Jasinsky, B. Weber, C. Burger, G. K. von Schulthess, E. A. Koller, and V. Pavlicek. Changes of cerebral blood flow during short-term exposure to normobaric hypoxia. *J Cereb Blood Flow Metab*, 18:906–910, 1998. 33, 37
- [18] H. Bundgaard, K. Jensen, G. E. Cold, B. Bergholt, R. Frederiksen, and S. Pless. Effects of perioperative indomethacin on intracranial pressure, cerebral blood flow, and cerebral metabolism in patients subjected to craniotomy for cerebral tumors. *J Neurosurg Anesthesiol*, 8:273–279, 1996. 54
- [19] R. B. Buxton and L. R. Frank. A model for the coupling between cerebral blood flow and oxygen metabolism during neural stimulation. *J Cereb Blood Flow Metab*, 17:64–72, 1997. 9, 13, 14, 25, 42
- [20] R. B. Buxton, E. C. Wong, and L. R. Frank. Dynamics of blood flow and oxygenation changes during brain activation: the balloon model. *Magn Reson Med*, 39:855–864, 1998. 10, 16
- [21] R.B. Buxton, K. Uludag, D.J. Dubowitz, and T.T. Liu. Modeling the hemodynamic response to brain activation. *Neuroimage*, 23 Suppl 1:S220–33, 2004. 9, 10, 45
- [22] E.R. Cohen, E. Rostrup, K. Sidaros, T.E. Lund, O.B. Paulson, K. Ugurbil, and S.G. Kim. Hypercapnic normalization of BOLD fMRI: comparison across field strengths and pulse sequences. *Neuroimage*, 23:613–24, 2004. 58
- [23] E.R. Cohen, K. Ugurbil, and S.G. Kim. Effect of basal conditions on the magnitude and dynamics of the blood dependent fMRI response. *J Cereb Blood Flow Metab*, 22:1042–53, 2002. 8, 29, 30, 46, 47

- [24] D.R. Corfield, K. Murphy, O. Josephs, L. Adams, and R. Turner. Does hypercapnia-induced cerebral vasodilation modulate the hemodynamic response to neural activation? *Neuroimage*, 13:1207–11, 2001. 43, 46
- [25] M. Czisch, R. Wehrle, C. Kaufmann, T.C. Wetter, F. Holsboer, T. Pollmacher, and D.P. Auer. Functional mri during sleep: BOLD signal decreases and their electrophysiological correlates. *Eur J Neurosci*, 20:566–74, 2004. 57
- [26] S.R. Dager and S.D. Friedman. Brain imaging and the effects of caffeine and nicotine. *Ann Med*, 32:592–9, 2000. 55
- [27] S.R. Dager, M.E. Layton, W. Strauss, T.L. Richards, A. Heide, S.D. Friedman, A.A. Artru, C.E. Hayes, and S. Posse. Human brain metabolic response to caffeine and the effects of tolerance. *Am J Psychiatry*, 156:229–37, 1999. 55
- [28] T. L. Davis, K. K. Kwong, R. M. Weisskoff, and B. R. Rosen. Calibrated functional MRI: Mapping the dynamics of oxidative metabolism. *Proc Natl Acad Sci U S A*, 95:1834–1839, 17 1998. 9, 24, 59
- [29] E.M. Dopperberg, A. Zauner, R. Bullock, J.D. Ward, P.P. Fatouros, and H.F. Young. Correlations between brain tissue oxygen tension, carbon dioxide tension, pH, and cerebral blood flow – a better way of monitoring the severely injured brain? *Surg Neurol*, 49:650–4, 1998. 19
- [30] J.F. Dunn, Y.Z. Wadghiri, and M.E. Meyerand. Regional heterogeneity in the brain’s response to hypoxia measured using BOLD MR imaging. *Magn Reson Med*, 41:850–854, 1999. 37
- [31] T.Q. Duong, C. Iadecola, and S.G. Kim. Effect of hyperoxia, hypercapnia, and hypoxia on cerebral interstitial oxygen tension and cerebral blood flow. *Magn Reson Med*, 45:61–70, 2001. 19, 33
- [32] T.Q. Duong and S.G. Kim. In vivo MR measurements of regional arterial and venous blood volume fractions in intact rat brain. *Magn Reson Med*, 43:393–402, 2000. 18
- [33] M.V. Dutka, B.E. Scanley, M.D. Does, and J.C. Gore. Changes in CBF-BOLD coupling detected by MRI during and after repeated transient hypercapnia in rat. *Magn Reson Med*, 48:262–70, 2002. 49
- [34] L. Edvinsson and D. Krause. *Cerebral Blood Flow and Metabolism*. Lippincott Williams & Wilkins, 2002. 27
- [35] I. Ellingsen, A. Hauge, G. Nicolaysen, M. Thoresen, and L. Walloe. Changes in human cerebral blood flow due to step changes in $P_{A}O_2$ and $P_{A}CO_2$. *Acta Physiologica Scandinavica*, 129:157–163, 1987. 33

- [36] M. Esposito, L.Y. Deouell, and A. Gazzaley. Alterations in the BOLD fMRI signal with ageing and disease: a challenge for neuroimaging. *Nat Rev Neurosci*, 4:863–72, 2003. 56
- [37] M. Esposito, E. Zarahn, G.K. Aguirre, and B. Rypma. The effect of normal aging on the coupling of neural activity to the BOLD hemodynamic response. *Neuroimage*, 10:6–14, 1999. 56
- [38] K.C. Evans, R.B. Banzett, L. Adams, L. McKay, R.S. Frackowiak, and D.R. Corfield. BOLD fMRI identifies limbic, paralimbic, and cerebellar activation during air hunger. *J Neurophysiol*, 88:1500–11, 2002. 33
- [39] T.F. Floyd, J.M. Clark, R. Gelfand, J.A. Detre, S. Ratcliffe, D. Guvakov, C.J. Lambertsen, and R.G. Eckenhoff. Independent cerebral vasoconstrictive effects of hyperoxia and accompanying arterial hypocapnia at 1 ATA. *J Appl Physiol*, 95:2453–61, 2003. 34
- [40] S.S. Foo, D.F. Abbott, N. Lawrentschuk, and A.M. Scott. Functional imaging of intratumoral hypoxia. *Mol Imaging Biol*, 6:291–305, 2004. 40
- [41] P. T. Fox and M. E. Raichle. Focal physiological uncoupling of cerebral blood flow and oxidative metabolism during somatosensory stimulation in human subjects. *Proc Natl Acad Sci*, 83:1140–1144, 1986. 42, 43, 44, 47
- [42] J. Frahm, K. D. Merboldt, W. Hanicke, A. Kleinschmidt, and H. Boecker. Brain or vein-oxygenation or flow? On signal physiology in functional MRI of human brain activation. *NMR Biomed*, 7:45–53, 1994. 7
- [43] K. Garde, E. Rostrup, P. B. Toft, and O. Henriksen. In vivo monitoring of cerebral energy metabolism during hypoxic hypoxemia. A ^{31}P and ^1H magnetic resonance study. *Acta Physiologica Scandinavica*, 145(2):185–191, 1995. 34
- [44] A. Gjedde. Cerebral blood flow change in arterial hypoxemia is consistent with negligible oxygen tension in brain mitochondria. *Neuroimage*, 17:1876–81, 2002. 21
- [45] A. Gjedde, P.H. Poulsen, and L. Ostergaard. On the oxygenation of hemoglobin in the human brain. In *Oxygen Transport to Tissue*, volume 471, book chapter 9, pages 67–81. Plenum, 1999. 9, 21
- [46] J. H. Greenberg, A. Alavi, M. Reivich, D. Kuhl, and B. Uzzell. Local cerebral blood volume response to carbon dioxide in man. *Circulation Research*, 43:324–331, 1978. 28
- [47] P. Grieb, R.E. Forster, D. Strome, C.W. Goodwin, and P.C. Pape. O_2 exchange between blood and brain tissues studied with $^{18}\text{O}_2$ dilution technique. *J Appl Physiol*, 58:1929–41, 1985. 19
- [48] J.R. Griffiths, N.J. Taylor, F.A. Howe, M.I. Saunders, S.P. Robinson, P.J. Hoskin, M.E. Powell, M. Thoumine, L.A. Caine, and H. Baddeley. The response of human tumors to carbogen breathing, monitored by gradient-recalled echo magnetic resonance imaging. *Int J Radiat Oncol Biol Phys*, 39:697–701, 1997. 41

- [49] R. L. Grubb, Jr., M. E. Raichle, J. O. Eichling, and M. M. Ter Pogossian. The effects of changes in $P_{A}CO_2$ on cerebral blood volume, blood flow, and vascular mean transit time. *Stroke*, 5:630–639, 1974. 17, 28
- [50] S. Gustard, E.J. Williams, L.D. Hall, J.D. Pickard, and T.A. Carpenter. Influence of baseline hematocrit on between-subject BOLD signal using gradient echo and asymmetric spin echo EPI. *Magnetic Resonance Imaging*, 21:599–607, 2003. 53
- [51] T. C. Harvey, M. E. Raichle, M. H. Winterborn, J. Jensen, N. A. Lassen, N. V. Richardson, and A. R. Bradwell. Effect of carbon dioxide in acute mountain sickness: a rediscovery. *Lancet*, 2:639–641, 1988. 27
- [52] G.M. Hathout, S.S. Gambhir, R.K. Gopi, K.A. Kirlew, Y. Choi, G. So, D. Gozal, R. Harper, R.B. Lufkin, and R. Hawkins. A quantitative physiologic model of blood oxygenation for functional magnetic resonance imaging. *Invest Radiol*, 30:669–82, 1995. 9
- [53] R. Hemmingsen, M. Hertz, and D. I. Barry. The effect of propranolol on cerebral oxygen consumption and blood flow in the rat: measurements during normocapnia and hypercapnia. *Acta Physiol Scand*, 105:274–281, 1979. 54
- [54] L. Henriksen, O.B. Paulson, and R.J. Smith. Cerebral blood flow following normovolemic hemodilution in patients with high hematocrit. *Ann Neurol*, 9:454–7, 1981. 39
- [55] O. Henriksen, H. B. W. Larsson, P. Ring, E. Rostrup, A. Steensgaard, M. Stubgaard, F. Ståhlberg, L. Søndergaard, C. Thomsen, and P. B. Toft. Functional MR imaging at 1.5 T. *Acta Radiologica*, 34:101–103, 1993. 7
- [56] S. Herold, M. M. Brown, R. S. Frackowiak, A. O. Mansfield, D. J. Thomas, and J. Marshall. Assessment of cerebral haemodynamic reserve: correlation between PET parameters and CO_2 reactivity measured by the intravenous ^{133}Xe injection technique. *J.Neurol.Neurosurg.Psychiatry*, 51:1045–1050, 1988. 40
- [57] R. D. Hoge, J. Atkinson, B. Gill, G. R. Crelier, S. Marrett, and G. B. Pike. Investigation of BOLD signal dependence on cerebral blood flow and oxygen consumption: the deoxyhemoglobin dilution model. *Magn Reson Med*, 42:849–863, 1999. 9, 14, 24, 44, 46, 59, 60
- [58] E.W. Hsu, L.W. Hedlund, and J.R. MacFall. Functional MRI of the rat somatosensory cortex: effects of hyperventilation. *Magn Reson Med*, 40:421–6, 1998. 46
- [59] Y.Y. Hsu, C.N. Chang, S.M. Jung, K.E. Lim, J.C. Huang, S.Y. Fang, and H.L. Liu. Blood oxygenation level-dependent MRI of cerebral gliomas during breath holding. *J Magn Reson Imaging*, 19:160–7, 2004. 41
- [60] A.G. Hudetz. Mathematical model of oxygen transport in the cerebral cortex. *Brain Research*, 817:75–83, 1999. 13, 24

- [61] S.A. Huettel, J.D. Singerman, and G. McCarthy. The effects of aging upon the hemodynamic response measured by functional mri. *Neuroimage*, 13:161–175, 2001. 56
- [62] P.D. Hurn and R.J. Traystman. Changes in arterial gas tension. In *Cerebral Blood Flow and Metabolism*, book chapter 24, pages 384–394. Lippincott Williams & Wilkins, 2002. 27, 33, 34
- [63] H. Ito, M. Ibaraki, I. Kanno, H. Fukuda, and S. Miura. Changes in the arterial fraction of human cerebral blood volume during hypercapnia and hypocapnia measured by positron emission tomography. *J Cereb Blood Flow Metab*, 25:852–7, 2005. 18
- [64] H. Ito, I. Kanno, M. Ibaraki, H. Hatazawa, and S. Miura. Changes in human cerebral blood flow and cerebral blood volume during hypercapnia and hypocapnia measured by positron emission tomography. *J Cereb Blood Flow Metab*, 23:665–670, 2003. 28, 29
- [65] H. Ito, K. Takahashi, J. Hatazawa, S. G. Kim, and I. Kanno. Changes in human regional cerebral blood flow and cerebral blood volume during visual stimulation measured by positron emission tomography. *J Cereb Blood Flow Metab*, 21(5):608–12, 2001. 18
- [66] H. Ito, I. Yokoyama, H. Iida, T. Kinoshita, J. Hatazawa, E. Shimosegawa, T. Okudera, and I. Kanno. Regional differences in cerebral vascular response to $P_a\text{CO}_2$ changes in humans measured by positron emission tomography. *J Cereb Blood Flow Metab*, 20:1264–70, 2000. 27
- [67] K.P. Ivanov, A.N. Derry, E.P. Vovenko, M.O. Samoilov, and D.G. Semionov. Direct measurements of oxygen tension at the surface of arterioles, capillaries and venules of the cerebral cortex. *Pflugers Arch*, 393:118–20, 1982. 16, 19
- [68] L.K. Jacobsen, J.C. Gore, P. Skudlarski, C.M. Lacadie, P. Jatlow, and J.H. Krystal. Impact of intravenous nicotine on BOLD signal response to photic stimulation. *Magn Reson Imaging*, 20:141–5, 2002. 55
- [69] F.F. Jobsis, J.H. Keizer, J.C. LaManna, and M. Rosenthal. Reflectance spectrophotometry of cytochrome aa3 in vivo. *J Appl Physiol*, 43:858–72, 1977. 13
- [70] B. Jodal, J. Elfverson, and C. von Essen. Cerebral blood flow, cerebrovascular resistance and cerebral metabolic rate of oxygen in severe arterial hypoxia in dogs. *Acta Neurol Scand*, 60:26–35, 1979. 33
- [71] A.J. Johnston, L.A. Steiner, A.K. Gupta, and D.K. Menon. Cerebral oxygen vasoreactivity and cerebral tissue oxygen reactivity. *Br J Anaesth*, 90:774–86, 2003. 33, 34
- [72] S.S. Kannurpatti, B.B. Biswal, and A.G. Hudetz. Baseline physiological state and the fMRI-BOLD signal response to apnea in anesthetized rats. *NMR Biomed*, 16:261–8, 2003. 38

- [73] K. Kashikura, J. Kershaw, A. Kashikura, T. Matsuura, and I. Kanno. Hyperoxia-enhanced activation-induced hemodynamic response in human V1: an fMRI study. *Neuroreport*, 11:903–6, 2000. 49, 50
- [74] I.G. Kassissia, C.A. Goresky, C.P. Rose, A.J. Schwab, A. Simard, P.M. Huet, and G.G. Bach. Tracer oxygen distribution is barrier-limited in the cerebral microcirculation. *Circ Res*, 77:1201–11, 1995. 19
- [75] A. Kastrup, V. Happe, C. Hartmann, and M. Schabet. Gender-related effects of indomethacin on cerebrovascular CO₂ reactivity. *J Neurol Sci*, 162:127–32, 1999. 27
- [76] A. Kastrup, G. Kruger, G. H. Glover, T. Neumann-Haefelin, and M. E. Moseley. Regional variability of cerebral blood oxygenation response to hypercapnia. *Neuroimage*, 10:675–681, 1999. 27
- [77] A. Kastrup, G. Kruger, T. Haefelin, G.H. Glover, and M.E. Moseley. Changes of cerebral blood flow, oxygenation, and oxidative metabolism during graded motor activation. *Neuroimage*, 15:74–82, 2002. 24, 60
- [78] A. Kastrup, G. Kruger, T. Haefelin, and M.E. Moseley. Assessment of cerebrovascular reactivity with functional magnetic resonance imaging: Comparison of CO₂ and breath holding. *Magn Reson Imaging*, 19:13–20, 2001. 29, 38, 40
- [79] A. Kastrup, T. Li, G. Kruger, G.H. Glover, and M.E. Moseley. Relationship between cerebral blood flow changes during visual stimulation and baseline flow levels investigated with functional MRI. *Neuroreport*, 10:1751–1756, 1999. 43
- [80] A. Kastrup, T. Q. Li, A. Takahashi, G. H. Glover, and M. E. Moseley. Functional magnetic resonance imaging of regional cerebral blood oxygenation changes during breath holding. *Stroke*, 29:2641–2645, 1998. 56
- [81] L.J. Kemna and S. Posse. Effect of respiratory CO₂ changes on the temporal dynamics of the hemodynamic response in functional MR imaging. *Neuroimage*, 14:642–649, 2001. 46, 47
- [82] L.J. Kemna, S. Posse, L. Tellmann, T. Schmitz, and H. Herzog. Interdependence of regional and global cerebral blood flow during visual stimulation: an O-15-butanol positron emission tomography study. *J Cereb Blood Flow Metab*, 21:664–70, 2001. 43, 47
- [83] S. S. Kety and C. F. Schmidt. The effects of altered arterial tensions of carbon dioxide and oxygen on cerebral blood flow and cerebral oxygen consumption of normal young men. *J Clin Invest*, 27:484–492, 1948. 21, 22, 23, 24, 27, 28, 34, 35, 36, 60
- [84] A. Keyeux, D. Ochrymowicz Bemelmans, and A. A. Charlier. Induced response to hypercapnia in the two-compartment total cerebral blood volume: Influence on brain vascular reserve and flow efficiency. *J Cereb Blood Flow Metab*, 15:1121–1131, 1995. 27

- [85] S. G. Kim, E. Rostrup, H. B. W. Larsson, S. Ogawa, and O.B. Paulson. Determination of relative CMRO₂ from CBF and BOLD changes: Significant increase of oxygen consumption rate during visual stimulation. *Magn Reson Med*, 41:1152–61, 1999. 2, 6, 9, 42, 45, 49, 59, 60
- [86] S. G. Kim and K. Ugurbil. Comparison of blood oxygenation and cerebral blood flow effects in fMRI: Estimation of relative oxygen consumption change. *Magnetic Resonance in Medicine*, 38:59–65, 1997. 9
- [87] K. K. Kwong, J. W. Belliveau, D. A. Chesler, I. E. Goldberg, R. M. Weisskoff, B. P. Poncelet, D. N. Kennedy, B. E. Hoppel, M. S. Cohen, and R. Turner. Dynamic magnetic resonance imaging of human brain activity during primary sensory stimulation. *Proc.Natl.Acad.Sci.*, 89:5675–5679, 1992. 7
- [88] P.J. Laurienti, A.S. Field, J.H. Burdette, J.A. Maldjian, Y.F. Yen, and D.M. Moody. Dietary caffeine consumption modulates fMRI measures. *Neuroimage*, 17:751–7, 2002. 55
- [89] M. Lauritzen. Reading vascular changes in brain imaging: Is dendritic calcium the key? *Nat Rev Neurosci*, 6:77–85, 2005. 8
- [90] I. Law, R. C. Roach, N. V. Olsen, S. Holm, M. Nowak, T. F. Hornbein, and O. B. Paulson. Oxygen delivery to the brain during behavioral activation at acute normobaric hypoxemia. *International Congress Series*, 1235:87–98, 2002. 33, 50
- [91] J.M. Lee, K.D. Vo, H. An, A. Celik, Y. Lee, C.Y. Hsu, and W. Lin. Magnetic resonance cerebral metabolic rate of oxygen utilization in hyperacute stroke patients. *Ann Neurol*, 53:227–32, 2003. 59
- [92] S.P. Lee, T.Q. Duong, G. Yang, C. Iadecola, and S.G. Kim. Relative changes of cerebral arterial and venous blood volumes during increased cerebral blood flow: Implications for BOLD fMRI. *Magn Reson Med*, 45:791–800, 2001. 17, 18, 46
- [93] J.M. Levin, B. Frederick, M.H. Ross, J.F. Fox, H.L. Rosenberg, M.J Kaufman, N. Lange, J.H. Mendelson, B.M. Cohen, and P.F. Renshaw. Influence of baseline hematocrit and hemodilution on BOLD fMRI activation. *Magnetic Resonance Imaging*, 19:1055–1062, 2001. 53
- [94] T. Q. Li, A. Kastrup, A. M. Takahashi, and M. E. Moseley. Functional MRI of human brain during breath holding by BOLD and FAIR techniques. *Neuroimage*, 9:243–249, 1999. 38
- [95] T.Q. Li, A. Kastrup, M.E. Moseley, and G.H. Glover. Changes in baseline cerebral blood flow in humans do not influence regional cerebral blood flow response to photic stimulation. *J Magn Reson Imaging*, 12:757–62, 2000. 43

- [96] W. Lin, R. P. Paczynski, A. Celik, C. Y. Hsu, and W. J. Powers. Experimental hypoxemic hypoxia: effects of variation in hematocrit on magnetic resonance T_2^* -weighted brain images. *J Cereb Blood Flow Metab*, 18:1018–1021, 1998. 37, 39
- [97] W. Lin, R.P. Paczynski, A. Celik, C.Y. Hsu, and W.J. Powers. Effects of acute normovolemic hemodilution on T_2^* -weighted images of rat brain. *Magn Reson Med*, 40:857–64, 1998. 39
- [98] N.K. Logothetis and B.A. Wandell. Interpreting the BOLD signal. *Annu Rev Physiol*, 66:735–69, 2004. 8
- [99] H. Lu and P.C. van Zijl. Experimental measurement of extravascular parenchymal BOLD effects and tissue oxygen extraction fractions using multi-echo vasa fmri at 1.5 and 3.0 t. *Magn Reson Med*, 53:808–16, 2005. 59
- [100] D.W. Lubbers, H. Baumgartl, and W. Zimelka. Heterogeneity and stability of local PO_2 distribution within the brain tissue. *Adv Exp Med Biol*, 345:567–74, 1994. 19
- [101] D. J. Lythgoe, S. C. Williams, M. Cullinane, and H. S. Markus. Mapping of cerebrovascular reactivity using BOLD magnetic resonance imaging. *Magn Reson Imaging*, 17:495–502, 1999. 40
- [102] V. MacMillan and B.K. Siesjo. Brain energy metabolism in hypoxemia. *Scand J Clin Lab Invest*, 30:127–36, 1972. 34
- [103] M. Menzel, A. Rieger, S. Roth, J. Soukup, I. Furka, I. Miko, P. Molnar, C. Peuse, C. Hennig, and J. Radke. Comparison between continuous brain tissue pO_2 , pCO_2 , pH, and temperature and simultaneous cerebrovenous measurement using a multisensor probe in a porcine intracranial pressure model. *J Neurotrauma*, 15:265–76, 1998. 19
- [104] M.A. Mintun, B.N. Lundstrom, A.Z. Snyder, A.G. Vlassenko, G.L. Shulman, and M.E. Raichle. Blood flow and oxygen delivery to human brain during functional activity: Theoretical modeling and experimental data. *Proc Natl Acad Sci*, 98:6859–6864, 2001. 8, 21, 24, 33, 50
- [105] S. Morii, A.C. Ngai, K.R. Ko, and H.R. Winn. Role of adenosine in regulation of cerebral blood flow: effects of theophylline during normoxia and hypoxia. *Am J Physiol*, 253:H165–75, 1987. 34
- [106] T.A. Mulderink, D.R. Gitelman, M.M. Mesulam, and T.B. Parrish. On the use of caffeine as a contrast booster for BOLD fmri studies. *Neuroimage*, 15:37–44, 2002. 55
- [107] K. Nakada, D. Yoshida, M. Fukumoto, and S. Yoshida. Chronological analysis of physiological T_2^* signal change in the cerebrum during breath holding. *J Magn Reson Imaging*, 13:344–51, 2001. 38

- [108] K. Niwa, C. Haensel, M.E. Ross, and C. Iadecola. Cyclooxygenase-1 participates in selected vasodilator responses of the cerebral circulation. *Circ Res*, 88:600–8, 2001. 54
- [109] S. Ogawa, T. M. Lee, A. R. Kay, and D. W. Tank. Brain magnetic resonance imaging with contrast dependent on blood oxygenation. *Proc Natl Acad Sci*, 87:9868–9872, 1990. 7, 33
- [110] S. Ogawa, T. M. Lee, A. S. Nayak, and P. Glynn. Oxygenation-sensitive contrast in magnetic resonance image of rodent brain at high magnetic fields. *Magnetic Resonance in Medicine*, 14:68–78, 1990. 7
- [111] S. Ogawa, R. S. Menon, D. W. Tank, S. G. Kim, H. Merkle, J. M. Ellermann, and K. Ugurbil. Functional brain mapping by blood oxygenation level-dependent contrast magnetic resonance imaging. a comparison of signal characteristics with a biophysical model. *Biophys.J.*, 64:803–812, 1993. 7, 9, 14, 37
- [112] S. Ogawa, D. W. Tank, R. Menon, J. M. Ellermann, S. G. Kim, H. Merkle, and K. Ugurbil. Intrinsic signal changes accompanying sensory stimulation: functional brain mapping with magnetic resonance imaging. *Proc Natl Acad Sci*, 89:5951–5955, 1992. 7
- [113] J.M. Oja, J.S. Gillen, R.A. Kauppinen, M. Kraut, and P.C. van Zijl. Determination of oxygen extraction ratios by magnetic resonance imaging. *J Cereb Blood Flow Metab*, 19:1289–95, 1999. 59
- [114] J. Olesen, O. B. Paulson, and N. A. Lassen. Regional cerebral blood flow in man determined by the initial slope of the clearance of intra-arterially injected ^{133}Xe . *Stroke*, 2:519–540, 1971. 27
- [115] L. Ostergaard, D.A. Chesler, R.M. Weisskoff, A.G. Sorensen, and B.R. Rosen. Modeling cerebral blood flow and flow heterogeneity from magnetic resonance residue data. *J Cereb Blood Flow Metab*, 19:690–9, 1999. 25
- [116] S. Posse, L.J. Kemna, B. Elghahwagi, S. Wiese, and V. G. Kiselev. Effect of graded hypo- and hypercapnia on fMRI contrast in visual cortex: Quantification of T_2^* changes by multiecho EPI. *Magn Reson Med*, 46:264–271, 2001. 8, 29, 46
- [117] S. Posse, U. Olthoff, M. Weckesser, L. Jancke, H.W. Gartner, and S.R. Dager. Regional dynamic signal changes during controlled hyperventilation assessed with blood oxygen level-dependent functional MR imaging. *Am J Neuroradiol*, 18:1763–70, 1997. 29
- [118] F. Prielmeier, Y. Nagatomo, and J. Frahm. Cerebral blood oxygenation in rat brain during hypoxic hypoxia. quantitative MRI of effective transverse relaxation rates. *Magnetic Resonance in Medicine*, 31:678–681, 1994. 37
- [119] M.E. Raichle, A.M. MacLeod, A.Z. Snyder, W.J. Powers, D.A. Gusnard, and G.L. Shulman. A default mode of brain function. *Proc Natl Acad Sci U S A*, 98:676–82, 2001. 10, 24, 42

- [120] S.C. Ramsay, K. Murphy, S.A. Shea, K.J. Friston, A.A. Lammertsma, J.C. Clark, L. Adams, A. Guz, and R.S. Frackowiak. Changes in global cerebral blood flow in humans: effect on regional cerebral blood flow during a neural activation task. *J Physiol*, 471:521–34, 1993. 43, 47
- [121] A. Riecker, W. Grodd, U. Klose, J.B. Schulz, K. Groschel, M. Erb, H. Ackermann, and A. Kastrup. Relation between regional functional mri activation and vascular reactivity to carbon dioxide during normal aging. *J Cereb Blood Flow Metab*, 23:565–73, 2003. 56
- [122] I. Roberts and G. Schierhout. Hyperventilation therapy for acute traumatic brain injury. *The Cochrane Database of Systematic Reviews*, 4, 1997. 27
- [123] P. E. Roland. *Brain Activation*. Wiley-Liss, 1993. 18, 21, 43
- [124] E.L. Rolett, A. Azzawi, K.J. Liu, M.N. Yongbi, H.M. Swartz, and J.F. Dunn. Critical oxygen tension in rat brain: a combined (31)P-NMR and EPR oximetry study. *Am J Physiol Regul Integr Comp Physiol*, 279:R9–R16, 2000. 13, 19
- [125] E. Rostrup, G.M. Knudsen, I. Law, S. Holm, H.B. W. Larsson, and O.B. Paulson. The relationship between cerebral blood flow and volume in humans. *Neuroimage*, 24:1–11, 2005. 6, 17, 27, 28, 29
- [126] E. Rostrup, H. B. W. Larsson, P. B. Toft, K. Garde, and O. Henriksen. Signal changes in gradient echo images of human brain induced by hypo- and hyperoxia. *NMR Biomed*, 8:41–47, 1995. 6, 8, 33, 34, 36, 37, 60
- [127] E. Rostrup, H. B. W. Larsson, P. B. Toft, K. Garde, P. Ring, and O. Henriksen. Susceptibility contrast imaging of CO₂-induced changes in blood volume of human brain. *Acta Radiologica*, 37:813–822, 1996. 6, 24, 27, 28
- [128] E. Rostrup, H. B. W. Larsson, P. B. Toft, K. Garde, C. Thomsen, P. Ring, L. Søndergaard, and O. Henriksen. Functional MRI of CO₂ induced increase in cerebral perfusion. *NMR Biomed*, 7:29–34, 1994. 6, 8, 28, 29, 60
- [129] E. Rostrup, H.B.W. Larsson, G.M. Knudsen, A.P. Born, and O.B. Paulson. Changes in BOLD and ADC weighted imaging in acute hypoxia and altitude adaptation. *Neuroimage*, 28:947–955, 2005. 6, 8, 49, 50
- [130] E. Rostrup, I. Law, M. Blinkenberg, H. B. W. Larsson, P. Born, S. Holm, and O. B. Paulson. Regional differences in the CBF response to hypercapnia. - a combined PET and MRI study. *Neuroimage*, 11:87–89, 2000. 6, 27, 29
- [131] E. Rostrup, I. Law, F. Pott, K. Ide, and G. M. Knudsen. Cerebral hemodynamics measured with simultaneous PET and near-infrared spectroscopy in humans. *Brain Res*, 954:183–93, 2002. 6, 11, 31, 32

- [132] IK Schmalbruch, R Linde, OB Paulson, and PL Madsen. Activation-Induced Resetting of Cerebral Metabolism and Flow Is Abolished by beta-Adrenergic Blockade With Propranolol. *Stroke*, 33(1):251–5, 2002. 55
- [133] G. H. Schneider, A. S. Sarrafzadeh, K. L. Kiening, T. F. Bardt, A. W. Unterberg, and W. R. Lanksch. Influence of hyperventilation on brain tissue- PO_2 , PCO_2 , and pH in patients with intracranial hypertension. *Acta Neurochir Suppl (Wien)*, 71:62–65, 1998. 31
- [134] C. Schwarzbauer and W. Heinke. Investigating the dependence of BOLD contrast on oxidative metabolism. *Magn Reson Med*, 41:537–543, 1999. 60
- [135] C. Schwarzbauer and M. Hoehn. The effect of transient hypercapnia on task-related changes in cerebral blood flow and blood oxygenation in awake normal humans: A functional magnetic resonance imaging study. *NMR Biomed*, 13:415–9, 2000. 49
- [136] E. Seifritz, D. Bilecen, D. Hanggi, R. Haselhorst, E.W. Radu, S. Wetzel, J. Seelig, and K. Scheffler. Effect of ethanol on BOLD response to acoustic stimulation: implications for neuropharmacological fmri. *Psychiatry Res*, 99:1–13, 2000. 55
- [137] C. Seki, J. Kershaw, P.J. Toussaint, K. Kashikura, T. Matsuura, H. Fujita, and I. Kanno. ^{15}O radioactivity clearance is faster after intracarotid bolus injection of ^{15}O -labeled oxy-hemoglobin than after ^{15}O -water injection. *J Cereb Blood Flow Metab*, 23:838–44, 2003. 20
- [138] J. W. Severinghaus and N. Lassen. Step hypocapnia to separate arterial from tissue PCO_2 in the regulation of cerebral blood flow. *Circulation Research*, 20:272–278, 1967. 27
- [139] M. Sharan, M. D. Jones, Jr., R. C. Koehler, R. J. Traystman, and A. S. Popel. A compartmental model for oxygen transport in brain microcirculation. *Ann Biomed Eng*, 17(1):13–38, 1989. 16, 18
- [140] A. Shiino, Y. Morita, A. Tsuji, K. Maeda, R. Ito, A. Furukawa, M. Matsuda, and T. Inubushi. Estimation of cerebral perfusion reserve by blood oxygenation level-dependent imaging: Comparison with single-photon emission computed tomography. *J Cereb Blood Flow Metab*, 23:121–35, 2003. 38, 40
- [141] S. Shimojyo, P. Scheinberg, K. Kogure, and O.M. Reinmuth. The effects of graded hypoxia upon transient cerebral blood flow and oxygen consumption. *Neurology*, 18:127–33, 1968. 21, 23, 33, 34
- [142] E. Shimosegawa, I. Kanno, J. Hatazawa, H. Fujita, H. Iida, S. Miura, M. Murakami, A. Inugami, T. Ogawa, and H. Itoh. Photic stimulation study of changing the arterial partial pressure level of carbon dioxide. *J Cereb Blood Flow Metab*, 15:111–114, 1995. 43, 47

- [143] B.K. Siesjo and M. Ingvar. Ventilation and brain metabolism. In *Handbook of physiology, Section 3: The respiratory system*, volume 2, book chapter 5, pages 141–161. Am. Phys. Society, 1986. 33
- [144] M. K. Stehling, F. Schmitt, and R. Ladebeck. Echo-planar MR imaging of human brain oxygenation changes. *J.Magn.Reson.Imaging*, 3:471–474, 1993. 38
- [145] N.J. Taylor, H. Baddeley, K.A. Goodchild, M.E. Powell, M. Thoumine, L.A. Culver, J.J. Stirling, M.I. Saunders, P.J. Hoskin, H. Phillips, A.R. Padhani, and J.R. Griffiths. BOLD MRI of human tumor oxygenation during carbogen breathing. *J Magn Reson Imaging*, 14:156–63, 2001. 41
- [146] S. Tominaga, S. Strandgaard, K. Uemura, K. Ito, and T. Kutsuzawa. Cerebrovascular CO₂ reactivity in normotensive and hypertensive man. *Stroke*, 7:507–10, 1976. 27
- [147] R. Turner, D. Le Bihan, C. T. Moonen, D. Despres, and J. Frank. Echo-planar time course MRI of cat brain oxygenation changes. *Magnetic Resonance in Medicine*, 22:159–166, 1991. 7, 33, 38
- [148] J. A. Ulatowski, J. M. Oja, J. I. Suarez, R. A. Kauppinen, R. J. Traystman, and P. C. van Zijl. In vivo determination of absolute cerebral blood volume using hemoglobin as a natural contrast agent: An MRI study using altered arterial carbon dioxide tension. *J Cereb Blood Flow Metab*, 19:809–817, 1999. 57
- [149] M.S. Vafae and A. Gjedde. Model of blood-brain transfer of oxygen explains nonlinear flow-metabolism coupling during stimulation of visual cortex. *J Cereb Blood Flow Metab*, 20:747–54, 2000. 21
- [150] M.S. Vafae and A. Gjedde. Spatially dissociated flow-metabolism coupling in brain activation. *Neuroimage*, 21:507–15, 2004. 42
- [151] R. Valabregue, A. Aubert, J. Burger, J. Bittoun, and R. Costalat. Relation between cerebral blood flow and metabolism explained by a model of oxygen exchange. *J Cereb Blood Flow Metab*, 23:536–545, 2003. 9, 13, 16, 21
- [152] P. C. van Zijl, S. M. Eleff, J. A. Ulatowski, J. M. E. Oja, A. M. Ulug, R. J. Traystman, and R. A. Kaupinnen. Quantitative assessment of blood flow, blood volume and blood oxygenation effects in functional magnetic resonance imaging. *Nature Medicine*, 4:159–167, 1998. 17, 37, 50, 57, 59
- [153] J.P. Wade, G.H. du Boulay, J. Marshall, T.C. Pearson, R.W. Russell, J.A. Shirley, L. Symon, G. Mein, and E. Zilkha. Cerebral blood flow, haematocrit and viscosity in subjects with a high oxygen affinity haemoglobin variant. *Acta Neurol Scand*, 61:210–5, 1980. 39

- [154] Q. Wang, O. B. Paulson, and N. A. Lassen. Indomethacin abolishes cerebral blood flow increase in response to acetazolamide-induced extracellular acidosis: a mechanism for its effect on hypercapnia? *J Cereb Blood Flow Metab*, 13:724–727, 1993. 54
- [155] M. Weckesser, S. Posse, U. Olthoff, L. Kemna, S. Dager, and G. ä. Müller. Functional imaging of the visual cortex with BOLD-contrast MRI: Hyperventilation decreases signal response. *Magn Reson Med*, 41:213–216, 1999. 46
- [156] R. M. Weisskoff and S. Kiihne. MRI susceptometry: Image-based measurement of absolute susceptibility of MR contrast agents and human blood. *Magnetic Resonance in Medicine*, 24:375–383, 1992. 13, 14
- [157] R.M. Winslow, M. Samaja, N.J. Winslow, L. Bernardi, and R.I. Shrager. Simulation of continuous blood O₂ equilibrium curve over physiological pH, DPG, and PCO₂ range. *J Appl Physiol*, 54:524–9, 1983. 12
- [158] D. A. Yablonskiy and E. M. Haacke. Theory of NMR signal behavior in magnetically inhomogeneous tissues: the static dephasing regime. *Magnetic Resonance in Medicine*, 32:749–763, 1994. 59
- [159] S. Ziyeh, J. Rick, M. Reinhard, A. Hetzel, I. Mader, and O. Speck. Blood oxygen level-dependent MRI of cerebral CO₂ reactivity in severe carotid stenosis and occlusion. *Stroke*, 36:751–6, 2005. 40

Summary in English

One of the very fascinating applications of MRI is mapping the functional anatomy of the human brain. During the last decade the methodology has developed tremendously, and the majority of current brain mapping studies relies on the BOLD (blood oxygenation level dependent) technique, rather than radiotracer based methods. During brain activation the supply of oxygen is known to increase more than its use, resulting in a decrease of deoxy-hemoglobin levels. Because deoxy-hemoglobin is paramagnetic, this results in a more homogeneous magnetic field, as can be detected by appropriate MR techniques. These techniques are primarily sensitive to the total amount of deoxy-hemoglobin per unit of tissue, which is determined from a balance between oxygen supply and use, but also depends on blood volume and other properties such as hematocrit, pH and P_aO_2 .

The BOLD effect is therefore not specific to neural activation. In the present work the term $BOLD_A$ has been used for BOLD responses caused by neural activation, and $BOLD_B$ for those caused by factors such as hypercapnia, hypoxia or other changes in blood composition or supply. These non-neural factors are very relevant both because they represent a tool by which basic brain physiology can be studied, and because they interact with the $BOLD_A$ responses, thereby adding to their intra- and inter-subject variability.

The present work aims to review the literature regarding the basic physiological mechanisms common to $BOLD_A$ and $BOLD_B$ responses, and with a special emphasis on the influence of variations in arterial blood gases. Furthermore, a mathematical model of the BOLD response is introduced, which includes, as a novel feature, the contributions from both the arterial, capillary and venous compartments. The model is used to guide the interpretation of experimental results obtained by the present and other authors.

From the modeling results it appeared that the level of tissue oxygenation in the brain is critically dependent on the permeability of the blood-brain barrier to O_2 diffusion, and it is suggested that O_2 metabolism under some, but not all conditions may be limited by arterial O_2 delivery.

In BOLD measurements the baseline signal increases with arterial CO_2 -tension as suggested by several studies, and this is mainly due to increased blood flow and brain oxygenation. These findings are confirmed by the present modeling results, which further indicate that the $BOLD_B$ response may be influenced by pH and P_aO_2 changes in addition to the hemodynamic changes during hypercapnia. During hypoxia the $BOLD_B$ signal decreases in spite of regulatory CBF increases that minimise the change in oxygen delivery to the brain. Hemodilution also influences the $BOLD_B$ signal, and this effect seem to be related to an accompanying increase in flow.

The magnitude of the $BOLD_A$ response detected after neural activation is dependent on several baseline parameters. Conditions with high baseline flow, such as hypercapnia, generally diminish the response magnitude. Hypoxia has also been shown to diminish the $BOLD_A$ response, and the effects of arterial deoxy-hemoglobin is proposed as an additional factor in hypoxia. Decreased baseline flow may enhance the $BOLD_A$ response, as long as O_2 metabolism is uncompromised.

In conclusion, several physiological factors influence the magnitude and detectability of BOLD responses, and should be accounted for in order to minimise variability between experimental groups. A quantitative understanding now seems possible, due to recent progress in

modeling and data acquisition techniques. In quantitative terms the inter-individual variability is unknown, and this is an area that should be pursued further.

Dansk Resumé

Kortlægningen af den menneskelige hjernes funktioner er en af de meget vigtige anvendelser af magnetisk resonans (MR) scanning, som er blevet muliggjort af de sidste 10 års teknologisk udvikling indenfor området. Størstedelen af alle hjernekortlægnings studier foregår idag vha. den såkaldte BOLD teknik (for Blood Oxygenation Level Dependent) fremfor med metoder baseret på indgift af radioaktive stoffer. Baggrunden for teknikken er, at aktivering af hjernen medfører en stigning i O_2 -tilførsel, som er større end stigningen i O_2 -forbrug, hvilket igen medfører et fald i det regionale deoxyhæmoglobin-indhold. Fordi deoxyhæmoglobin er et paramagnetisk stof, skabes der herved en bedre homogenitet af det magnetiske felt, og det er denne effekt som kan detekteres med passende MR-målinger. BOLD teknikkerne er derfor først og fremmest sensitive overfor mængden af deoxyhæmoglobin pr. volumen-enhed, og denne afhænger af balancen mellem tilførsel og forbrug af O_2 , men også af det lokale blod volumen, samt andre faktorer såsom hæmatokrit, pH og P_aO_2 .

BOLD effekten er derfor ikke specifik for neural aktivering, og det er praktisk at skelne mellem $BOLD_A$ -effekter der skyldes neural aktivering, og $BOLD_B$, som skyldes andre faktorer, såsom hyperkapni, hypoxi eller andre ændringer i blodets sammensætning. De non-neurale faktorer er vigtige, dels fordi de repræsenterer en mulighed for at undersøge hjernens basale fysiologi og ilt-balance, dels fordi de interagerer med $BOLD_A$ responset og øger variabiliteten på målinger både indenfor og mellem individer.

Denne afhandling har som mål at belyse og gennemgå litteraturen angående de basale fysiologiske mekanismer som er fælles for $BOLD_A$ og $BOLD_B$ responserne, specielt hvad angår betydningen af arterielle blod gasser. Desuden præsenteres en matematisk model for BOLD responset, som redegør for betydning af både arterielle, kapillære og venøse bidrag, og som her anvendes til at støtte fortolkningen af eksperimentelle resultater fra forfatterens egne og andres tidligere arbejder.

De model-baserede resultater viste først og fremmest at hjernens iltningegrad synes at være kritisk afhængig af diffusions-barrierer for ilt-transporten fra blod til væv. Det foreslås derfor at hjernens O_2 -metabolisme under nogle, men ikke nødvendigvis alle omstændigheder er direkte begrænset af den arterielle O_2 -tilførsel.

I BOLD målinger stiger baseline signalet når P_aCO_2 øges, hovedsageligt pga. øget flow, som sammen med en konstant O_2 -metabolisme medfører højere venøs ilt-saturation. Disse fund bekræftes af model-beregninger, som desuden viser, at også pH og P_aO_2 kan have en betydning for $BOLD_B$ responset, udover den hæmodynamiske baggrund. Under hypoxi falder BOLD signalet på trods af den kompensatoriske øgning i CBF, som tenderer mod at holde O_2 -forsyningen konstant. Blodets hæmoglobin koncentration er også en af de faktorer som påvirker BOLD signalet, og dette synes at være en effekt, som er tæt bundet til de ledsagende ændringer i CBF.

Størrelsen af det $BOLD_A$ respons, som fremkaldes af neural aktivering afhænger også af et antal fysiologiske parametre. Tilstande med højt flow, som f.eks. hyperkapni, formindsker generelt $BOLD_A$ responset. Også hypoxi er vist at nedsætte $BOLD_A$ responset, og omend dette delvist kan skyldes det øgede flow, er det sandsynligt at også den øgede arterielle koncentration af deoxyhæmoglobin har en mere direkte effekt. Nedsat baseline flow ses f.eks. under hypokapnia, eller som farmakologisk effekt, og under forudsætning af at O_2 -metabolismen ikke nedsættes,

kan dette medføre en øget $BOLD_A$ effekt.

Det konkluderes at adskillige fysiologiske faktorer fremkalder ændringer i cerebral oxygenering, og dermed både fremkalder ændringer i baseline signal, samt indvirker på størrelsen af det respons som skyldes cerebral aktivering. En nærmere forståelse af BOLD effekten synes mulig, pga. fremskridt indenfor såvel MR-data opsamling, som matematisk modellering af den cerebrale O_2 -balance. Rent kvantitativt mangler der dog fortsat data som belyser den individuelle variabilitet i disse faktorer, deres praktiske betydning for BOLD effekten, samt generelt for hjernens O_2 -metabolisme og funktion.

Index

- 2,3-diphosphoglycerate, 14, 60
 - molar ratio, 19
- 7 T, 7, 53
- acetazolamide, 60
- activation
 - additive model, 49
 - proportional model, 49
- aging, 63
- air hunger, 38
- anemia, 60
- anoxia
 - vs apnea, 44
- Balloon Model, 11
- baseline, 10
- beta-receptor blockade, 61
- Bohr effect, 35
- BOLD
 - interactions, 10, 52
 - main effects, 10
- breath-holding, 44
- butanol, 54
- caffeine, 62
- carbogen, 47
- carbonic anhydrase, 60
- carotid stenosis, 46
- cerebral blood flow
 - CO₂ reactivity, 29, 34
 - and O₂ metabolism, 24
 - and tissue PO₂, 22
- cerebral blood volume
 - CO₂ reactivity, 32
 - effect on BOLD_A, 55
 - effect on BOLD_B, 27
- cyclooxygenase inhibition, 61
- cytochrome, 21
- default state, 28
- deoxy-hemoglobin, 7
- echo-planar imaging, 7
- ethanol, 62
- Ficks principle, 9
- Grubbs relation, 19
- Haldane effect, 41
- hematocrit, 15
 - and gender, 59
- hemodilution, 45
- hemoglobin
 - concentration, 15
 - properties, 12
 - transport, 15
- hypercapnia, 29
 - effect on BOLD_A, 52
 - graded, 52
 - regional variation, 31
- hypercapnic
 - calibration, 67
 - normalisation, 65
- hyperoxia, 56
 - effect on BOLD_A, 59
 - flow change, 43
- hypocapnia, 52
 - effect on BOLD_A, 53
 - respiratory alkalosis, 34
- hypoxia, 39, 56
 - and activation, 27
 - effect on BOLD_A, 56
 - regional variation, 43
- indomethacin, 29, 61
- inter-individual variation, 8
- Kety-Schmidt
 - CBF quantification, 29
- lactate, 40, 62
- mass-balance, 11

- near infrared spectroscopy, 36
- nicotine, 62
- nitric oxide, 29
- oxygen
 - O₂ limitation model, 10
 - affinity (of Hb), 60
 - delivery, 24, 38, 60
 - diffusion, 23, 27
 - dissociation curve, 12
 - extraction fraction, 12, 27, 48
 - metabolism, 24
- parameters
 - typical values, 18, 19
- perfluorocarbon, 20
- permeability-surface product, 13
- pH, 55
 - effect of CO₂, 29
 - in hypercapnia, 31
 - oxygen affinity, 34
- Poiseuilles law, 20
- positron emission tomography, 7
 - CO₂ reactivity, 31
 - additive/proportional, 50
 - arterial blood volume, 20
 - CBF-CBV relationship, 19
 - hypoxia, 39
 - neuronal activation, CO₂, 38
 - regional variation, 31
 - sleep, 64
- propranolol, 61
- relaxation rate, 15
- resonance shift, 16
- sleep, 64
- susceptibility, 15
- transit time
 - intra/extravascular tracers, 23
- tumor oxygenation, 47
- vascular
 - CO₂ reactivity, 32
 - compartments, 20
 - heterogeneity, 28
 - reserve capacity, 46
 - volumes, 20
- visual stimulation, 53